Snow avalanche hazard assessment in the French Alps using a combination of dendrogeomorphic and statistical approaches

Romain Schläppy

Université Paris 1 Panthéon-Sorbonne
École Doctorale
de Géographie de Paris

Université Berne
Décanat de la Faculté
des Sciences naturelles

PhD thesis

Geography

SCHLÄPPY Romain

Snow avalanche hazard assessment in the French Alps using a combination of dendrogeomorphic and statistical approaches

Supervisors of PhD thesis: Dr. Vincent JOMELLI / Prof. Dr. Markus STOFFEL

Defended on 23 April 2014

Commitee:

Dr. Vincent JOMELLI, Université Paris 1 Panthéon-Sorbonne, co-director
Prof. Dr. Markus STOFFEL, Université de Berne, co-director
Dr. Nicolas ECKERT, Irstea, Grenoble, co-supervisor
Prof. Dr. Daniel GERMAIN, Université Québec, reviewer
Dr. Luuk DORREN, Universität für Bodenkultur, Vienne, reviewer
Prof. Dr. Pierre PECH, Université Paris 1 Panthéon-Sorbonne, examiner
Dr. Frédéric BERGER, Irstea, Grenoble, examiner

Université Paris 1 Panthéon-Sorbonne
École Doctorale
de Géographie de Paris

Université Berne
Décanat de la Faculté
des Sciences naturelles

Thèse de Doctorat

Géographie

SCHLÄPPY Romain

Caractérisation de l'aléa avalancheux dans les Alpes françaises. Combinaison d'approches dendrogéomorphologique et statistique

Thèse dirigée par: Dr. Vincent JOMELLI / Prof. Dr. Markus STOFFEL

Soutenue le 23 avril 2014

Jury:

Dr. Vincent JOMELLI, Université Paris 1 Panthéon-Sorbonne, co-directeur
Prof. Dr. Markus STOFFEL, Université de Berne, co-directeur
Dr. Nicolas ECKERT, Irstea, Grenoble, co-encadrant
Prof. Dr. Daniel GERMAIN, Université Québec, rapporteur
Dr. Luuk DORREN, Universität für Bodenkultur, Vienne, rapporteur
Prof. Dr. Pierre PECH, Université Paris 1 Panthéon-Sorbonne, examinateur
Dr. Frédéric BERGER, Irstea, Grenoble, examinateur

Summary

Snow avalanches are a significant natural hazard that impact roads, structures and threaten human lives in mountainous terrain. Although relatively few people are killed during ''normal" winters, extreme winters may still claim victims, as winter 1998/1999 showed very clearly throughout the Alps. Hence, specification of expected runout distances and related return periods are the most important steps for zoning in snow avalanche prone terrain. Runout distances can be identified through a combination of field observations, historical records or the analysis of aerial photos and topographic maps. However, as long and continuous historical observations are generally scarce, the extent of avalanches is usually evaluated using topographic or statistic models. These models are well capable to simulate contemporary events with return periods typically ≤ 30 yr, but uncertainties increase as soon as longer return periods are investigated. Thus, there is a real need for validation of modeling procedures to corroborate model predictions.

Dendrogeomorphology has been recognized as a powerful tool to reconstruct past activity of avalanches with annual resolution and for risk assessment. The approach has also been used to find relations between snow and weather variables and avalanche activity. Surprisingly, little attention has been paid so far to assess the accuracy and relevance of dendrogeomorphology for these particular uses in the field of snow avalanche science. It is therefore the aim of this PhD thesis to (i) propose a new tree-ring-based semi-quantitative approach for the identification of avalanche events and to evaluate the quality and completeness of tree-ring records, to (ii) densify and extend existing avalanche data in different paths within the French Alps and to (iii) evaluate runout distances and related return periods for extreme events, to (iv) perform the first cross-validation of high return period avalanche information derived from a locally calibrated statistical-dynamical model and the long-term, higher-return period information gathered from tree-ring records, and to (v) evaluate the actual contribution of dendrogeomorphic data to the assessment of avalanche-climate relations at the path scale.

In the first paper, a total of 1169 samples extracted from 587 conifers (*Larix decidua* Mill., *Picea abies* (L.) Karst., and *Abies alba* Mill.) in three different avalanche paths was investigated. Using an alternative tree-ring-based semi-quantitative approach, we were able to reconstruct a total of 75 avalanche events for the period 1799—2010. As the approach relies on the assessment of the number and position of disturbed trees within avalanche paths as well as the intensity of reactions in trees, the principal objective of this study was to demonstrate that no bias was induced by the dendrogeomorphic expert. Based on a statistical evaluation (Classification Trees, or CART) of the approach, we were able to point out the consistency and replicability of the procedure. Moreover, comparison between the avalanche years recorded in a substantial database in a well-documented path in Chamonix and those defined with dendrogeomorphic techniques shows that the avalanche record reconstructed from tree-ring series contains 38% of the observed events.

In the second paper, a total of 713 samples extracted from 297 conifers (*L. decidua* and *P. abies*) were used to reconstruct avalanche activity in two avalanche paths using the semi-quantitative approach validated previously. The objective was to perform the first cross-validation of high return period avalanches derived from a locally calibrated statistical-dynamical model and the long-term, higher-return period information gathered from tree-ring records. Based on the reconstructed distribution of runout distance of 25 events for the period 1799—2010 and mean event frequencies, we successfully derived runout values for events with return periods of $\leq$ 300 yr. Comparison of relations between runout distances and return periods between both approaches shows very good agreement. Within the classical intervals used in hazard zoning (i.e. 10—300 yr), mean and mean square errors amounted to $\sim$20 and 30—45 m, respectively.

The main objective of the last part of this PhD thesis was to evaluate the relevance of climate–avalanche relationships inferred from tree-ring chronologies at the local scale, given that dendrogeomorphic reconstructions may miss a significant number of avalanches. Firstly, past avalanche activity was reconstructed in five paths in different areas of the French Alps with various site-related characteristics. Based on refined daily snow and weather data for the period 1959—2009, we defined a large set of potential variables that could explain

avalanche activity and picked up the most pertinent of them using a variable selection procedure implemented within a logistic regression framework. A similar approach was used with event chronologies derived from historical archives as well as with a third data set composed of a combination of both chronology types. Obtained logistic regression models suggest that tree rings preferentially record events that occurred during cold winter storms with heavy precipitation. Conversely, an important proportion of those events may be missed by human observation on remote paths or on paths were risk exposure is low.

In conclusion, this PhD thesis provides new insights into the possibilities and limitations of tree-ring analyses in snow avalanche research. The new semi-quantitative approach used in this work has been proven to be consistent and applicable in different types of paths. This approach is not restricted to the identification of high-magnitude avalanches but also allows determination of relatively small events. Although tree-ring reconstructions may miss a significant number of avalanches, dendrogeomorphic data can be seen as an extremely valuable data pool for the assessment of runout distances and return periods of extreme avalanche events, and in particular for the hazard zoning on forested paths with limited or no historical data. Furthermore, tree-ring records contribute to a better understanding of link between snow, climate and avalanche activity, but only up to a certain extent, specifically for avalanche events occurring during cold episodes accompanied by heavy precipitation. It seems, however, that combining tree-ring and historical event chronologies for refining the study of climate-avalanche relations remains a difficult and open problem. In the current context of climate warming, similar approaches are needed at the regional scale to evaluate the contribution of dendrogeomorphic data for documenting the response of avalanche activity to climate change.

Keywords: *snow avalanche, dendrogeomorphology, tree ring, hazard assessment, runout distance, return period, avalanche-climate relations, statistical-dynamical model, logistic regression, French Alps, validation.*

Résumé

Dans les régions de montagne, les avalanches sont susceptibles d'affecter le réseau routier et les infrastructures bâties, mettant ainsi en péril la population résidante. Bien que l'on dénombre relativement peu de victimes d'avalanches spontanées durant les hivers considérés comme «normaux», les hivers extrêmes peuvent parfois se révéler très meurtriers, comme ce fut le cas durant l'hiver 1998/1999 dans les Alpes. Ainsi, la caractérisation des distances d'arrêt des avalanches et l'évaluation des périodes de retour associées représentent l'étape la plus importante pour un zonage réaliste en aval des couloirs. Les distances d'arrêt peuvent être identifiées à l'aide de plusieurs méthodes telles que les observations de terrain, la consultation d'archives historiques ou encore l'analyse de photos aériennes et de cartes topographiques. Cependant, ces données sont souvent lacunaires et limitées dans le temps. Pour cette raison, l'extension des avalanches est généralement évaluée à l'aide de modèles physiques et/ou statistiques. Ces modèles sont très performants lorsqu'il s'agit de simuler des évènements relativement fréquents dont la période de retour est inférieure ou égale à 30 ans. A l'inverse, les incertitudes tendent à augmenter rapidement dès lors que l'on considère des périodes de retour supérieures. Il est donc indispensable de valider les procédures de modélisation afin de confirmer les prédictions qui en découlent

La dendrogéomorphologie a prouvé son utilité pour reconstituer l'activité avalancheuse passée au pas de temps annuel. Cette technique a également été utilisée pour caractériser les relations entre des variables liées au manteau neigeux et météorologiques, et l'activité avalancheuse. De manière assez surprenante, peu d'intérêt a été porté sur l'évaluation de la précision et la pertinence de l'approche dendrogéomorphologique dans le domaine de l'étude des avalanches. L'objectif de ce travail de thèse est donc de (i) proposer une nouvelle approche semi-quantitative fondée sur l'étude des cernes d'arbres pour l'identification des évènements avalancheux et d'évaluer la qualité et l'exhaustivité de cet outil naturaliste; (ii) densifier et étendre les données existantes sur les avalanches dans plusieurs couloirs des

Alpes françaises et (iii) évaluer les distances d'arrêt et les périodes de retour associées pour les évènements extrêmes; (iv) réaliser la première validation croisée entre des avalanches à période de retour très élevées prédites par un modèle statistique-dynamique calibré localement et des informations sur des périodes de retour d'avalanches similaires obtenues grâce à l'étude des séries de cernes d'arbres impactés; (v) évaluer la contribution effective des données dendrogéomorphologiques pour la caractérisation des relations avalanche—climat à l'échelle locale.

La première étude de ce travail se fonde sur l'analyse de 1169 échantillons extraits de 587 conifères (*Larix decidua* Mill., *Picea abies* (L.) Karst., and *Abies alba* Mill.) dans trois couloirs d'avalanches. Grâce à l'utilisation d'une nouvelle approche dendrogéomorphologique semi-quantitative, un total de 75 évènements avalancheux a été reconstitué pour la période 1799—2010. Cette approche se fonde sur l'évaluation du nombre et de la position des arbres impactés par les avalanches situés dans les couloirs ainsi que sur l'intensité des réactions dans les arbres. L'objectif principal était donc de démontrer qu'aucun biais ne résulte de l'expertise dendrogéomorphologique. Une évaluation statistique (arbres de classification) de l'approche a permis de confirmer la cohérence et la transférabilité de la procédure utilisée. Par ailleurs, la comparaison entre les années avalancheuses reportées dans une base de données substantielle et celles identifiées par l'approche dendrogéomorphologique dans un couloir très bien documenté à Chamonix montre que la chronique issue des séries de cernes d'arbres contient 38% des évènements observés.

La seconde étude se fonde sur un total de 713 échantillons extraits de 297 conifères (*L. decidua* and *P. abies*) et a permis de reconstituer l'activité avalancheuse dans deux couloirs à l'aide de l'approche semi-quantitative évaluée préalablement. L'objectif était de réaliser la première validation croisée entre des avalanches à période de retour très élevées prédites par un modèle statistique-dynamique calibré localement et des informations sur des périodes de retour d'avalanches similaires obtenues grâce à l'étude des séries de cernes d'arbres impactés. Se fondant sur la distribution des distances d'arrêt de 25 évènements reconstitués dans deux couloirs et sur la fréquence évènementielle moyenne pour la période 1799—2010, il a été possible de déduire l'extension spatiale pour des évènements dont la

période de retour est égale ou inférieure à 300 ans. Les relations entre distances d'arrêt et périodes de retour issues des deux approches ont été comparées. Les résultats montrent une bonne concordance entre les deux approches. En effet, considérant les intervalles traditionnellement utilisés en zonage, i.e. 10—300 ans, les écarts moyens ainsi que les écarts quadratiques moyens s'élèvent à ~20 et 30—45 mètres, respectivement.

L'objectif principal de la troisième étude de ce travail était d'évaluer la pertinence des relations climat—avalanches dérivées des séries de cernes d'arbres impactés à l'échelle locale, considérant la non-exhaustivité des reconstructions dendrogéomorphologiques. Dans un premier temps, l'activité avalancheuse a été reconstituée dans cinq couloirs dispersés dans les Alpes françaises. Se fondant sur des données journalières ré-analysées liées au manteau neigeux et aux conditions météorologiques pour la période 1959—2009, nous avons défini un important jeu de variables pouvant potentiellement expliquer l'activité avalancheuse et les plus pertinentes ont été sélectionnées à l'aide d'une procédure mise en place dans le cadre d'une régression logistique. Une approche similaire a été utilisée avec les chronologies évènementielles dérivées des archives historiques et d'un troisième jeu de données composé d'une combinaison des deux types de chronologie. Les modèles obtenus de la régression logistique suggèrent que les cernes d'arbres enregistrent de manière préférentielle les évènements qui ont eu lieu durant des épisodes froids associés à des tempêtes hivernales accompagnées de fortes précipitations. A l'inverse, ce genre d'évènements échappe régulièrement aux observateurs en charge de la surveillance des couloirs situés dans des zones reculées ou pour lesquels le risque d'exposition est faible.

En conclusion, ce travail de thèse fournit de nouvelles connaissances concernant les apports et les limites de l'étude des cernes d'arbres dans le domaine de la prévention des avalanches. Nous avons démontré que l'approche semi-quantitative utilisée pour cette recherche est cohérente et peut être appliqué dans différents types de couloir. L'utilisation de cette approche n'est pas restreinte à l'identification des avalanches extrêmes mais permet également la caractérisation d'évènements relativement confinés. Bien que les reconstitutions dendrogéomorphologiques tendent à manquer un certain nombre d'évènements avalancheux, les séries de cernes d'arbres impactés par les avalanches

peuvent être très utiles pour l'évaluation des distances d'arrêt des évènements extrêmes et des périodes de retour associées, en particulier en ce qui concerne le zonage à proximité des couloirs boisés pour lesquels les archives historiques sont lacunaires, voire inexistantes. Par ailleurs, les données dendrogéomorphologiques peuvent, dans une certaine mesure, contribuer à une meilleure compréhension des relations entre le manteau neigeux, le climat et l'activité avalancheuse, particulièrement pour les évènements ayant lieu durant les épisodes hivernaux froids accompagnés de fortes précipitations. Cependant, l'étude des relations climat—avalanches se fondant sur la combinaison de chronologies d'évènements dérivées des archives historiques et des cernes d'arbres demeure compliquée et reste une problématique ouverte. Dans le contexte actuel de réchauffement climatique, il paraît indispensable de conduire des approches similaires à l'échelle régionale afin d'évaluer la contribution des analyses dendrogéomorphologiques pour documenter la réponse de l'activité avalancheuse aux changements climatiques.

Mots-clés: *avalanche, dendrogéomorphologie, cerne d'arbre, caractérisation des aléas, distance d'arrêt, période de retour, relations avalanche-climat, modèle statistique-dynamique, régression logistique, Alpes françaises, validation.*

Table of contents

CHAPTER C : EVALUATION OF RUNOUT DISTANCES AND RETURN PERIODS

CHAPTER D : ASSESSMENT OF AVALANCHE-CLIMATE RELATIONS

CHAPTER F : APPENDICES

List of tables

List of figures

Acknowledgements

I would like to gratefully acknowledge my two co-directors, Dr. Vincent Jomelli and Prof. Markus Stoffel, as well as my co-supervisor Dr. Nicolas Eckert for their guidance, support, insight and contributions throughout the process of completing my PhD thesis. They have assisted me during my whole work and offered me the great opportunity to live a 4-year experience in the world of scientific research. I would also like to thank the other members of my examination committee, Drs. Daniel Germain, Luuk Dorren, Pierre Pech and Frédéric Berger, for accepting to review this thesis.

Special thanks to Delphine Grancher and Daniel Brunstein, who were present every day to answer my questions, to provide me technical as well as psychological support and to reassure me during this pretty long work. In addition, I would also thank Drs. Michelle Schneuwly-Bollschweiler, Christophe Corona, Jérôme Lopez Saez, Mohamed Naaim, as well as Michaël Deschâtres and Claude Legentil for their worthy scientific contribution and the great discussions we had together.

I gratefully acknowledge Louis Manière, Jonathan Dumani and Matthieu Schläppy for their assistance in the field as well as Marie-Adélaïde Bouquet for her help in sample analysis. I also want to thank the Office National des Forêts (ONF), and especially Didier Bois, as well as the provosts in Lanslevillard, Modane, Chamonix and Montgenèvre for sampling permissions and technical assistance. Many thanks as well to the Compagnie du Mont-Blanc for providing me free access to the Planpraz cable car during sampling campaigns.

I would like to acknowledge wholeheartedly the Laboratoire de Géographie Physique “Pierre Birot” (LGP) in Meudon, for hosting me during all these years, and especially its former director Catherine Kuzucuoglu and its secretary Michelle Pennec, for their effective administrative assistance. In addition, I would like to gratefully thank Irina, Salomé, Valentina, Nathalie, Céline, Marie, Clélia, Marina, Anne, Marion, Anne-Kyria, Charlotte, Sèverine, Sterenn, Thomas, Alex, Édouard, Clément, Vincent R., Vincent T., Aurélien,

Frédéric, Fouzi, Antoine, Jean-Marc, Yohan and Tim. Without the countless coffee breaks, fit of laughter, parties and nice moments, I would probably not have succeeded in finishing my work. Many thanks to all the LGP members for having shared out their valuable human and scientific qualities.

Furthermore, this research would not have been possible without the support provided by the French National Research Agency (ANR-09-RISK-007-01) and the Swiss National Science Foundation (project P1SKP2_148492).

My thoughts also go to Caro, Marie, Thibault, Chris, Lilian, Steven, Laurent, Manu, Artus, and Guillaume, who allowed me to break with routine during hundreds of hours of very good music. I would also acknowledge all IMBC92 members for the great sporty moments that allowed me to retrieve a balanced body and mind.

Special thanks to my long-time friends Lili, Véro, Jon, Youri, Louis, Kevin and Mouloud for having been present during my journeys in Switzerland and for visiting me sometimes. I would also like to thank my flatmates Marine, Alex and Jenny, as well as Sophie and Mat, Julie, Antoine and Dorothée, Marie, Alain, Cécilia and Alex, Auré and François, Alice and Stéphane, Lilou and Mat, Constance and Alexis, Johana and Xavier, Emma, Bastien, Émilie and Flo, Marie and Antoine, Nathalie and Thomas, Élo and Jim, Lulu and Alex, Stéphanie and Thom, Trifon and Mariam, and Olivier for the very nice time we spent together.

I would like to express my gratitude to my mother and Pierre, Mélanie and Matthieu, Céline and Bastien, Soleïa, Lénaë, Gabrielle, Aléïna and Ayan, as well as Violaine and Tico, Johanna, Sylvie, for their support, smiles and humor. I am very proud to be part of such a beautiful family. I would also like to thank sincerely Françoise and Mao, Marion and Akram, Sandrine and Nico, Eileen, Leïla, Betty and Henri-Paul, Aurélie and Julien, Julie and Alex, Iléa, Florence and Fréd, as well as Lorn for all the very pleasant moments we shared together.

Finally, many, many thanks to Sophie, for her great patience and support during the last 3 years and for making me happy every day.

Preamble

This PhD thesis has been realized within the framework of the MOPERA (Modélisation Probabiliste pour l'Évaluation du Risque d'Avalanche) project funded by the French National Research Agency and headed by Dr. Nicolas Eckert from Irstea (Institut national de recherche en sciences et technologies pour l'environnement et l'agriculture), Grenoble, France.

Research of this thesis has been conducted at the Laboratoire de Géographie Physique "Pierre Birot" (LGP) research unit of the Centre National de la Recherche Scientifique (CNRS) directed by Dr. Catherine Kuzucuoglu, Université Paris 1 Panthéon-Sorbonne, as well as at Dendrolab.ch directed by Prof. Markus Stoffel, University of Berne.

Noteworthy, the main part of this thesis is composed of three papers.

CHAPTER A

GENERAL INTRODUCTION

1 Introduction

1.1 Snow avalanche process

The following section is essentially based on McClung and Schaerer (2006).

1.1.1 Definition

Snow avalanches are rapid downslope transfers of snow, often with great destructive power, which are significant natural hazards in areas of steep terrain (Luckman, 2010). They can contain rocks, soil, vegetation, or ice (Schweizer et al., 2003). Snow avalanches vary in size from a few to several million cubic meters of snow ranging in character from dry powder avalanches to dense wet snow.

1.1.2 Snow avalanche formation

There are two general types of snow avalanche release: loose-snow avalanche and slab avalanche (Schweizer et al., 2003). Loose-snow avalanches start at or near the surface and they usually involve only surface or near-surface snow. They start at a single area or point and spread out as they move down the slope in a triangular pattern (inverted V-shape) as more snow is pushed down the slope and entrained into the slide (McClung and Schaerer, 2006; Figure 1).

Slab avalanches initiate by a failure associated with a thin weak layer at depth in the snow cover, ultimately resulting in a block of snow, usually approximating a rectangular shape, that is entirely cut out by propagating fractures in the snow (Figure 1b). When a slab avalanche releases, it generally leaves a set of readily identifiable failure surfaces in the surrounding snowpack.

These two types can be further described as to whether they are wet or dry. Wet snow avalanches have a water content of $>$ 3% (McClung and Schaerer, 2006).

Snow avalanche activity depends on the interaction between terrain variables that control slope characteristics and meteorological/climatic conditions that control the accumulation patterns of snow (Luckman, 2010). The terrain characteristics usually determine the locations within the landscape where snow can accumulate to sufficient depth on an adequate slope (usually between 25° and 55°) to generate avalanches. However, avalanches result from the mechanical failure of the snow cover when it becomes unstable. This may be the result of direct loading during precipitation events (either snow or rain on snow), changes in the physical characteristics of the snow cover over time (mainly related to wind activity, temperature variations, and solar radiation) or inherent instability of the snow cover due to its depositional history and stratigraphy (Luckman, 2010). On the other hand, an avalanche may be actively triggered, meaning a release initiated due to a disturbance such as the presence of a skier, cornice fall, snowmobile, or explosive (Delparte, 2008).

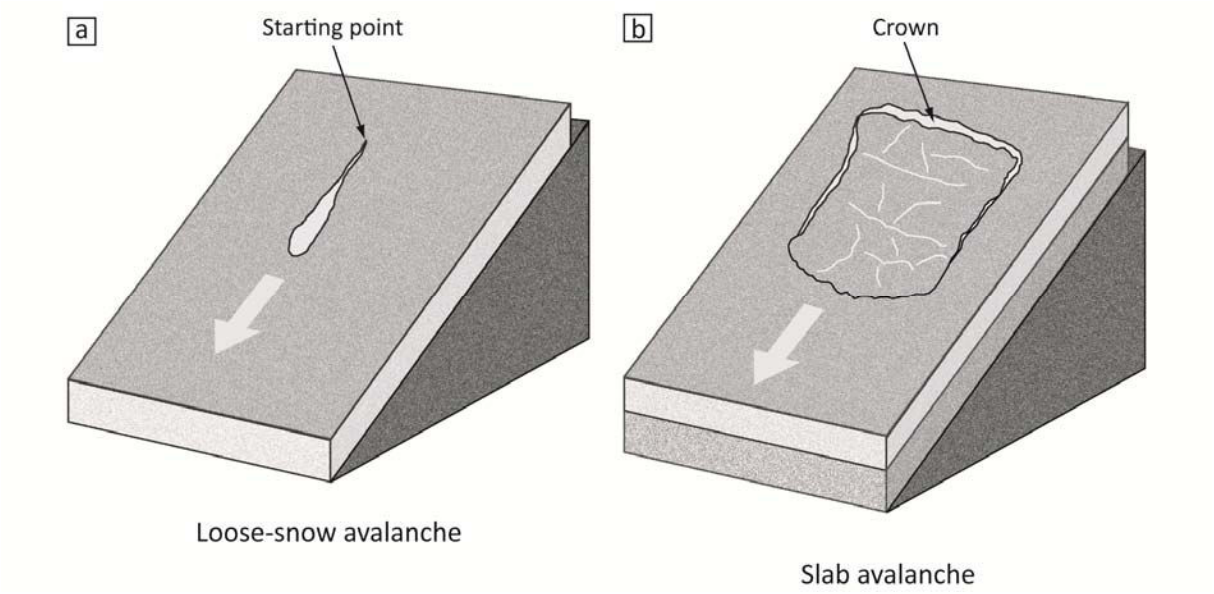

Figure 1. *Illustration of (a) loose and (b) slab avalanche failure types (after* McClung and Schaerer, 2006).

1.1.3 Path characteristics

An avalanche path is a fixed locality within which an avalanche moves. Avalanche paths may cover a vertical distance of only 50 m or may fall the full length of a mountainside with a vertical drop of 2000 m or more (McClung and Schaerer, 2006). Within a path, smaller avalanches may start and stop at various places, each avalanche having its own starting zone, track, and runout zone. The starting zone is the location where the unstable snow failed and began to move (Figure 2). The crown (Figure 1b) of a slab avalanche and the initiation point of a loose-snow avalanche (Figure 1a) define the upper limit of the starting zone for each avalanche (McClung and Schaerer, 2006). A combination of variables affect the avalanche starting zone character: slope incline, wind exposure, orientation to the sun (aspect), forest cover, ground surface, slope dimensions, altitude, as well as crown and flank locations.

The track is the slope below the starting zone that connects the starting zone with the zone where debris collects: the runout zone (Figure 2). While the track is the major terrain feature for large avalanches, it is often ill-defined in avalanches with a short running distance. Avalanche speed attains its maximum value in the track, with accelerating flow at the start of the track and decelerating flow at the end (McClung and Schaerer, 2006). The track is typically in the 15°—30° slope range (Mears, 1992). It can be confined, unconfined or a combination of both. A confined track is characterized by small drainages or gullies and has the effect of increasing flow depth and runout distances. Unconfined tracks occur on large open slopes where increased deposition may be observed at abrupt slope transitions such as benches along the avalanche path (Delparte, 2008).

The runout zone is the area where deceleration is rapid, snow and transported material is deposited, and the avalanche stops (Figure 2). It can be a wide bench, a talus slope, a valley bottom, the opposite side of a valley, or anywhere that an avalanche stops running. Typical slope angles for the runout zone are 15° or less (McClung and Schaerer, 2006).

The three zones can vary for individual avalanches within an avalanche path. A forest in the runout zone can retard avalanche flow, depending on the tree spacing, tree height, and elasticity and type of avalanche. However, forest cover cannot be relied on to stop all

avalanches because these may either move through the trees or break them, especially on steep slopes above the runout zone.

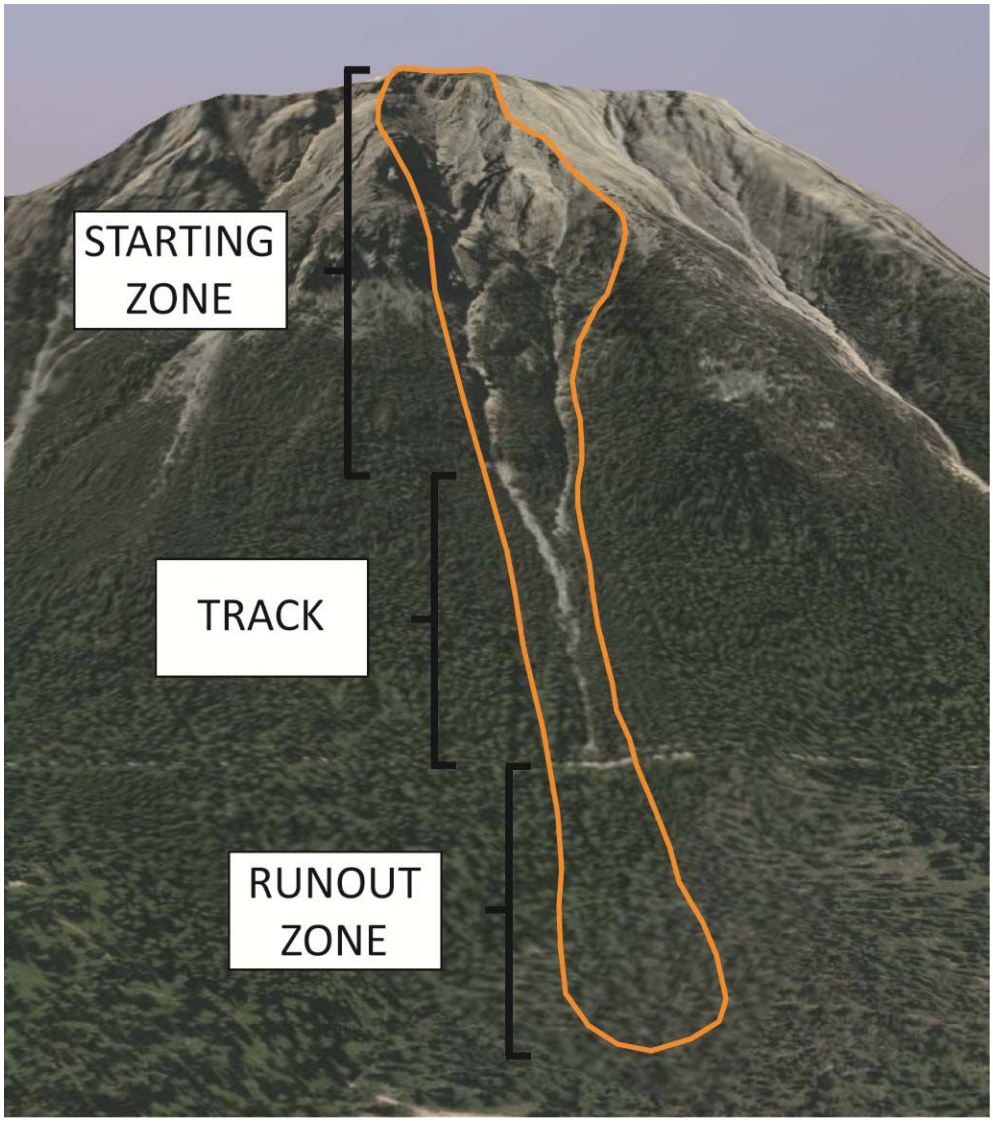

Figure 2*.The three principal subdivisions in an avalanche path.*

1.2 Main issues

Snow avalanches are a significant natural hazard that impact roads, structures and threaten human lives in mountainous terrain (Delparte, 2008). In France, even if around 600 townships are strongly susceptible to snow avalanche danger, only few people are killed

during ''normal" winters. Conversely, extreme winters may still claim victims, as February 1999 showed with terrifying clarity (12 persons were killed at Montroc; Ancey et al., 2000). Hence, specification of expected runout distances and related return periods (i.e. the average interval of time within which a given runout distance is reached or exceeded) are the most important steps for zoning in snow avalanche prone terrain (McClung, 2000).

Runout distances can be identified through a combination of field observations, historical records or the analysis of aerial photos and topographic maps (Ancey et al., 2004; Mears, 1992; Weir, 2002). However, as long and continuous historical observations are generally scarce, the extent of avalanches is usually evaluated using topographic or statistic models (Bovis and Mears, 1976; Eckert et al., 2007b; Keylock, 2005; Lied and Bakkehøi, 1980; McClung and Lied, 1987). These models are well capable to simulate contemporary events (i.e., corresponding to return periods ≤ 30 yr) on which they could be calibrated, but uncertainties increase as soon as longer return periods are investigated. For long-term avalanche forecasting, the interval which is of highest relevance corresponds to return periods varying between 30 and 300 yr (Salm et al., 1990). Consequently, there is a clear need for validating modeling procedures to corroborate model predictions on this range.

On forested paths, dendrogeomorphology (Alestalo, 1971; Stoffel et al., 2010) has been demonstrated to represent a powerful tool to reconstruct past activity of avalanches with annual resolution and for periods covering past decades to centuries (Butler and Sawyer, 2008). The approach is based on the fact that trees form one increment ring per year in temperate climates and that trees affected by mass movements record the evidence of geomorphic disturbance in their growth-ring series (Stoffel and Bollschweiler, 2008; Stoffel et al., 2013). Since the 1970s, dendrogeomorphology has been repeatedly used for the identification of snow avalanche activity worldwide (e.g., Butler and Malanson, 1985; Casteller et al., 2008; Corona et al., 2012; Germain et al., 2010; Voiculescu, 2008).

In addition, several researchers have used this approach to explore the link between snow and weather factors and avalanche activity (Corona et al., 2010; Germain et al., 2009; Hebertson and Jenkins, 2003; Reardon et al., 2008).

Surprisingly enough, little attention has been paid so far to assess the accuracy and relevance of dendrogeomorphology for these different uses in the field of snow avalanche science.

1.3 Objectives

The present PhD thesis aims at improving snow avalanche hazard assessment in the French Alps using a combination of conventional dendrogeomorphic techniques and statistical methods. Based on the study of tree-ring series, a preliminary objective is to propose a new semi-quantitative approach for the identification of snow avalanche events. As this approach relies on the analytical skills of the dendrogeomorphic expert, an effort will be made to statistically evaluate the consistency and transferability of the approach. Moreover, quality and completeness of tree-ring records for the reconstruction of snow avalanche activity will be evaluated in an unusually well-documented path. Event reconstruction in several avalanche paths will allow the densification and extension of existing snow avalanche database.

Second, based on the resulting event chronologies, an effort will be made to evaluate runout distances and related return intervals for extreme events, i.e., corresponding to return periods $\geq$ 30 yr. These empirical data will be used to perform the first cross-validation of high return period avalanche information derived from an up-to-date locally calibrated statistical-dynamical model and the long-term, higher-return period information gathered from tree-ring records.

Finally, the last objective of this thesis is to evaluate the actual contribution of dendrogeomorphic data to the assessment of avalanche-climate relationships at the local scale on different case studies.

1.4 Structure of the thesis

The thesis starts with a general introduction containing information on the snow avalanche process and the use of tree-ring based techniques to reconstruct snow avalanche activity (CHAPTER A). Main issues and related objectives are defined and dendrogeomorphic

techniques are presented in detail. CHAPTER A continues with a “state of the art” of dendrogeomorphology in the field of snow avalanche science and ends with an overview on the localization of the different paths studied.

The main part of this thesis is composed of three papers: The first paper (CHAPTER B) proposes a statistical evaluation of a new tree-ring-based, semi-quantitative approach for the identification of snow avalanche events. The second paper (CHAPTER C) presents a validation of extreme snow avalanches and related return periods derived from a statistical-dynamical model using tree-ring techniques. The third paper (CHAPTER D) discusses the actual contribution of dendrogeomorphic data to the assessment of avalanche-climate relationships at the path scale.

An overall conclusion of the main findings and suggested further research (CHAPTER E), as well as 3 appendices complement this work (CHAPTER F). The manuscript ends with an overall bibliography.

2 Dendrogeomorphology: a valuable tool for the reconstruction of snow avalanche activity

The following section is essentially based on Bollschweiler (2007) and Stoffel and Bollschweiler (2008).

2.1 Principles of dendrochronology

Dendrochronology depends on the fact that trees growing in the temperate regions can form distinct annual growth rings. In conifer trees, reproductive cambium cells form large, thin-walled tracheids during the early stages of the growing season (Camarero et al., 1998; Rigling et al., 2002) in spring and early summer. These earlywood cells serve the transport or nutrients and water. At the end of the growing season in late summer and early autumn, smaller cells with thicker walls are formed (Schweingruber, 1996) and serve to increase the stability of the tree. These latewood layers are darker in appearance due to thicker cell walls.

The width and character of each tree ring is influenced by biotic as well as abiotic factors. Biotic factors include the genetic makeup as well as the aging of trees and are individual for each species and each tree. Abiotic factors include e.g., light, temperature, water, nutrient supply or influence of strong wind and are more or less common for all trees growing at a specific site (Fritts, 1976; Schweingruber, 1996). Therefore, trees growing at the same site will record the same environmental impacts and fluctuations (e.g., temperature or precipitation) in their tree-ring series. This similarity in relative ring widths allows accurate dating of tree-ring series of unknown age. The method used for the absolute dating of wood is called “cross-dating” and allows the construction of long tree-ring series by overlapping the inner parts of younger trees with the outer parts of older trees (Figure 3; Schweingruber, 1983).

Apart from the use of tree rings for pure dating purposes in dendroarcheology, the information contained in the growth sequences have been used repeatedly to retrieve information from the environment of the tree or the stand analyzed (dendroecology; Bräuning, 1995).

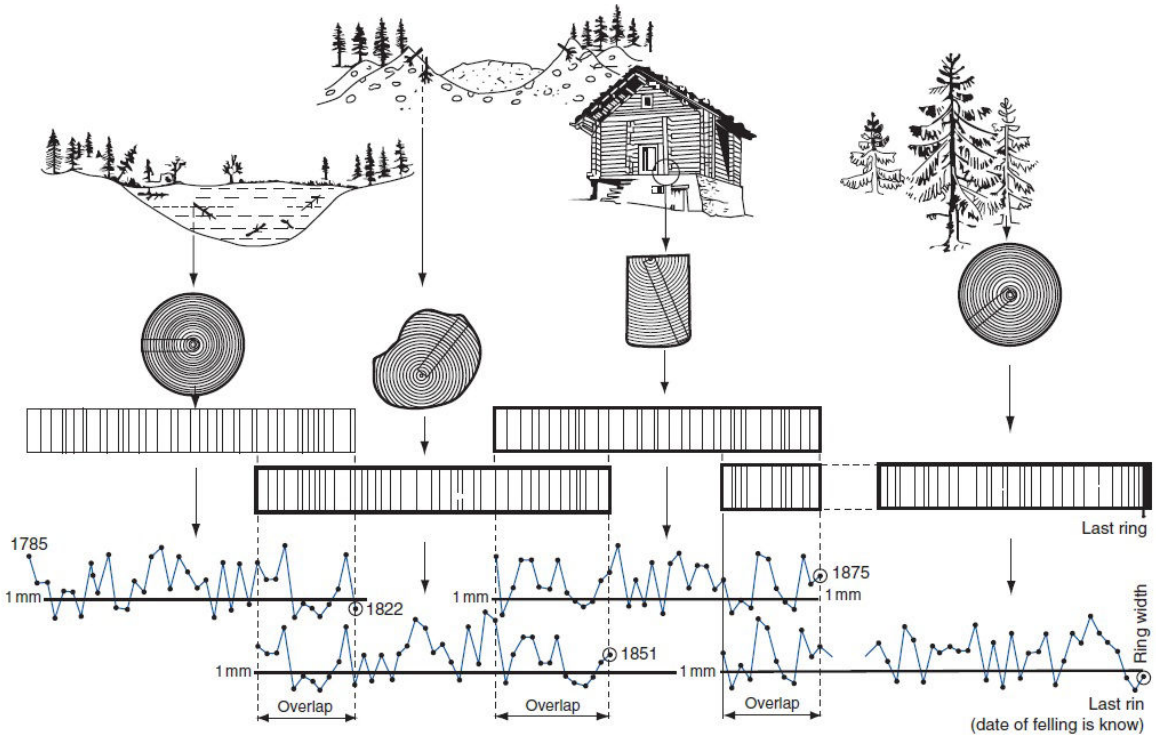

***Figure 3**. Cross-dating of tree-ring series of unknown age from houses or moraines with younger series from living trees illustrated with the raw data as seen on the cross-sections as well as in the form of measured ring-width series (Source: Schweingruber, 1983).*

2.2 Influence of snow avalanches on trees and their reactions to the disturbance

The analysis of geomorphic processes through the study of growth anomalies in tree-ring series is called dendrogeomorphology (Alestalo, 1971; Stoffel et al., 2010). Tree-ring analyses of geomorphic processes are based on the concept of “process-event-response” as defined by Shroder (1978). A mass movement, such as snow avalanches, represents the process. When the geomorphic process impacts a tree (event), the latter will react to this

intrusive event with a characteristic growth response (Bollschweiler, 2007). In the following sections, we present the different types of events caused by snow avalanches, as well as the responses of trees.

2.2.1 Growth injuries (wound) and formation of traumatic resin ducts

Clastic material, logs and other objects (rock, boulders, etc.) transported in snow avalanche mass can hit, abrade and injure the stems of trees growing in the flow path (Figure 4a). When impact locally destroys the cambium, increment cell formation is disrupted and new cell formation ceases in the injured segment of the tree (Stoffel et al., 2010). In order to minimize rot and insect attacks after damage, the injured tree will (i) compartmentalize the wound (Shigo, 1984) and (ii) almost immediately start production of chaotic callus tissue at the edges of the injury (Figure 4c; Schweingruber, 2001). Through the production of callus tissue (Schneuwly et al., 2009a; Stoffel et al., 2010), cambium cells will continuously overgrow the injury from its edges (Figure 4b; Sachs, 1991; Larson, 1994) and ideally can lead to the complete closure of the wound.

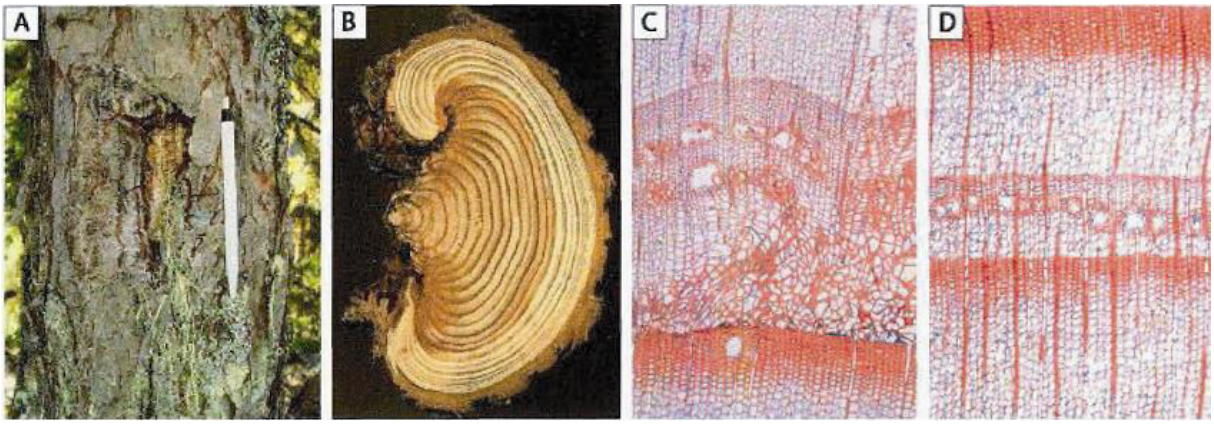

***Figure 4**. Injuries in a Larix decidua Mill.: (a) Injured stem (b) Cross-section with overgrowth starting from the lateral edges of the injury. (c) Callus tissue as observed in the overgrowing cell layers bordering the injury. (d) Tangential row of traumatic resin ducts migrating from earlywood towards later portions of the tree ring with increasing distance from the wound (Source: Bollschweiler, 2007).*

Following injury, tangential rows of traumatic resin ducts (TRD; Bollschweiler et al., 2008; Schneuwly et al., 2009; Stoffel and Hitz, 2008) are produced in the developing

secondary xylem of many conifer species (Pallardy, 2007; Schweingruber, 2007) e.g., European larch (*Larix decidua* Mill.), Norway spruce (*Picea abies* (L.) Karst.) or Silver fir (*Abies alba* Mill.; Figure 4d). They extend both tangentially and axially from the injury (Bannan, 1936; Nagy et al., 2000; Bollschweiler et al., 2008). Depending on the impact energy and the relative size of the damage, an injured tree will concentrate the formation of tree rings to those parts essential for survival and limit growth in other segments in the years succeeding the impact. This may result in missing or partial rings from certain areas of the trunk (Stoffel et al., 2010).

2.2.2 Tilting of trunks

Tilting (or inclination) of trees result from the sudden pressure induced directly by geomorphic impacts or by the associated deposition of snow. The trunk of tilted conifers will always try to regain its vertical position (Figure 5a). The reaction will be most clearly visible in that segment of the tree to which the center of gravity has been moved by the inclination of the stem axis (Mattheck, 1993). In the tree-ring series, eccentric growth will be visible in the cross-section after a tilting event and thus allow accurate dating of the disturbance (Figure 5c).

In coniferous trees, compression wood will be produced on the underside of the trunk. Individual rings will be considerably larger here and slightly darker in appearance as compared to the upslope side (Figure 5b; Stoffel, 2010). The difference in color is due to the much thicker and rounded cell walls of early- and latewood tracheids (Timell, 1986; Schweingruber, 2001; Du and Yamamoto, 2007). In addition to the formation of different types of reaction wood, trees may also respond with reduced growth after tilting (Bollschweiler, 2007).

2.2.3 Decapitation of trees and elimination of branches

The windblast of snow avalanches may decapitate trees or remove branches (Figure 6). The loss of the crown of branches is more common in bigger trees, where trunks have lost their suppleness (Stoffel et al., 2010). Following decapitation, trees react with abrupt radial growth reduction in the years following the impact (Butler and Malanson, 1985). One or

several lateral branches will form a “leader” that replaces the broken crown, resulting in a tree morphology called “candelabra” growth (Stoffel et al., 2005).

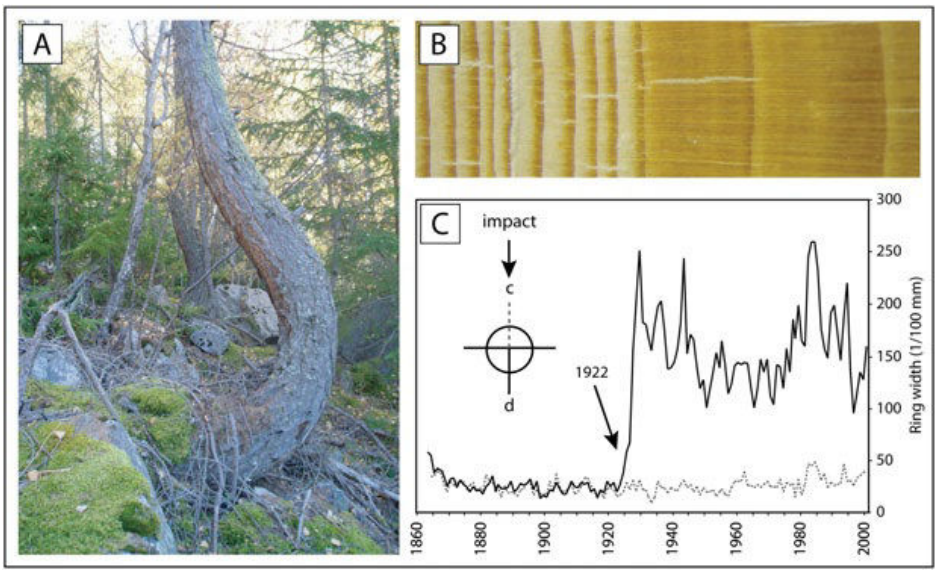

Figure 5. *(a) Tree morphology and (b) cross-sections of a tilted Larix decidua Mill. (c) Increment curves of a Picea abies (L.) Karst. tree (Source: Stoffel and Bollschweiler, 2008).*

Figure 6. *Tree decapitation and branches removing caused by the windblast of a snow avalanche event.*

2.3 Dendrogeomorphic procedure

2.3.1 Field approach

As shown in the previous sections, different types of growth defects can be identified in tree rings. However, a visual inspection of the increment rings will in no case allow determination of the process that was causing the disturbance (Stoffel and Bollschweiler, 2008). Therefore, preceding the sampling of trees in the field, we carried out a detailed identification of geomorphic processes present at the study site as well as an accurate identification of features related to previous events.

The identification of geomorphic processes and features present on a study site started with the examination of topographic sheets, geological maps as well as the interpretation of aerial photographs. In addition, archival data were consulted to obtain data on the time and the locations of occurrence of previous events. This step was a prerequisite in order to select study sites where snow avalanches are the only active geomorphic process present. It allowed us to avoid a misinterpretation of growth disturbances in trees originating from other processes or anthropogenic activity as stated by Stoffel and Bollschweiler (2008).

2.3.2 Sampling design and methods

At an individual site, the choice of sampling design and selection of the trees to be sampled depends on the purpose of the investigation. As our main goal was to maximize the likelihood of identifying the maximum reach of avalanche events, we restricted our sampling area to the lower track of the path and its runout zone. We considered only *L. decidua*, *P. abies* or *A. alba* as these species are known to clearly record the different types of growth disturbances presented in Influence of snow avalanches on trees and their reactions to the disturbance. We carried out a balanced sampling of older and younger trees as recommended by Stoffel et al. (2013). As discrete processes, snow avalanches are more accurately reconstructed with a large sample depth (Corona et al., 2012). Consequently, we realized a systematic sampling of ~100 trees in the runout zone as well as a few target trees damaged at the margin of an event. No preference was given to trees with visible growth

defects, but rather trees were chosen along vertical and/or horizontal transects (Stoffel et al., 2013)

On trees that were selected, the following information were noted: (i) determination of the tree's position within the path using GPS devices; (ii) description and sketches of the visible disturbances in the tree morphology; (iii) position of the samples taken on the stem surface; (iv) diameter measurement at breast height; and (v) data on neighboring trees. A photo documentation of each tree completed information for a better understanding and interpretation of reactions in the laboratory as recommended by Stoffel and Bollschweiler (2008).

Growth disturbances of past events can be analyzed on cross-sections or increment cores. As forests often have protective functions and as they effectively reduce the risk of snow avalanche from reaching transportation corridors and/or inhabited areas (Dorren et al., 2007; Stoffel et al., 2006), trees are sometimes protected and cannot normally be felled for analysis. This is why our tree-ring studies were essentially realized with cores (Figure 7c) extracted with an increment borer (Figure 8). Grissino-Mayer (2003) provides a technical description on how to properly use these increment borers.

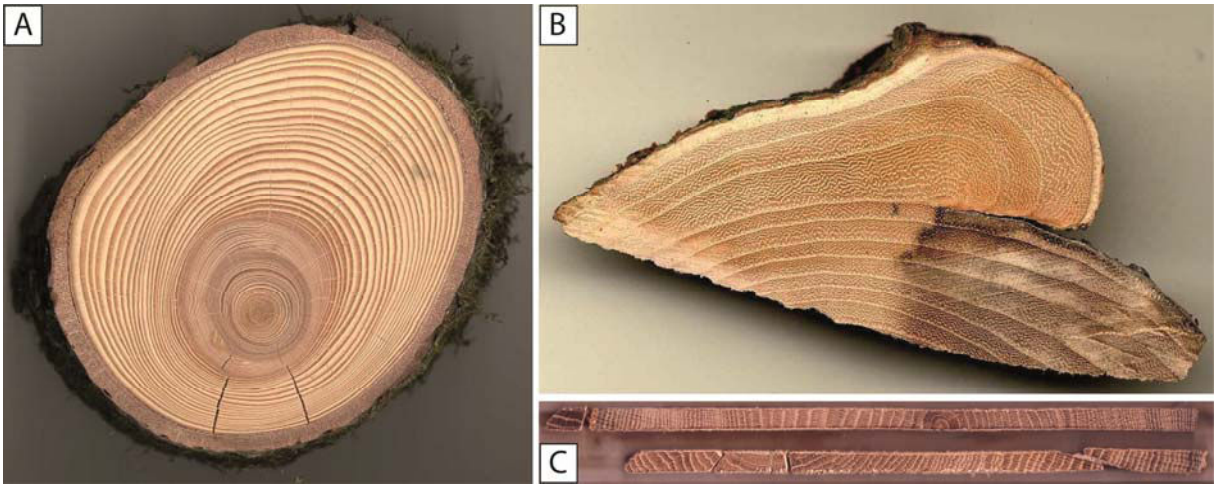

***Figure 7**. Different types of sample extracted from trees. (a) Cross-section (b) Wedge (c) Increment cores.*

The nature of the visible growth defect as observed in the tree's morphology will strongly influence the sampling height, sampling directions and the minimum number of samples to be taken per tree (Stoffel and Bollschweiler, 2008). As it appears more difficult to identify growth disturbances on increment cores, as opposed to cross-sections (Figure 7b), special attention needs to be taken with the sampling position on the tree (Bollschweiler, 2007).

Figure 8*. Increment borer used in forestry to extract cores.*

Decapitated trees were sampled as close to the ground as possible to obtain the largest number of tree rings possible. Two cores were extracted from these trees, one in the direction of the impact and another one on the opposite side of the stem. In the case of tilted stems, we extracted at least two cores per tree at the height of the angle-change, one in the direction of the tilting and the other on the opposite side of the trunk, where the presence of compression wood is expected (Stoffel and Bollschweiler, 2008). Finally, sampling of trees with visible injury consisted in the extraction of at least three cores. Two samples were taken from the lateral edges of the injury where signs of the impact were visible in the tree-ring series, but where no rings were missing due to abrasion

(Bollschweiler, 2007). Figure 9 illustrates the recommended position for the extraction of increment cores in injured trees. In addition, one more sample was taken from the opposite side of the stem.

In some young trees with large visible scars, destructive sampling was selected in some cases and cross-sections (Figure 7b) were lopped off with a hand- or chainsaw, at the location where the injury was the largest. Through this procedure, we facilitated identification of the onset of callus tissue production and TRD formation. Alternatively, wedges (Figure 7a) were sometimes sawn from the overgrowing callus and an increment core extracted from the side opposite of the wound.

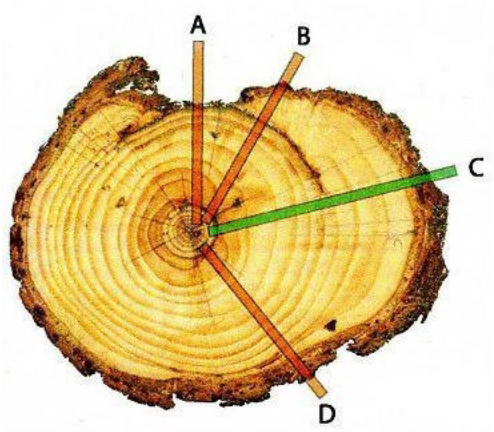

Figure 9*. When sampling injured trees, special attention needs to be addressed to the sampling position. Samples taken (a) inside the wound or (b) from the overgrowing callus tissue will provide an incomplete tree-ring record, as wounds are closed from their edges. (c) Ideally, increment cores are extracted just next to the injury where the presence of overgrowing callus tissue and TRD will allow accurate dating. (d) Cores taken too far away from the wound will not necessarily show signs of the disturbing event and thus prevent dating (Source: Stoffel and Bollschweiler, 2008).*

In addition to the disturbed trees sampled on the site, we selected about 30 undisturbed reference trees from nearby forest stand. For the reference chronology, as a rule, the selection of trees was based on the following two criteria: (i) absence of obvious signs of injuries or diseases to minimize non-climatic influences on ring growth; (ii) oldest trees in order to maximize the age of sampled trees and the length of the tree-ring chronology (Stoffel and Bollschweiler, 2008). In contrast to the disturbed trees, two

increment cores were extracted perpendicular to the slope and at breast height (~130 cm). Finally, we labeled and stored the samples in a receptacle for transport.

2.3.3 Sample preparation, counting of tree-rings and growth disturbance analysis

Increment cores were glued onto a wooden support, with special attention being made to the direction of the wood fibers, which need to be vertical to allow further analysis (Iseli and Schweingruber, 1989). Increment cores, wedges and cross-sections were then sanded. In the laboratory, tree rings were counted, starting from the outermost ring which represents the year of sampling. All samples were analyzed visually, and rings with particular growth characteristics noted on skeleton plots (for more details, see Schweingruber et al., 1990). Special attention was focused on extremely narrow, as well as large, tree rings. In addition, all changes in the wood structure, such as tangential rows of traumatic resin ducts, callus tissue, abrupt growth reduction or compression wood were noted on the skeleton plots. This method primarily assists the cross-dating of samples by identifying false or missing rings (Bollschweiler, 2007). Hence, characteristic years present in a large number of samples (i.e. pointer years; Schweingruber et al., 1990) could be identified. As an example, in *L. decidua*, outbreaks of larch budmoth (*Zeiraphera diniana* Gn.; Figure 10) occur at more or less regular intervals, and are identified in the tree-ring series as very narrow rings with almost no latewood (Baltensweiler and Rubli, 1999; Weber, 1997). The inclusion of larch budmoth chronologies for the study sites was crucial in order to avoid misinterpretation of growth reduction in trees impacted by snow avalanches.

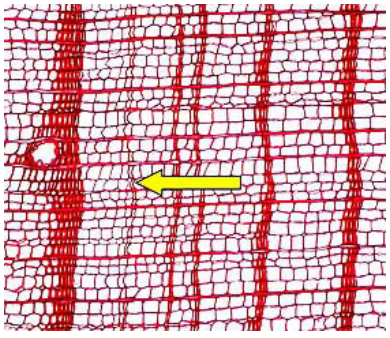

***Figure 10**. Narrow tree ring of larch with regard to larch budmoth outbreak under the microscope (Photo: F. Schweingruber / WSL).*

2.3.4 Reference chronology

In undisturbed trees, growth reductions are driven by climate or the influence of insect outbreaks. Trees belonging to the same species and growing at the same site are considered to be benefiting of suffering from the same environmental conditions and are thus supposed to show the same growth patterns in their tree-ring series. Consequently, the general growth patterns of one species at a specific site can be summarized in a reference chronology (Cook and Kairiukstis, 1990; Schweingruber, 1996).

In a first step, we thus built a reference chronology with the increment cores of the undisturbed reference trees. Ring widths of the increment cores were measured using a LINTAB positioning table coupled to a Leica stereomicroscope (Rinntech, 2014a). In this study, the software used for the measurement of the ring width is called TSAP (Time Series Analyses and Presentation; Rinntech, 2014b). Each ring-width measurement series was then indexed and standardized in order to remove age trends or effects of stand dynamics (Cook and Kairiukstis, 1990; Vaganov et al., 2006). As typical with tree-ring chronologies, sample depth (i.e. the number of measured ring-width series included in the chronology) usually decreases with time before the sampling years (Wigley et al., 1984). In order to guarantee adequacy of sample replication in the early years of the chronology, reference chronologies was limited to the time period with a sample depth of at least five trees (Stoffel and Bollschweiler, 2008).

Ring widths of the disturbed samples were measured as well, and the series were then graphically and statistically compared with the reference chronology. Overall, these comparisons served the separation of insect attacks or climatically driven fluctuations in tree growth from growth disturbances caused by geomorphic processes (Stoffel and Bollschweiler, 2008). Further details on the realization of reference chronologies, the statistical approaches used in dendrochronology or on the improvement of growth series with missing rings can be found in Fritts (1976), Cook and Kairiukstis (1990) or Vaganov et al. (2006).

Once all tree-ring series had been checked and missing rings added, growth curves are analyzed visually to identify the tree's reactions to snow avalanches like the initiation of

abrupt growth reduction (McAuliffe et al., 2006; Schweingruber, 2001). In the case of tilted stems, the growth curve data are analyzed to approximate the moment of the tilting (Fantucci and Sorriso-Valvo, 1999; Figure 4c), but, in addition, the appearance of the cells (i.e. structure of the reaction wood cells) is investigated on the samples as well. Other features like callus tissue overgrowing scars or the presence of tangential rows of traumatic resin ducts (TRD) formed following cambium damage can only be identified through a visual inspection of the cores and cross-sections (Bollschweiler et al., 2008; Perret et al., 2006; Stoffel et al., 2005). Finally, the first decade of juvenile growth should never be included in the analysis, as tree rings in seedlings tend to be more susceptible to snow pressure or the fraying and browsing of ungulates, so that this produces more reaction wood or resin ducts per unit area in general (Stoffel and Bollschweiler, 2008).

All growth reactions identified in the samples are noted in order to identify events. One growth disturbance identified in one single tree will not be considered an event. The reconstruction of past events needs to be based on quantitative (i.e. indices; Dubé et al., 2004; Germain et al., 2005; Butler and Sawyer, 2008; Reardon et al., 2008) or qualitative (Stoffel and Bollschweiler, 2009a) thresholds identified from a number of trees or lines of evidence.

3 Dendrogeomorphology applied to snow avalanche science – a state of the art

The use of damage in trees growing within and along the margins of avalanche paths has become well established in natural hazard research using the principles of dendrogeomorphology as elucidated by Alestalo (1971) and Shroder (1980). Pioneering dendrogeomorphic work on snow avalanche dates back to the late 1960s when Potter (1969) and Schaerer (1972) developed the first reconstructed time series of snow avalanches for sites in North America. In the recent decades, numerous studies have been successfully conducted in both the USA (Butler and Malanson, 1985; Butler et al., 2010; Hebertson and Jenkins, 2003; Reardon et al., 2008) and Canada (Boucher et al., 2003; Dubé et al., 2004; Germain et al., 2005, 2009, 2010; Larocque et al., 2001). Dendrogeomorphic studies of snow avalanches are also becoming increasingly common in Europe, with works in the Pyrenees (Muntán et al., 2004, 2009), the Alps (Casteller et al., 2007; Corona et al., 2010, 2012a, 2012b; Garavaglia and Pelfini, 2011; Stoffel et al., 2013, 2006), the Carpathians (Voiculescu and Onaca, 2013; Voiculescu, 2008; Voiculescu et al., 2012) as well as in Iceland (Arbellay et al., 2013; Decaulne and Sæmundsson, 2008; Decaulne, 2006; Decaulne et al., 2012, 2014) and Norway (Decaulne et al., 2013). Furthermore, a few studies have also been conducted in Argentina (Casteller et al., 2011, 2008; Mundo et al., 2007), Japan (Kajimoto et al., 2004), Turkey (Köse et al., 2009) and Northern India (Laxton and Smith, 2008).

Tree-ring data are used to identify individual avalanche events and to build “event chronologies” at the site level. In general, the morphological criteria examined in trees damaged by snow avalanching are the same as those in other areas of dendrogeomorphology (Butler and Sawyer, 2008; see Influence of snow avalanches on trees and their reactions to the disturbance). These tree-ring responses have been widely utilized in creating to-the-year chronologies of avalanching and seem to be the most accurate (Burrows and Burrows, 1976; Carrara, 1979). Recently, the onset of traumatic resin ducts within annual rings of damaged trees has been used as a new valuable annual dating tool

(e.g., Casteller et al., 2007; Corona et al., 2012b; Larocque et al., 2001; Stoffel et al., 2006; Stoffel and Hitz, 2008). Analyzing these growth disturbances allows the dating and determination of multiple events from the same tree. However, all of these phenomena vary in their expression within the tree, e.g. reaction wood series differ in duration, radial encompassment and degree of development (Stoffel et al., 2010). The choice of ring responses varies among dendrogeomorphic practitioners and with experience, and so some workers have attempted to standardize the quality of tree-ring reactions (e.g., Frazer, 1985; Reardon et al., 2008; Germain et al., 2009; Corona et al., 2012a). However, at this time, there is no agreement among dendrogeomorphologists studying snow avalanche chronologies about which, if any, of these systems of "ring damage rating" should be employed, or indeed if such a semi-quantitative categorization is actually necessary for a skilled dendrogeomorphologist (Butler and Sawyer, 2008).

There is also no easy answer for the related question of what the minimum number of trees would be to ensure a reasonable sampling of the avalanche history of a site (Stoffel et al., 2010). Butler and Sawyer (2008) suggested ten "good" trees could be adequate but obviously 100 trees would be better, while Germain et al. (2010) suggested diminishing returns when sampling more than 40 trees in a track. More recently, Corona et al. (2012a) demonstrated that snow avalanches are more accurately reconstructed with larger sample sizes, and that a plateau apparently exists above ~100 trees.

The question on how to accurately and unambiguously define an event from tree rings also remains under debate. Several authors have used quantitative approaches based on the proportion of disturbed vs. existing trees (index number) to date events to a given year (Butler and Sawyer, 2008), with thresholds used ranging from 10% (e.g., Dubé et al., 2004) to 40% (e.g., Butler and Malanson, 1985). Similar approaches were used by Corona et al.(2010), Germain et al.(2005) and Reardon et al.(2008), which in addition added a minimal number of trees showing GD in a specific year (generally 10) to render dating more accurate (Stoffel et al., 2013). Corona et al. (2012a, 2012b) recommended the use of a variable index number and GD thresholds, which would need to be adjusted to change with sample size so as to capture a maximum of past snow avalanche events without introducing noise.

A dendrogeomorphic avalanche record allows estimation of the minimum frequency of high-magnitude avalanches at the path scale. However, very few works have studied the actual completeness of tree-ring records (Corona et al., 2012a). Hence, stakeholders and engineers show little interest in tree-ring data, waiting for an evaluation of their usefulness for establishing spatio-temporal variations of high-magnitude events and calculations of runout distance. Based on extreme events, i.e., $\geq$ 30 year return interval, runout distances are usually evaluated using physical or statistical models that need to be calibrated with historical and/or filed data (Germain et al., 2010). Statistical runout models known as alpha-beta (Lied and Bakkehøi, 1980; McClung and Lied, 1987) or runout-ratio models (McClung and Mears, 1991; McClung et al., 1989) are easier to use because they are based on topographic parameters. Dendrogeomorphic methods may be very useful for the calibration of such models, but surprisingly very little attention has been paid to tree-ring based avalanche records. So far, only Casteller et al. (2008) attempted to validate numerical simulations of snow avalanches using dendrogeomorphic methods in the Argentinean Andes. Knowledge of avalanche frequencies at the head of runout zones would allow theoretical estimation of effective return interval as a function of position along a given slope (McClung, 2000). Tree-ring methods thus appear as a practical tool for zoning applications when used in conjunction with runout models (Germain et al., 2010).

An additional effort has been increasingly made to examine relationships between climate and snow avalanche activity. Hebertson and Jenkins (2003) as well as Corona et al. (2010) found that mean January snowfall was significantly related to the probability of major avalanche in the western U.S. and the French Alps, respectively. High-magnitude avalanche years were significantly correlated to positive snowpack anomalies in the U.S. (Reardon et al., 2008) or snowy winters, with total snowfall well above average in Canada (Dubé et al., 2004; Germain et al., 2009). Similarly, Casteller et al. (2011) found a significant correlation between years with large avalanche activity and abundant precipitation from May to October in Argentina. All these studies have provided information on the link between climate and avalanche occurrence at the local scale. However, given that tree-ring reconstructions may miss a significant number of avalanches and their poor temporal

(annual) resolution, it seems necessary to evaluate the relevance of climate-avalanche relationships inferred from tree-ring chronologies.

4 Study sites

Fieldwork was conducted at different sites in the Rhône-Alpes and Provence-Alpes-Côte d'Azur regions of the French Alps. The selection of sites was driven by the presence of well localized starting zone of snow avalanches, a straight avalanche path, the existence of stopping zones in forests as well as by the availability of historical archives on past avalanche activity. Five avalanches paths were selected, the *Avalanche des Pylônes* and *Pèlerins* paths near Chamonix-Mont-Blanc (Haute-Savoie), the *Ressec* path near Lanslevillard (Savoie), the *Château Jouan* path near Montgenèvre (Hautes-Alpes) and the *Ourcière* path near La Grave (Hautes-Alpes). An overview of the different study sites is provided in Figure 11. Details of the individual study sites are provided in the different chapters.

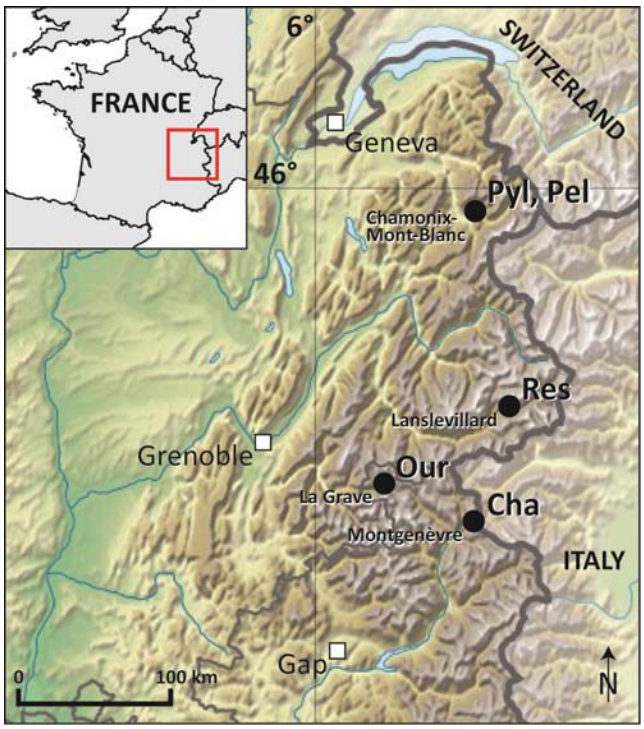

***Figure 11**. Study sites analyzed in this PhD thesis are located in the northern part of the French Alps: Pyl = Avalanche des Pylônes; Pel = Pèlerins; Res = Ressec; Our = Ourcière; Cha = Château Jouan.*

CHAPTER B

IDENTIFICATION OF PAST SNOW AVALANCHE ACTIVITY

IDENTIFICATION OF PAST SNOW AVALANCHE ACTIVITY

Romain Schläppy[1], Vincent Jomelli[1], Delphine Grancher[1], Markus Stoffel[2,3], Christophe Corona[2,4], Daniel Brunstein[1], Nicolas Eckert[5], Michaël Deschatres[5]

"A new tree-ring-based, semi-quantitative approach for the determination of snow avalanche events: use of classification trees for validation"

[1] *Laboratoire de Géographie Physique, Université Paris 1 Panthéon-Sorbonne, UMR 8591 CNRS*
[2] *Dendrolab.ch, University of Berne, Institute of Geological Sciences*
[3] *Climatic Change and Climate Impacts, University of Geneva, Institute for Environmental Sciences*
[4] *Laboratoire de Géographie Physique et Environnementale, Université Blaise Pascal Clermont-Ferrand 2, UMR 6042 CNRS*
[5] *Irstea, UR ETGR Érosion Torrentielle Neige et Avalanches / Université Grenoble Alpes*

Published in *Arctic, Antarctic, and Alpine Research*, Vol. 45(3), p. 383—395
Submission: 16 August 2012, acceptance: 20 February 2013

Abstract
On forested paths, dendrogeomorphology has been demonstrated to represent a powerful tool to reconstruct past activity of avalanches, an indispensable step in avalanche hazard assessment. Several quantitative and qualitative approaches have been shown to yield reasonable event chronologies but the question of the completeness of tree-ring records remains to be rather debated. Here, we present an alternative semi-quantitative approach for the determination of past snow avalanche events. The approach relies on the assessment of the number and position of disturbed trees within avalanche path as well as on the intensity of reactions in trees. In order to demonstrate that no bias was induced by the dendrogeomorphic expert, we carry out a statistical evaluation (Classification and regression trees, or CART) of the approach. Results point to the consistency and replicability of the procedure and to the fact that the approach is not restricted to the identification of high-magnitude avalanches. Evaluation of the semi-quantitative approach is illustrated on a well-documented path in Chamonix, French Alps. For the period 1905—2010, comparison between the avalanche years recorded in a substantial database (Enquête Permanente sur les Avalanches, or EPA) and those defined with dendrogeomorphic techniques shows that the avalanche record reconstructed from tree-ring series contains 38% of the observed events.

Keywords
snow avalanche, dendrogeomorphology, event determination, semi-quantitative approach, CART, hazard assessment, French Alps

1 Introduction

Documenting past avalanche activity represents an indispensable step in avalanche hazard assessment (Ancey et al., 2004). Nevertheless, (i) archival records of past avalanche events do not normally yield data with satisfying spatial and temporal resolution and (ii) precision concerning runout distance (Casteller et al., 2008; Keylock et al., 1999; Lied and Bakkehøi, 1980) and/or avalanche type is generally poorly defined (Corona et al., 2012a). In addition, historic documentation is most often (iii) biased toward events that caused damage to structure or loss of life on the one hand and (iv) undersampled in unpopulated areas on the other hand (Bollschweiler et al., 2011).

On forested paths, dendrogeomorphology (Alestalo, 1971; Stoffel et al., 2010) has been demonstrated to represent a powerful tool to reconstruct past activity of avalanches with annual resolution and for periods covering the past decades to centuries (Butler and Sawyer, 2008). External scars, reaction wood, growth asymmetry and tangential rows of traumatic resin ducts have been the most frequently used avalanche indicators since they allow the dating and determination of multiple events from the same tree (Luckman, 2010). As all of these growth disturbances (hereafter referred to as GDs) vary in their expression within the tree (e.g. duration, radial encompassment and degree of development), a series of graduated classes allows a discrimination of features that are clearly associated with avalanche activity, so as to differentiate them from disturbances which can be induced by a variety of other, non-geomorphic factors (Corona et al., 2012a). Different empirical rating systems have been proposed and improved in the past ten years (Corona et al., 2012a; Dubé et al., 2004; Reardon et al., 2008), but the question of how accurately an event or a time series of events can be reconstructed from tree-ring records remains debatable.

Some authors used quantitative methods based on the proportion of disturbed trees (i.e. index number) to date an event in a given year (Butler and Sawyer, 2008). Dubé et al. (2004), Germain et al. (2005), Pederson et al. (2006) and Reardon et al. (2008) used an index number but also took account of the total number of disturbed trees. Conversely, Stoffel et al. (2006) used a qualitative approach where the nature and spatial distribution of trees with GDs were analyzed visually to determine years with avalanche activity. These approaches

have provided reasonable event chronologies. Nevertheless, as Corona et al. (2012a) emphasized, quantitative methods tend to underestimate activity due to the very stringent and arbitrary thresholds used that are better adapted to the determination of high-magnitude events. On the other hand, qualitative approaches may be very useful in cases with a limited sample depth, either on the temporal or on spatial domains, depending strongly on the context at the site (Luckman, 2010).

Recently, Corona et al. (2012a) evaluated the potential of tree-ring records to produce a dendrogeomorphic time series on an extensively and accurately documented avalanche path in the Chamonix valley (French Alps). The authors defined optimal values for the number of GDs and the index number such that the match between avalanches documented in archival data (Enquête Permanente sur les Avalanches, hereafter referred to as EPA[1] and those observed in the tree-ring records was maximized. Their study pointed out the importance of a large sample depth (~100 trees) and suggested adaptation of the thresholds (related to the index number and the number of disturbed trees) with increasing/decreasing sample depth. However, the thresholds they used depend on the nature and amount of data gathered in this particular path and cannot be applied to other sites.

To compensate for these difficulties, a semi-quantitative approach is developed in this paper. The aim of this study therefore was to (i) promote this new approach for the determination of past snow avalanche years based on the analytical skills of the dendrogeomorphic expert and to (ii) demonstrate its consistency and replicability using a Classification and regression trees (CART) approach; to (iii) highlight the high potential of this approach in terms of past avalanche activity reconstruction; and to (iv) validate its reliability in a very well-documented path.

[1] see 2.4 Historical archives, below.

2 Study area and historical archives

This study was conducted in the French Alps, in the Rhône-Alpes and Provence-Alpes-Côte d'Azur regions. Three avalanche paths were selected, the *Pèlerins* path near Chamonix-Mont-Blanc (Haute-Savoie), the *Ressec* path near Lanslevillard (Savoie) and the *Château Jouan* path near Montgenèvre (Hautes-Alpes; Figure 12).

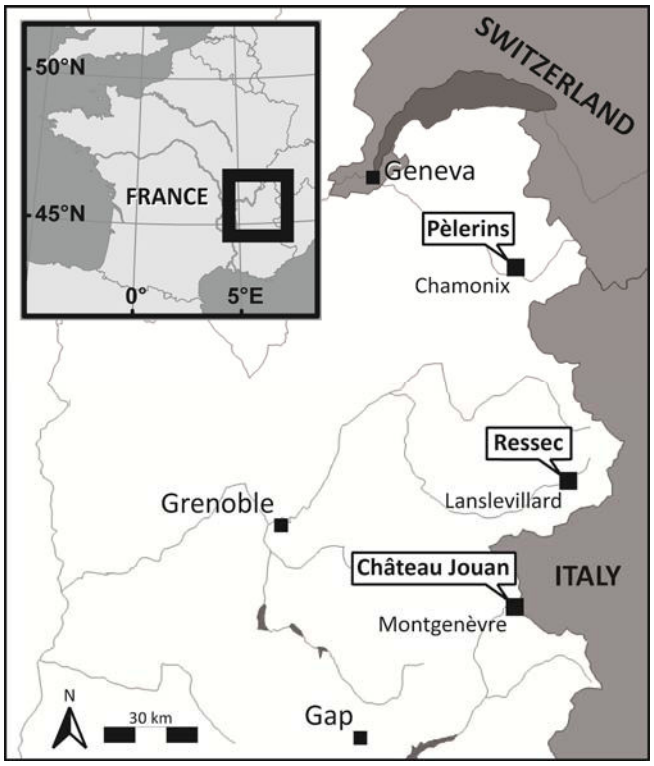

***Figure 12**. Location of the three study sites (Pèlerins, Ressec and Château Jouan paths) in the French Alps.*

2.1 Pèlerins path

The *Pèlerins* avalanche path on the north-facing slope of the Arve Valley dominates the hamlet of Les *Pèlerins*, located 2 km southwest of downtown Chamonix (Table 1). It passes under the Aiguille du Midi cable car (*Les Pèlerins—La Para*), which was constructed for the first Winter Olympics in 1924. Snow avalanches are commonly triggered from a starting zone

located between 3650 and 2750 m asl where an orthogneissic rockwall is partly covered by the *Pèlerins* glacier. The access road to the Mont Blanc Tunnel crosses the runout zone several times below 1275 m asl (Figure 13a). This tunnel is a major north-south connection for Europe and two million vehicles use this road each year, of which 33% are trucks (Corona et al., 2012a).

The inner zone of the track is colonized by dense shrubs and shade-intolerant pioneer tree species with flexible stems. Toward the outer zone, *L. decidua* and *P. abies* are becoming dominant. Located in the upper mountain stage, the runout zone is covered by a dense forest dominated by *P. abies*. According to the data from the nearby meteorological station of Chamonix (1054 m asl), annual (DJF) temperature is 6.6°C (−2.5°C) for the period 1935−1990 and the annual (DJF) precipitation amounts to 1262 mm (311 mm) for the period 1934−1990.

Path name	Maximum elevation (m)	Minimum elevation (m)	Path length (m)	Mean slope angle (degree)	Starting zone area (ha)	Runout zone area (ha)	Solar exposure
Pèlerins	3650	1085	4900	35	110	70	north
Ressec	3060	1770	2550	30	55	15	north
Château Jouan	2500	1700	1700	29	12	7	north

***Table 1**. Site-related characteristics in the Pèlerins, Ressec and Château Jouan paths. The three paths exhibit quite different features although their solar exposure and mean slope are rather similar. The Pèlerins path represents a very-extended avalanche path, while the Ressec and Château Jouan paths are smaller in size.*

2.2 *Ressec* path

The *Ressec* avalanche path on the north-facing slope of the Arc Valley dominates the hamlet of Chantelouve, located 3 km northeast of downtown Lanslevillard (Table 1). Snow avalanches are commonly triggered from a starting zone located between 3060 and 2300 m

asl. A 5-m deep ephemeral torrent that cuts into the runout zone may have a channelizing effect on snow avalanches (Figure 13b).

The avalanche path is located in a zone composed of lustrous schists resulting in particularly poor soils. As a consequence, woody vegetation is mostly absent above 2000 m asl, except for a few pioneering *L. decidua*. The runout zone is covered by a dense forest dominated by *P. abies* and *L. decidua*, *A. alba* is scarce (1%). The nearby meteorological station of Lanslebourg-Mont-Cenis (1720 m asl) indicates annual (DJF) temperatures of 2.4°C (−4.3°C) and annual (DJF) precipitation of 995 mm (393 mm) for the period 1959−1973.

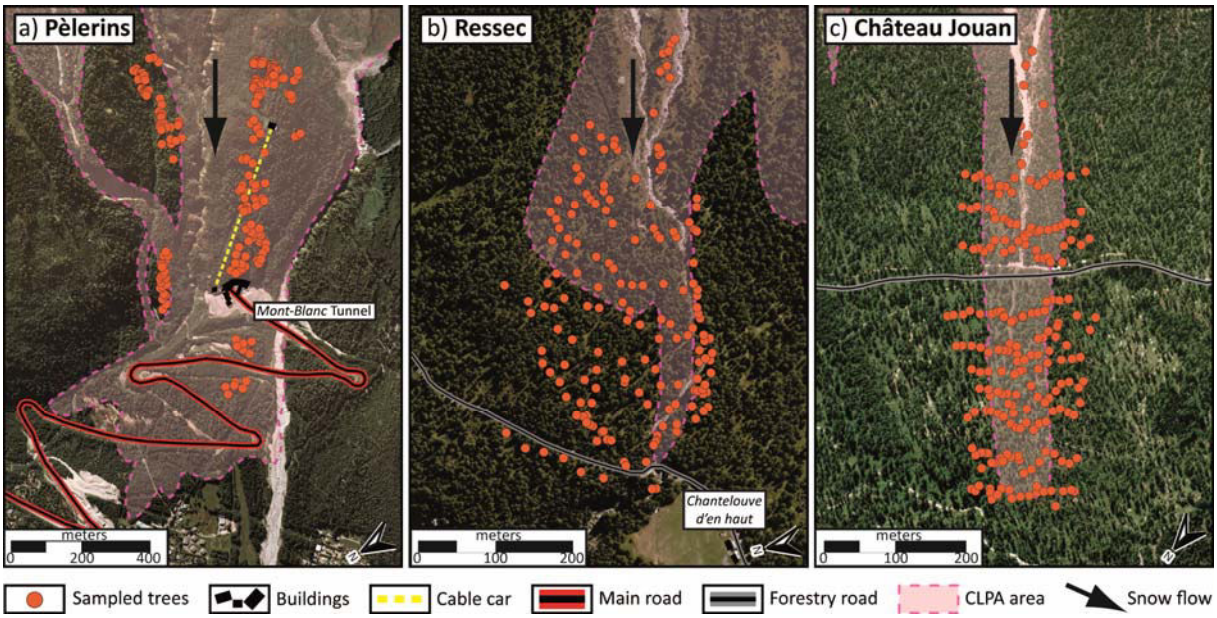

***Figure 13**. Location of sampled trees in the (a) Pèlerins, (b) Ressec and (c) Château Jouan snow avalanche paths. The CLPA (Carte de Localisation des Phénomènes d'Avalanche) represents historical spatial limits of snow avalanches derived from technical reports and photographs.*

2.3 *Château Jouan* path

The *Château Jouan* avalanche path on the north-facing slope of the Durance Valley is located 2 km southwest of downtown Montgenèvre (Table 1). Snow avalanches are commonly triggered from a starting zone located between 2500 and 2000 m asl.

The path of *Château Jouan* is located in a zone composed of Triassic dolomites and limestones. *L. decidua* is the only tree species present in this area (Figure 13c). According to the data from the nearby meteorological station of Briançon (1212 m asl), annual (DJF) temperature was 8.0°C (0.4°C) and the annual (DJF) precipitation amounted to 755 mm (174 mm) for the period 1970—2004.

2.4 Historical archives

In France several documentary sources provide information about past snow avalanche events. In the EPA, the avalanche history of ~3900 recognized paths in the French Alps and the Pyrenees with a length > 200 m is recorded since the early 20th century at most sites (Mougin, 1922). However, only avalanche events reaching a determined observation threshold have to be recorded. The EPA therefore represents a very substantial database and provides a huge quantity of information about past snow avalanches. These data have proved useful for risk assessment at the local (Eckert et al., 2007b, 2010c) and regional scales and for the quantification of inter-annual variation of avalanche activity. EPA records are usually complemented with a map (Carte de Localisation des Phénomènes Avalancheux, hereafter referred to as CLPA) in which the release zones and maximal runout extent for different types of snow avalanches are recorded. Additional information can be found in other archives such as technical reports, aerial and terrestrial photographs, incidental narratives, diaries, municipal archives and paintings (Corona et al., 2012a).

As a result of the potential threat to infrastructure, the *Pèlerins* avalanche path has received considerable attention in the past and activity has been documented continuously and with unusual accuracy, especially since the beginning of the 20th century. In total, 47 avalanche years have been documented for the period 1779—2010, with most of them (37) during the EPA time extent 1905—2010. Conversely, the *Ressec* and *Château Jouan* paths only threaten forestry roads which are used by a very limited number of people during winter season. As a result, 20 and 19 events, respectively, have been recorded in the EPA in these two paths for the period 1907—2010. The lack of a significant element at risk may have led to a less accurate survey in these areas, especially during the first half of the 20th century,

indicating that the real activity was certainly largely underestimated. No other historical archives have been found for these two avalanche paths.

3 Tree-ring based snow avalanche event chronologies

3.1 Dendrogeomorphic analysis

For this study, sampling areas were restricted to the lower track and runout zone of the paths. The goal was to maximize the likelihood of identifying the maximal extent of avalanche events. Based on the CLPA, we also aimed to select trees close to the recorded lateral limits. All samples were extracted from conifers (*L. decidua*, *P. abies* and *A. alba*). We used impact scars (Corona et al., 2013; Trappmann and Stoffel, 2013), the appearance of callus tissue (Schneuwly et al., 2009a, 2009b) and tangential rows of traumatic resin ducts (referred hereafter as to TRD; (Bollschweiler et al., 2008; Stoffel and Hitz, 2008; Stoffel, 2008), the initiation of compression wood (Timell, 1986) and abrupt growth reductions (Butler and Malanson, 1985) to determine the potential occurrence of avalanches. Selection of trees, sampling design as well as sample preparation and analysis followed the procedures well described in (Stoffel and Bollschweiler, 2008).

3.2 Determination of snow avalanche years

In a next step, intensities were assigned to GDs in order to emphasize features that are clearly associated with avalanche activity and to discriminate these from disturbances possibly induced by other factors (such as creeping snow, strong wind, etc.). We used a rating system (Table 2) similar to those described in the recent literature (Corona et al., 2012a; Germain et al., 2005; Reardon et al., 2008) and based on the visual quality of the evidence of reactions within each sample. With such an intensity scale, we assigned significant weight (classes 4 and 5) to GDs that were initiated by strong external forces directly related to avalanche flows. Class 3 is an intermediate category mainly used for compression wood which was clearly visible in the samples but which could, under certain circumstances, stem from other processes (i.e. creeping snow). Classes 1 and 2 point to reactions in the wood which can stem from disturbances but where an unambiguous attribution to a snow avalanche was not possible (Table 2).

GD data from individual trees were then summarized in a geographic information system with ArcGIS (ESRI, 2014). For each year of the chronology, trees that were living (i.e. trees which were present in a given year considering their age as obtained from sample analysis) were plotted according to their geographic coordinates. Disturbed trees were highlighted using a color gradient corresponding to the intensity of reaction. However, only disturbances of intermediate or strong intensity (classes 3—5) were considered for avalanche year assessment. As mentioned before, intensity classes 1 and 2 could not unambiguously be attributed to snow avalanche activity. The determination of snow avalanche years was based on a visual evaluation of the resulting maps and focused on several assessment criteria.

Intensity	Growth disturbances characterization
Class 5	Impact scars or dense TRD which can undoubtedly be associated to a scar.
Class 4	Obvious TRD (with some gaps in the rows), presence of callus tissue, obvious compression wood being formed for more than 3 successive growth years or abrupt growth reduction lasting for at least 5 years (associated with stem breakage).
Class 3	Obvious compression wood being formed for 1—3 successive growth years following disturbance.
Class 2	Compression wood present but not well defined or growth reduction lasting for less than 5 years.
Class 1	Scattered TRD.

***Table 2**. Growth disturbance intensity scale. This scale emphasizes features that are clearly associated with avalanche activity and discriminates against disturbances which may be induced by other factors. Thresholds related to growth reduction and compression wood have been defined based on the visual quality of these reactions within each sample. TRD = tangential rows of traumatic resin ducts.*

In the expert approach, each map (one per chronology year) was assessed separately by analyzing simultaneously the number of disturbed trees present, the proportion of strong intensity GDs (which are undoubtedly related to past avalanche activity) compared to intermediate ones as well as their distribution within the path. A minimum of three disturbed trees was required for a year to be qualified as an avalanche year. This threshold

aimed at minimizing the risk that one or two GD caused by other factors (possible influence of felling activity, scars induced by ungulate browsing) could mistakenly be attributed to avalanches. Years showing several GDs of strong intensity were unequivocally identified as avalanche years. For years where only few disturbed trees were observed, special attention was given to spatial criteria allowing the expert to determine whether the pattern was clustered or scattered. This allowed distinction between years with a dispersed pattern of reacting trees, where disturbance was not apparently induced by snow avalanches, and years where disturbed trees were grouped on the slope and thus attested to the occurrence of an avalanche. In the latter cases, only years with disturbed trees located in the upper track were assessed as avalanche years. Conversely, years showing a few disturbed trees in the runout zone but very few or no GDs in the trees located higher in the track were not considered avalanche years. This was justified by the fact that all avalanches that disturbed trees in the runout zone should also have been recorded in some of the trees located in the upper track. Thus, although the assessment of avalanche years resulted from an evaluation of criteria based on field knowledge, the expert remained as objective as possible when assigning a score (avalanche/non-avalanche) to each year of the chronologies.

3.3 Growth disturbances and past avalanche activity

Sampling campaigns were carried out during the summers of 2010 and 2011. A total of 209, 168 and 210 trees, respectively, were sampled in the *Pèlerins*, *Ressec*, and *Château Jouan* paths (Figure 13a—c). The samples from the *Pèlerins* path were those analyzed by Corona et al. (2012). All GDs observed in the latter path were reclassified according to the rating system used in the present study (Table 2). Sample analysis permitted identification of 660, 591 and 491 GDs, respectively (Table 3). In the *Pèlerins* path, growth reductions were the most frequently observed type of GD (56%), whereas TRD were predominantly identified in the *Ressec* (42.5%) and *Château Jouan* (46.5%) paths. Concerning GD intensity, class 2 was predominant in the *Pèlerins* (36%) and *Ressec* (33%) paths. By contrast, class 4 was most present (36.5%) in the *Château Jouan* path (Table 3).

Based on the procedure described in the previous section, 34 avalanche years were reconstructed in the *Pèlerins* path for the past 240 years (1771—2010). In the *Ressec* and

Château Jouan paths, a total of 24 and 17 avalanche years have been identified for the period 1870—2010 and 1799—2010, respectively.

	Pèlerins		*Ressec*		*Château Jouan*	
Sample analysis	Number	Percentage	Number	Percentage	Number	Percentage
Sampled trees	**209**	**-**	**168**	**-**	**210**	**-**
Sample type	**452**	**100%**	**401**	**100%**	**438**	**100%**
Cross section	0	0%	59	15%	63	14%
Increment core	452	100%	342	85%	375	86%
Growth disturbances	**660**	**100%**	**591**	**100%**	**491**	**100%**
a Impact scars	0	0%	28	5%	35	7%
TRD	115	17%	251	42.5%	229	46.5%
Compression wood	150	23%	155	26%	156	32%
Growth suppression	368	56%	155	26%	63	13%
Callus tissue	27	4%	2	0.5%	8	1.5%
b Intensity class 5	142	22%	69	11.5%	49	10.0%
Intensity class 4	219	33%	140	23.5%	183	36.5%
Intensity class 3	50	8%	105	18%	66	13.0%
Intensity class 2	240	36%	195	33%	110	22.0%
Intensity class 1	9	1%	82	14%	83	18.5%

***Table 3**. Sample depth, (a) types, and (b) intensity of growth disturbances in the Pèlerins, Ressec and Château Jouan paths. TRD = tangential rows of traumatic resin ducts.*

4 Statistical evaluation of the semi-quantitative approach

4.1 Classification trees and characterization of assessment criteria

The semi-quantitative approach used for the determination of snow avalanche years is based on a dendrogeomorphic expert approach. Each year of the tree-ring chronology is assessed in a similar way and based on the same criteria. To demonstrate that no bias is introduced by the expert, we assessed the consistency of approach statistically. For this purpose, a Classification and regression tree (hereafter referred to as CART; Breiman et al., 1984; Ripley, 1996) approach was used. CART is a statistical tree-building technique that explains the variation of a response variable using a set of explanatory independent variables, so-called predictors. The method is based on a recursive binary splitting of the data into mutually exclusive subgroups within which objects have similar values for the response variable. At each split, the CART imposes a "goodness of split criterion", similar to the method of least squares, so as to optimize splitting for each variable and ultimately minimize the overall probability of misclassifying the response variable. The CART adds variables until classification trees have grown to a maximum size and, in the final step, removes the variables that do not add any predictive power to the model. This allows the CART to select the best model adjusting the number of variables used in the analysis (for more details see Breiman et al., 1984).

In the present work, the response variable was characterized by the score assigned by the dendrogeomorphic expert during its assessment. Each year of the three tree-ring chronologies was thus classified as an avalanche or non-avalanche year. Explanatory variables were then characterized based on the assessment criteria. The first variable chosen was $GD_{tot}(t)$, i.e. the total number of GDs (classes 3 to 5) in each year t. We then calculated $GD_i(t)$ i.e. the number of GDs from each class of intensity i, in each year t. To have an idea of the proportion of GDs from each class related to the total number of GDs present in a given year, we computed:

$$GD_i^*(t) = \frac{GD_i(t)}{GD_{tot}(t)} \quad (1)$$

As both sample depth and the number of GDs decrease in the past, a standardization procedure was applied to take account of all values in the dataset and to avoid potential bias in the data. We therefore included the annual standardized anomaly for each intensity class into the analysis:

$$GD_i'(t) = \frac{(GD_i(t) - \overline{GD_i})}{\sigma_i} \quad (2)$$

where:

$$\overline{GD_i} = \frac{\sum_{t=1}^{T} GD_i(t)}{T} \quad (3)$$

$$\sigma_i = \sqrt{\frac{\sum_{t=1}^{T} (GD_i(t) - \overline{GD_i})^2}{T}} \quad (4)$$

and T corresponds to the extent of each tree-ring chronology.

The last criteria on which the dendrogeomorphic expert focused for the determination of avalanche years were the position and spread of disturbed trees along the path. No universally applicable rule could be defined for the characterization of the different patterns of GD location. Therefore, spatial criteria were not used in the statistical evaluation of the approach.

4.2 Consistency of the approach

Considering the seven characterized explanatory variables (GD_{tot}, GD_3^*, GD_4^*, GD_5^*, GD_3', GD_4', GD_5'), we evaluated consistency of the scores assigned by the dendrogeomorphic expert to each year of the tree-ring chronologies. Practically, data from both the *Pèlerins* and *Ressec* paths were combined to create a sufficiently large and representative dataset. Only

years where at least one GD was present in the tree-ring record were considered, since, from a dendrogeomorphic perspective, years without GD could not show evidence of a snow avalanche event. The combined dataset yielded data for 213 years. Using the 'rpart' routine (Therneau and Atkinson, 1997) of the R package (R Development Core Team, 2011), the classification tree was calibrated with the scores assigned (avalanche/non-avalanche year) as a response variable and based on values resulting from the explanatory variables. To test the performance of the model, we then carried out repeated random sub-sampling validation, where the dataset is randomly partitioned into training (90% of all years) and validation subsets (remaining 10%). For each of these splits, the model was fitted to the training subset and predictive accuracy was assessed using the validation subset (Breiman et al., 1984; Kohavi, 1995). The results were then averaged over the splits for 100 iterations. Cross-validation classification probabilities indicated that the model correctly classified the years in 89% of the cases.

4.3 Replicability of the approach based on an independent path

Illustration of the replicability of our approach represented the last step of the statistical evaluation. This procedure was required to demonstrate that the expert's assessment does not depend on site-related characteristics of a given path and can therefore be applied elsewhere. We therefore applied the classification tree resulting from the above-mentioned combined dataset (from both the *Pèlerins* and *Ressec* paths) to predict avalanche/non-avalanche years in an independent path. The calibrated model pointed to the prevalence of the total number of GDs in the assessment since the corresponding variable GD_{tot} was the first classification split (Figure 14). It also permitted to emphasize a hierarchy within the classification splits, from variables related to strong intensity (GD_5^*, GD_5') to weaker ones (GD_4^*, GD_3^*).

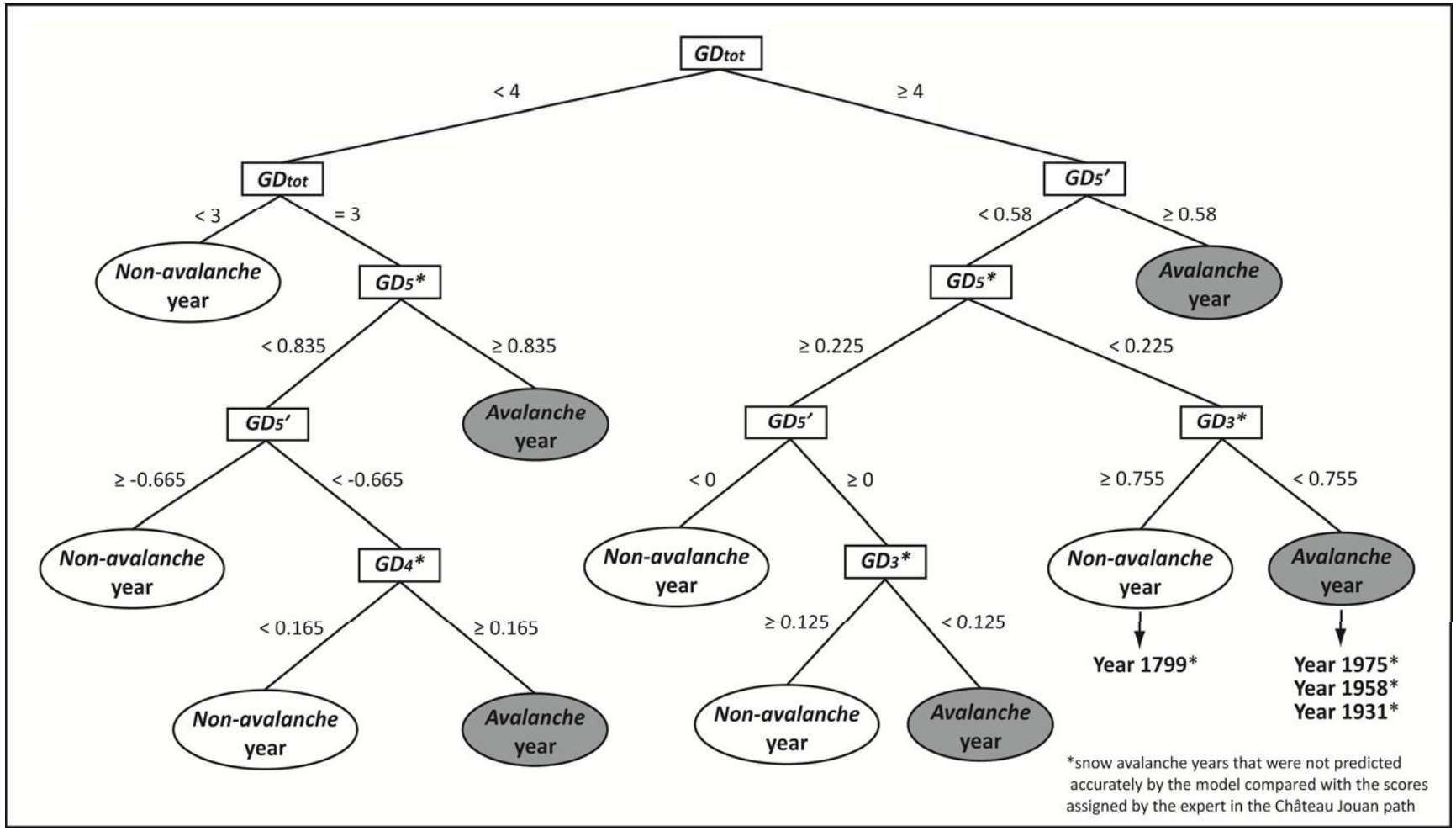

***Figure 14**. Classification tree calibrated from a combined dataset composed of tree-ring chronology years from both the Pèlerins and Ressec paths. It was used to predict scores (avalanche/non-avalanche years) in the Château Jouan path in order to demonstrate replicability of the semi-quantitative approach.*

Based on this classification tree, we predicted scores in the *Château Jouan* path. Comparison of the scores (avalanche/non-avalanche year) predicted and those initially assigned during assessment in this path was summarized in a confusion matrix. Results show that only four out of 128 years (3%) were incorrectly predicted (Table 4). A correct prediction means that the score assigned by the dendrogeomorphic expert is the same as the one predicted by the model. In fact, three years were considered non-avalanche years by the expert whereas the classification tree considered them as avalanche years (Figure 14 & Figure 15). Conversely, one year was considered an avalanche year during the expert's assessment and was predicted as non-avalanche year by the model.

		Scores predicted by the model		Total
		non-avalanche	*avalanche*	
Scores assigned by the expert	*non-avalanche*	108	3	111
	avalanche	1	16	17
%	*non-avalanche*	97.3	2.7	100
	avalanche	5.9	94.1	100

Table 4*. Confusion matrix of assigned and predicted avalanche occurrences in the Château Jouan path. The dendrogeomorphic expert initially assigned scores during assessment procedure. Predicted values result from the classification tree calibrated from a combined dataset composed of tree-ring chronology years from both Pèlerins and Ressec paths.*

4.4 An efficient tool to complement historical avalanche chronologies

The reliability of our procedure was tested at *Pèlerins* path where we compared results from dendrogeomorphic assessment with data recorded in the EPA and historical archives (Figure 16). For the period covered by the EPA (1905−2010), our approach allowed reconstruction of 14 out of 37 (38%) documented years. Furthermore, four undocumented events have been identified in 1932, 1948, 1993 and 1995. In a second step, comparison was realized for the entire period covered with tree-ring records (1771−2010), for which 18 out

of 47 (38%) documented events were reconstructed. A total of 16 avalanches could be added to the historical chronology (Figure 16).

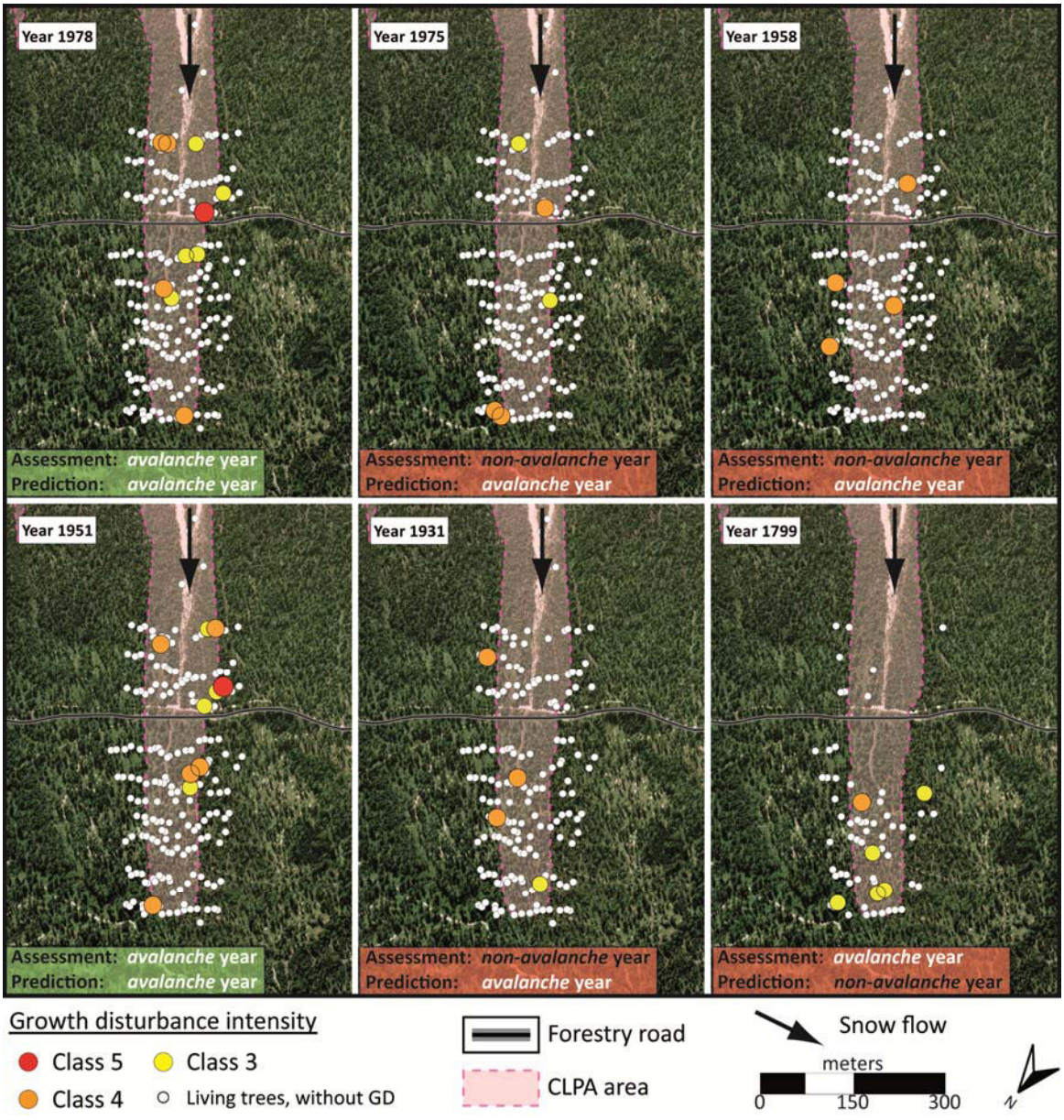

Figure 15. *Spatial distribution of disturbed trees for six years in the Château Jouan path. Initially, scores (avalanche/non-avalanche year) were assigned using "expert procedures" (see text for details). Scores were subsequently predicted using a classification tree calibrated from a combined dataset composed of tree-ring chronology years from both the Pèlerins and Ressec paths. Two examples (green underlined) represent years correctly predicted by the model. Conversely, four years (1975, 1958, 1931, and 1799) were incorrectly predicted (red underlined). These represent only 3% of all predicted years. GD = growth disturbance. CLPA areas represent historical limits of snow avalanches derived from technical reports and photographs.*

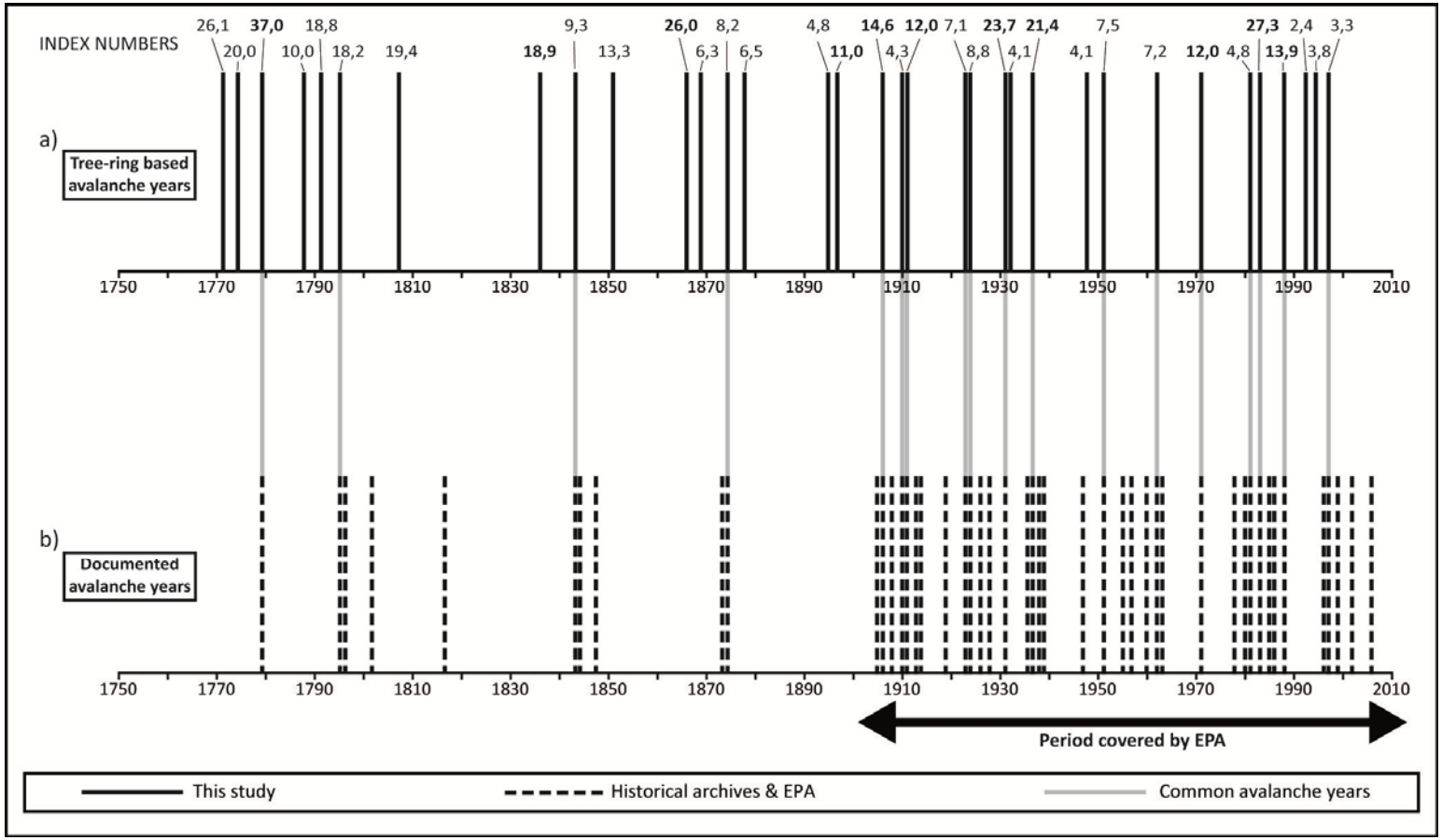

Figure 16. *Snow avalanche years in the Pèlerins path. Comparison of (a) tree-ring based reconstructed years from this study with (b) documented avalanche years from historical archives and the EPA database. EPA = Enquête Permanente sur les Avalanches. Index numbers correspond to the percentage of disturbed trees in a given year. Bold values emphasize years where both the fixed thresholds of GDs ≥ 10 and It ≥ 10 were reached.*

5 Discussion and conclusion

5.1 Contribution of the spatial information in avalanche assessment

The use of tree rings for the reconstruction of chronologies of snow avalanching has been progressively recognized over the past decades and has become popular worldwide in the early 2000s with studies in Canada (Dubé et al., 2004; Germain et al., 2010), the Alps (Casteller et al., 2007; Corona et al., 2010, 2012b; Kogelnig-Mayer et al., 2011; Stoffel et al., 2006), Pyrenees (Muntán et al., 2009) and South America (Casteller et al., 2011). Although all of these studies were based on the same fundamental dendrogeomorphic principles, the way to determine avalanche years as well as the criteria used varied strongly from one study to the other, depending on the objective pursued. In our approach, we considered only GDs of intermediate and strong intensities for the identification of avalanche years. We therefore minimized the risk of introducing bias due to GDs which were caused by external factors.

Most of the authors selected the use of arbitrary quantitative thresholds (i.e., Butler and Sawyer, 2008; Germain et al., 2005; Reardon et al., 2008) and attempted to track high-magnitude events (Dubé et al., 2004; Germain et al., 2009), whereas Stoffel et al. (2006) used a qualitative approach and could therefore also reconstruct much smaller events with a more limited spatial extent. In the present study, we present an alternative semi-quantitative approach which integrally relies on the analytical skills of the dendrogeomorphic expert. This approach allows identification of different types of avalanche events independently from their size. Even if it might be considered as open to operator bias, we here demonstrate objectivity of its results based on a statistical evaluation.

Cross-validation classification probabilities for a representative dataset from the *Pèlerins* and *Ressec* paths, where different site characteristics prevail (Table 1), indicate that the model correctly classified the years in 89% of the cases. This attests the accuracy of classification tree predictions and consecutively demonstrates the good consistency of our procedure. In other words, it confirms that similar decisions were taken during assessment

of each year of the chronology. The classification tree calibrated with the representative dataset emphasized the prevalence of a few variables such as GD_{tot}, GD_5^* and GD_5' (Figure 14), and is reflective of the typical strategy of a dendrogeomorphic expert's approach. The number of GDs appears to be the first criterion considered whereas strong intensity disturbances seem to be decisive as well.

Furthermore, we obtained a very satisfying match between scores (avalanche/non-avalanche years) predicted by the classification tree (Figure 14) and those initially assigned by the dendrogeomorphic expert in the *Château Jouan* path. Only four out of 128 years (3%) were incorrectly predicted and 16 out of the 17 avalanche years (94%) assessed by the expert were also predicted as avalanche years by the model (Table 4). During the expert's assessment, the years 1931, 1958 and 1975 were considered non-avalanche years since GDs were widely scattered in the path, which was already colonized by a large number of trees at that time (Figure 15). Moreover, a very small number of trees were disturbed in the lower portions of the track during these years. By contrast, the model predicted these years as avalanche years based on (i) the number of GDs exceeding three ($GD_{tot} \geq 4$), (ii) the low scores for both variables related to intensity class 5 ($GD_5' < 0.58$ & $GD_5^* < 0.225$) as well as (iii) the proportion of GDs with intensity class 3 (GD_3^*) that was lower than 0.755 (Figure 14). Conversely, the year 1799 was considered as an avalanche year during the expert's assessment while the classification tree did not confirm this choice. In this particular case, no disturbances were identified in the lower track where few living trees were present (Figure 15). All disturbed trees were observed in the lower part of the runout zone and were clustered. Accordingly, and even if most of GDs were classified as intermediate intensity (class 3), it seemed justified to consider this case as an avalanche year. The high proportion of GDs with intensity class 3 ($GD_3^* \geq 0.755$) explained why the model predicted this year as a non-avalanche year (Figure 14). Interestingly, the spatial component was decisive in all misclassified years which seems logical given that spatial criteria could not be included in the statistical evaluation of our semi-quantitative approach. This finding emphasizes quite clearly the added value of the expert's assessment, especially for years where GDs patterns are equivocal, and the necessity of further work devoted to the inclusion of spatial criteria into the CART modeling.

We therefore demonstrate that our semi-quantitative approach is replicable, considering the very good results from the CART approach (Table 4). However, since the datasets used in this study were quite small, the classification tree was rather sensitive. Hence, any modification in scores of the response variable may lead to a slightly different model. As a consequence, the classification tree presented in this work (Figure 14) cannot be used in its raw state for the determination of past snow avalanche years in other paths without care. In the future, calibration of such a model using a larger dataset with more avalanche paths could help to standardize dendrogeomorphic procedures and an improved determination of snow avalanche years.

5.2 A valuable approach for the determination of past snow avalanches

As a result of the combined use of both quantitative (number of GDs in a given year) and qualitative criteria (intensity and array of GDs), our approach allowed identification of a large number of snow avalanche years in three avalanche paths of the French Alps. The reconstruction was not limited to large extent events but also yielded data for smaller events (Figure 17). In the well-documented *Pèlerins* path, 14 out of 18 events defined by our approach were also recorded in the archives of the EPA for period 1905—2010. Within the four undocumented years, 1948 and 1993 exhibited GDs only above 1720 m asl (Table 5). As the EPA observation threshold (located at 1540 m asl in this path) was not reached, these events were not recorded in the database. Conversely, both years 1932 and 1995 showed disturbed trees down to an elevation of 1470 m asl which is slightly below the observation threshold. These two events could have been missed since they stopped sufficiently far away from critical infrastructure and consequently did not represent any imminent threat in a context of risk management, or simply because the event was not observed by witnesses.

Given the exceptional accuracy of the available historical records in the *Pèlerins* path, we had a unique opportunity to quantify the reconstruction rate of the semi-quantitative approach. Considering the period covered by the EPA (1905—2010), we were able to reconstruct 38% of all documented avalanche years. Although this result might be considered surprisingly low, it is in agreement with the main conclusions of Corona et al. (2012a). These authors applied a slightly different approach and concluded that the

dendrogeomorphic reconstruction underestimates years with natural avalanche activity by roughly 60% in the *Pèlerins* path. Several reasons may be invoked that explain why snow avalanche reconstruction has to be seen as a minimum frequency of natural avalanches. The main limiting factor is that major disturbances (tilting, scarring) may mask the evidence of later events in the same tree. Hence, trees are not consistent recorders of evidence over time i.e. the propensity to record damage varies with the age and size of the tree (Luckman, 2010).

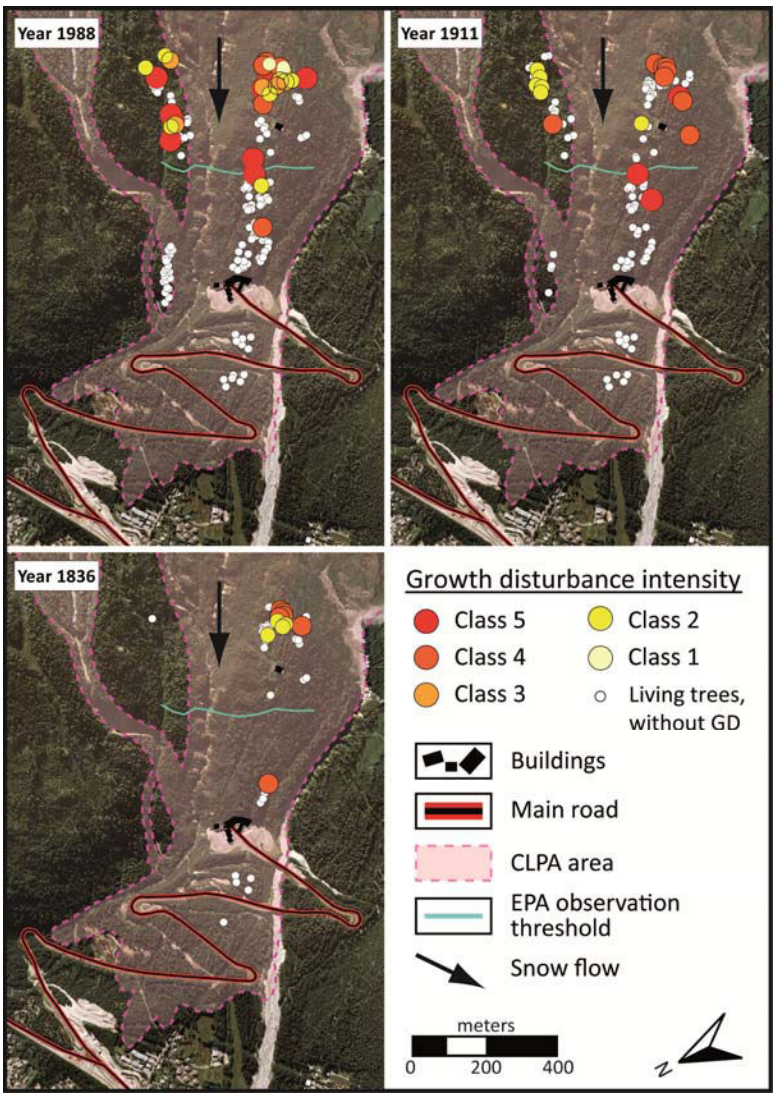

Figure 17. *Spatial distribution of disturbed trees in the Pèlerins path in 1836, 1911, and 1988. Note that only avalanches reaching a determined observation threshold are recorded in the EPA database. For discussion, see text.*

In order to highlight the strength of our approach for the determination of snow avalanche years, we followed a purely quantitative a posteriori method used in recent studies (e.g. Corona et al., 2010; Reardon et al., 2008). Thresholds related to the total number of GDs ($n \geq 10$) and the percentage of disturbed trees (index number ≥ 10) in a given year were applied to the tree-ring data from the *Pèlerins* path. In contrast to the strategy used in our semi-quantitative approach, the five intensity classes were considered here. Results showed that only eleven years were identified for the period 1771—2010 (Figure 16, Table 5). Hence, compared to the 34 years identified with the expert's approach, the total number of reconstructed events is reduced drastically if the fixed quantitative thresholds are being applied without any consideration of the spatial patterns of reacting trees. Furthermore, three years exhibited quite singular GD arrays (1836, 1911, and 1988). Most GDs in these years were located in the track but (almost) none in the runout zone (Figure 17). Considering the total number of GDs and index number, varying between 10 and 29, and between 12% and 19%, respectively (Figure 16, Table 5), these years would have been considered high-magnitude events in terms of damage (e.g., Dubé et al., 2004; Germain et al., 2009). Interestingly, these years do not correspond to large-extent events based on the position of GDs within the path and compared to historical limits derived from technical reports and photographs (CLPA) as well as the EPA observation threshold (Figure 17).

All in all, this paper highlights the contribution of semi-quantitative approaches for the determination of past snow avalanche years. The approach presented in this study is a valuable tool in snow avalanche hazard assessment, especially where there is little or no historical data available.

Snow avalanche years			Assessment criteria					Additionnal criterion
This study	Corona et al. (2012)	Historical archives	Total number of GDs	GDs Intensity class 5	GDs Intensity class 4	GDs Intensity class 3	Runout altitude (m, tree-ring)	Index number
1997		x	7	4	1	1	1570	3.3
1995			8	6	1	0	1470	3.8
1993			5	3	0	1	1720	2.4
1988	x	x	**29**	9	5	6	1530	**13.9**
1983	x	x	**57**	10	31	1	1180	**27.3**
1981	x	x	10	1	1	3	1740	4.8
1971	x	x	**25**	6	9	0	1280	**12.0**
1962	x	x	15	1	10	0	1450	7.2
1951	x	x	15	6	1	0	1460	7.5
1948			8	5	2	1	1760	4.1
1937	x	x	**37**	4	9	0	1330	**21.4**
1932	x		7	2	4	0	1470	4.1
1931	x	x	**40**	5	18	5	1330	**23.7**
1924	x	x	14	5	3	2	1470	8.8
1923	x	x	11	8	2	0	1450	7.1
1911	x	x	**17**	3	8	0	1470	**12.0**
1910		x	6	3	3	0	1780	4.3
1906	x	x	**20**	7	6	1	1450	**14.6**
1897	x		**14**	3	4	0	1320	**11.0**
1895			6	1	4	0	1640	4.8
1878	x		6	0	3	1	1590	6.5
1874	x	x	7	2	2	0	1810	8.2
1869	x		5	2	2	0	1780	6.3
1866	x		**20**	2	13	0	1340	**26.0**
1851	x		8	1	2	0	1780	13.3
1843	x	x	5	0	1	2	1740	9.3
1836	x		**10**	0	6	0	1760	**18.9**
1807	x		7	1	2	3	1740	19.4
1795	x	x	6	0	4	0	1780	18.2
1791	x		6	0	4	1	1740	18.8
1788			3	0	1	2	1730	10.0
1779	x	x	**10**	3	1	0	1750	**37.0**
1774	x		5	0	3	0	1740	20.0
1771	x		6	0	1	2	1780	26.1

Table 5*. Snow avalanche years reconstructed based on several assessment criteria in the Pèlerins path. This study reconstructed 34 event years for the period 1771−2010. In comparison, only eleven years (bold underlined) would have been identified based on the fixed thresholds of GDs ≥ 10 and It ≥ 10* (Corona et al., 2012a; Dubé et al., 2004; Reardon et al., 2008)*.*

Acknowledgments

The authors gratefully acknowledge Jonathan Dumani, Matthieu Schläppy and Louis Manière for their assistance in the field. We also want to thank the Office National des Forêts for sampling permissions. This work was realized within the framework of the MOPERA project funded by the French National Research Agency (ANR-09-RISK-007-01).

CHAPTER C

EVALUATION OF RUNOUT DISTANCES AND RETURN PERIODS

EVALUATION OF RUNOUT DISTANCES AND RETURN PERIODS

Romain Schläppy[1], Nicolas Eckert[2], Vincent Jomelli[1], Markus Stoffel[3,4], Delphine Grancher[1], Daniel Brunstein[1], Mohamed Naaim[2], Michaël Deschatres[2]

"Validation of extreme snow avalanches and related return periods derived from a statistical-dynamical model using tree-ring techniques"

[1] *Laboratoire de Géographie Physique, Université Paris 1 Panthéon-Sorbonne, UMR 8591 CNRS*
[2] *Irstea, UR ETGR Érosion Torrentielle Neige et Avalanches / Université Grenoble Alpes*
[3] *Dendrolab.ch, University of Berne, Institute of Geological Sciences*
[4] *Climatic Change and Climate Impacts, University of Geneva, Institute for Environmental Sciences*

Published in *Cold Regions Science and Technology*, Vol. 99, p. 12—26
Submission: 17 July 2013, acceptance: 1 December 2013

Abstract
Specification of expected runout distances and related return periods are the first and most important steps for zoning in snow avalanche prone terrain. In the past, runout distances of extreme events have often been evaluated with physically- or statistical-based numerical models. More recently, the statistical-dynamical modeling approach has been put forward, as it has the advantage of providing information on avalanche velocity, pressure, and flow depth at each point along a path quantified in terms of probabilities. Most often, calibration of statistical-dynamical modeling is based on existing data from historical archives so that current events with return periods $\leq$ 30 yr can normally be simulated with high confidence, but uncertainty increases as soon as one want to deal with longer return periods, thus calling for validation procedures to corroborate model predictions. In this context, we used dendrogeomorphic records of trees impacted by snow avalanches in their runout zone to reconstruct past activity in two avalanche paths of the French Alps. Based on the reconstructed distribution of runout distances of 25 events and mean event frequencies, we successfully derived runout values for events with return periods of $\leq$ 300 yr. Comparison of relations between runout distance and return periods between dendrogeomorphic data and predictions of a locally calibrated statistical-dynamical model show good agreement. Within the classical intervals used in hazard zoning (i.e. 10–300 yr), mean and mean square errors amounted to $\sim$20 and 30–45 m, respectively. These results suggest that dendrogeomorphic time series of snow avalanches can yield valuable information to anticipate future extreme events and that the employed statistical-dynamical model can be used with reasonable confidence to predict runout distances of avalanches with high return periods, despite some uncertainty inherent to the limits of both approaches.

Keywords
snow avalanche, dendrogeomorphology, event determination, semi-quantitative approach, CART, hazard assessment, French Alps

1 Introduction

Snow avalanches are major hazards to human lives in mountain ranges around the world (McClung and Schaerer, 2006). Mitigation against snow avalanches generally includes analysis of runout distances and related return periods (i.e. the average interval of time within which the runout distance is reached or exceeded at a given location) to designate hazard zones and to design defense structures. Runout distances can be identified through a combination of field observations, historical records, meteorological data or the analysis of aerial photos and topographic maps for vegetation and/or geomorphic evidence (Ancey et al., 2004; Mears, 1992; Weir, 2002). As long and continuous historical observations are generally scarce, the extent of avalanches often needs to be estimated using topographic (or statistic) models (Bovis and Mears, 1976; Eckert et al., 2007b; Keylock, 2005; Lied and Bakkehøi, 1980; McClung and Lied, 1987). These models typically consist of simple statistical regressions which explain observed runout distances with various topographic covariates. While they allow an estimation of maximum runout distances, they do not, however, provide estimates of avalanche size, speed, force or lateral extent (Delparte et al., 2008).

The more physical characteristics of snow avalanches can, in contrast, be gathered from dynamical models (Voellmy, 1955). Dynamical models require a careful representation of avalanche terrain and internal material properties and can consider interaction between different factors (Mears, 1989). Up-to-date models use the formal framework of continuum mechanics (Savage and Hutter, 1989) to reproduce different types of flows with remarkable accuracy (Bartelt et al., 2012). However, if they are used to simulate single events/scenarios – as generally suggested in the avalanche literature (Salm et al. 1990), they do not allow assessment of uncertainties in runout distance predictions in standard statistical terms (McClung, 1990).

More recently, propagation models and statistical analyses have been coupled explicitly using Monte Carlo simulations and are commonly summarized as statistical-dynamical modeling approaches (Barbolini and Keylock, 2002; Bozhinskiy et al., 2001; Eckert et al., 2008b; Keylock et al., 1999; Meunier and Ancey, 2004). Probability distributions are typically chosen for the input variables (e.g., release area and depth, friction coefficient, flow height)

and runout distances and related return periods are derived from a large set of model runs. In addition, data on avalanche velocity, pressure and flow depth can be retrieved at each position along the path and quantified in terms of probabilities.

Calibration of statistical-dynamical models with archival records improves the reliability of the approach considerably (Ancey and Meunier, 2004), but data available for calibration typically remains quite limited (Straub and Grêt-Regamey, 2006), non-explicit in nature, and difficult to be implemented in the friction law (i.e. friction parameters may be too numerous for a single solution of the inversion problem; Ancey et al., 2003). Bayesian methods have been used recently to overcome these difficulties, allowing consistent inference and prediction of high return periods with respect to the available information (Ancey, 2005; Eckert et al., 2009; Gauer et al., 2009; Grêt-Regamey and Straub, 2006).

Nevertheless, all models which are currently available are still hampered considerably by imperfect knowledge of the friction law representing snow in motion (Rognon et al., 2008) and difficulties to properly account for transition between different flow types (Issler, 1998). Furthermore, statistical-dynamical models are well capable to simulate contemporary events, corresponding to return period ≤ 30 yr on which they could be calibrated, but uncertainties increase as soon as longer return periods are investigated. A clear need thus exists to validate modeling procedures in order to corroborate model predictions. Recent work has used radar measurements on avalanche test sites (Vriend et al., 2013) to evaluate simulated velocity profiles (Fischer et al., 2014). However, such data from experimental sites will likely yield data on frequent events, but not on extreme runouts corresponding to large/rare events.

On forested paths, dendrogeomorphology (Alestalo, 1971; Stoffel et al., 2010) has been demonstrated to represent a powerful tool to reconstruct past activity of avalanches with annual resolution and for periods covering past decades to centuries (Butler and Sawyer, 2008). The approach is based on the fact that trees form one increment ring per year in temperate climates and that trees affected by mass movements record the evidence of geomorphic disturbance in their growth-ring series (Stoffel and Bollschweiler, 2008; Stoffel et al., 2013). Reactions of trees to snow avalanches are driven by the forces of the avalanche

and the mechanical impact of debris (i.e. rocks and boulder or broken trees) transported by the snow as well as by the size and flexibility of the tree itself (Bebi et al., 2009).

Typical reactions of trees to avalanche include tilting, wounding as a consequence of trunk, apex and branch breakage (Bartelt and Stöckli, 2001; Luckman, 2010). These external disturbances are reflected in the wood with anomalous anatomical features, which can be detected and accurately dated in tree-ring series using dendrogeomorphic techniques (Butler and Sawyer, 2008; Stoffel and Bollschweiler, 2008; Stoffel et al., 2012). Assessment of yearly patterns of growth anomalies enables identification of avalanche events based on either quantitative (Butler and Sawyer, 2008; Corona et al., 2012a; Germain et al., 2005; Pederson et al., 2006), qualitative (Stoffel et al., 2006), or semi-quantitative (Schläppy et al., 2013) approaches. Dendrogeomorphic data has been used repeatedly in the past to derive minimum avalanche frequency and magnitude within the path or to estimate avalanche return periods based on disturbance frequency of individual trees (Corona et al., 2010; Reardon et al., 2008).

Even if statistical properties of avalanches in forests (McClung, 2003; Teich et al., 2012) and, for instance, relations between forest terrain and avalanche dynamics (Bartelt and Stöckli, 2001; Feistl et al., 2012; Takeuchi et al., 2011) are now more and more investigated, little attention has been paid to the potential of dendrogeomorphic avalanche records for the calibration or validation of avalanche models so far (Germain et al., 2010). Casteller et al. (2008), for instance, used tree-ring records to validate numerical simulations in Argentina, but not with a focus on runout distance and/or its relation to return periods in a given path.

Hence, this study represents the first cross-validation of high return period avalanche information derived from a statistical-dynamical model and the long-term, higher-return period information gathered from tree-ring records. Using event chronologies from two avalanche paths located in the French Alps, its aim was to (i) reconstruct past avalanche activity using a semi-quantitative approach and (ii) evaluate runout distances, (iii) calculate return periods of specific events using the mean frequency and runout distance distribution of snow avalanches, and to (iv) compare dendrogeomorphic results with the predictions of

extreme avalanches as obtained with a locally calibrated statistical-dynamical model (Eckert et al., 2010c).

2 Study sites

This study was conducted at two sites in the Rhône-Alpes and Provence-Alpes-Côte d'Azur regions of the French Alps, namely at the *Avalanche des Pylônes* path near Chamonix-Mont-Blanc (Haute-Savoie) and the *Château Jouan* path near Montgenèvre (Hautes-Alpes; Figure 18). The selection of the sites was driven by the presence of well localized starting zones of snow avalanches, a straight avalanche path as well as by the existence of stopping zones in forests.

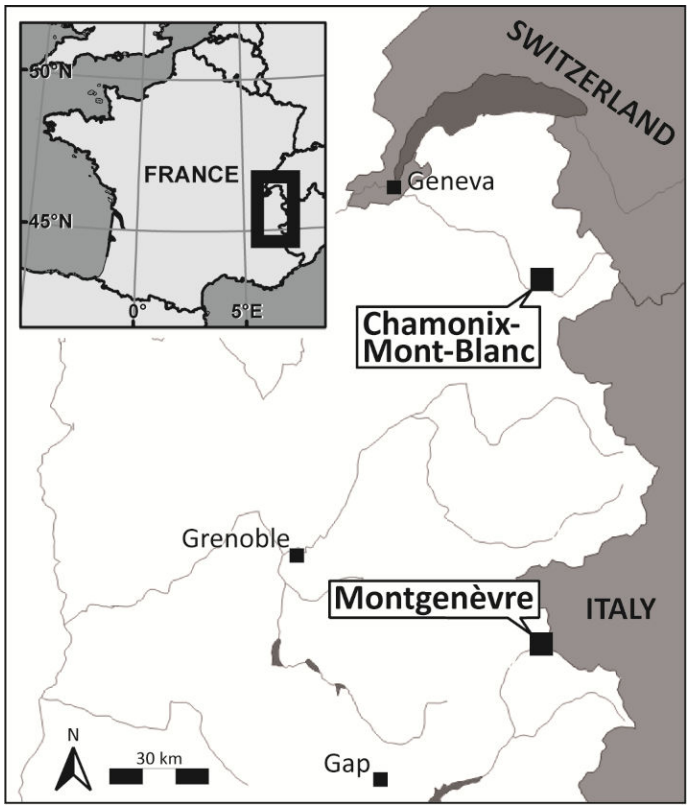

***Figure 18**. Location of the Château Jouan (Montgenèvre) and Avalanche des Pylônes (Chamonix-Mont-Blanc) avalanche paths in the French Alps.*

2.1 *Château Jouan* path

The *Château Jouan* path (44°55' N, 6°42' E) is located on a N-facing slope of the Durance Valley, 2 km SW of Montgenèvre (Figure 19a). At the study site, geology is composed of

Triassic dolomites and limestones. The nearby meteorological station of Briançon (1324 m asl) records mean annual air temperatures (MAAT) of 7.9°C (1971–2000) with coolest mean values in January (−4.8°C). Annual precipitation amounts to 770 mm. Between November and March, precipitation falls primarily as snow, and average annual snowfall reached 258 cm for the period 1961–2001.

Snow avalanches are commonly released from a starting zone located at 2500–2100 m asl (mean slope angle: 36°). Avalanches pass a short track before reaching the runout zone at 2000 m asl (mean slope angle: 22°). Vegetation in the upper part of the runout zone is dominated by shrubs and invasive trees species (e.g., *Pinus mugo* subsp. *mugo*), but *L. decidua* starts to dominate at 1800–1700 m asl. At 1810 m asl, the path is crossed by a forestry road which is used for cross-country skiing during winter (Figure 19a).

2.2 *Avalanche des Pylônes* path

The *Avalanche des Pylônes* path (45°55’ N, 6°51’ E) is located on the S-facing slope of the Arve Valley, immediately next to the first section of the Brévent cable car (Chamonix−Planpraz). MAAT at Chamonix-Mont-Blanc (1054 m, asl) was 6.6°C for the period 1935–1960 and annual precipitation amounts to 1257 mm. Precipitation falls primarily as snow between November and April (average snow cover period: 130 days; Bergue, 2000) and mean annual snowfall was 287 cm (± 121 cm) for the period 1960–2007.

Snow avalanches at the site are generally triggered from a starting zone at 1930–1600 m asl (mean slope angle: 47°). Once released, they pass through an incised path before reaching the runout zone (mean slope: 30°) extending from 1450 m to 1100 m asl. A characteristic transverse vegetation pattern (Malanson and Butler, 1984) can be observed across the starting zone and track. The inner zone is colonized exclusively by shrubs, except for a small scree slope located in the eastern part of the starting zone. In the outer zone, forest vegetation is mainly comprised of *P. abies* with exceptional *L. decidua* and *Alnus viridis*. The runout zone is relatively narrow and trees are very sparse in the central track above 1200 m asl. However, the outer part is covered by a relatively dense forest dominated by *P. abies* with sparse *Pinus sylvestris* L., *Betula pendula*, *A. alba* and some *Alnus alnobetula*

(Bergue, 2000). The path is crossed by a forestry road at 1170 m asl which is used as a skiing track during the winter season. The runout zone ends immediately above the uppermost houses of downtown Chamonix-Mont-Blanc (Figure 19b).

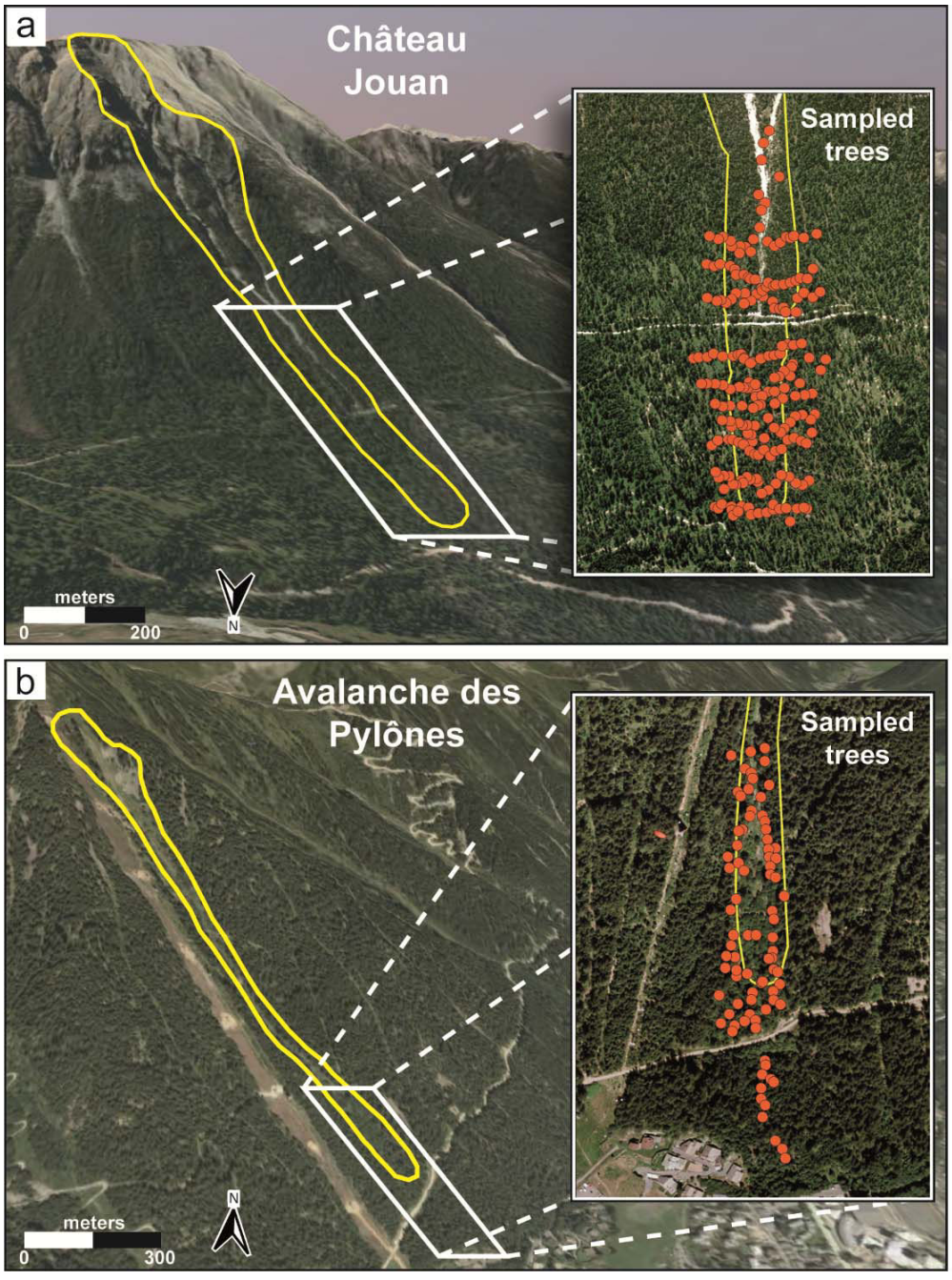

***Figure 19**. Localization of sampled trees in the (a) Château Jouan and (b) Avalanche des Pylônes paths.*

3 Data and methods

3.1 Avalanche historical data

In France, survey of avalanches was initiated by foresters in the 1900s (Mougin, 1922). Most avalanche events have been recorded in the “Enquête Permanente sur les Avalanches” (hereafter referred to as EPA), containing ~80,000 avalanche events in approximately 3900 recognized paths in the French Alps and the Pyrenees. Data on avalanches are gathered by forest rangers, who also record various quantitative (e.g., runout altitudes, deposit volumes) and qualitative (e.g., flow regime, snow quality) data (Jamard et al., 2002). For safety reasons, rangers do not actually measure runout altitudes, but estimate them from a distant observation point. As a consequence, recorded altitudes are more uncertain than avalanche counts, and have been missed repeatedly because of bad visibility.

All observations are stored in a database and complemented with data on meteorological conditions during the days preceding avalanche occurrence. For each surveyed path, EPA data is usually complemented with a map (Carte de Localisation des Phénomènes Avalancheux or CLPA) localizing the occurrence of avalanches, but these maps usually cover only a limited time span with frequent omissions of past events.

Locally, the quality of EPA records depends to a large extent on the rangers’ careful data recording making certain series poor, at least during years corresponding to a ranger’s career. In addition, Teich et al. (2012) state that in forested terrain, avalanches are sometimes badly documented as they are not of key importance compared to large destructive avalanches threatening settlements, infrastructure, and human lives in open terrain. More generally, the quality of observations in the different paths is strongly influenced by the potential threat to existing or projected infrastructure and ease of observation (Jamard et al., 2002). Nevertheless, EPA has repeatedly been found a valuable source of information for local scale risk evaluation (Eckert et al., 2008a), the design of defense structures (Naaim et al., 2010), and for larger-scale investigations of avalanche activity and related snow and weather drivers (Eckert et al., 2010a, 2010b; Jomelli et al., 2007).

In this study, we assume that historical records in the *Château Jouan* and *Avalanche des Pylônes* paths are sufficient for (i) the calibration of the statistical-dynamical model and for (ii) a comparison of predictions with dendrogeomorphic records. In the *Château Jouan* path, the first documented event dates back to winter 1926–7. Due to lacking data on type of avalanche, date of occurrence, or runout elevations, we only consider the period 1950–2011 here. In the *Avalanche des Pylônes* path, the avalanche survey dates back to winter 1985–6. Due to the presence of several critical infrastructures (i.e. cable car, road, houses) in the runout zone of the path, the quality of the avalanche survey is assumed to be satisfying for the period 1986–2012 for which historical archives exist. Note that for both paths, avalanches recorded in the EPA were dense flow avalanches.

3.2 A locally calibrated Bayesian statistical-dynamical model

The Bayesian statistical-dynamical model used in this study has been presented extensively in Eckert et al. (2010c). The main characteristics of the model are summarized in Statistical-dynamical model. It is based on Saint Venant equations solved numerically along a curvilinear profile $z = f_1(x)$, where z is the altitude and x the horizontal distance starting at the top of the path. The classical Voellmy (1955) friction law is used with its well-known friction coefficients pair, μ and ξ (see Appendix 1.1 for more details).

Avalanche frequency a and avalanche magnitude y are modeled as two independent random processes. Avalanche frequency is a scalar discrete random variable corresponding to the number of avalanches recorded each winter and whose long-range mean is necessary for computing return periods (see Evaluation of return periods). Avalanche magnitude is a random vector including all the correlated multivariate quantitative characteristics that vary from one event to another, namely runout distance, velocity and pressure profiles, or snow volume. The probabilistic model is noted $p(y, a|\theta_M, \theta_F)$, indicating that the joint distribution p of the random variables y and a is indexed by parameters (θ_M, θ_F).

Our data sets $y_i, i \in [1, n]$ and $a_t, t \in [1, T_{obs}]$ corresponding to the n avalanches registered at the study site during T_{obs} years of observation are assumed to be mutually independent. Bayesian inference (Bayes and Price, 1763) combines observations and a prior

distribution $\pi(\theta_M, \theta_F)$ which encodes prior knowledge about the unknowns, leading the joint posterior distribution of all parameters and latent variables, as detailed in Appendix 1.2. For each unknown, a point estimate could be derived as well as the related uncertainty quantified by the posterior standard deviation and credibility interval (Table 6, see Statistical-dynamical model for details of the meaning of each parameter). From the posterior estimates, the posterior distribution of model variables $p(y|\widehat{\theta_M})$ and $p(a|\widehat{\theta_F})$ could easily be obtained (Appendix 1.2).

Prior		Posterior							
		Château Jouan				Avalanche des Pylônes			
		mean	SD	2.5%	97.5%	mean	SD	2.5%	97.5%
a_1	$a_1 \sim U(0,10)$	0.69	0.23	0.32	1.19	2.25	0.75	1.02	3.87
a_2	$a_2 \sim U(0,10)$	0.9	0.31	0.4	1.62	11.74	4.23	4.82	21.03
b_1	$b_1 \sim N(3,1)$	1.08	0.13	0.82	1.34	1.07	0.15	0.79	1.36
b_2	$b_2 \sim N(0,1)$	0.15	0.25	−0.36	0.64	1.31	0.76	−0.23	2.81
σ_h	$\sigma_h^2 \sim Gamma(10,100)$	0.32	0.04	0.25	0.4	0.4	0.04	0.33	0.48
c	$c \sim N(0.5,0.2)$	0.49	0.03	0.43	0.56	0.51	0.02	0.46	0.55
d	$d \sim N(0,0.25)$	−0.02	0.05	−0.11	0.07	−0.01	0.06	−0.12	0.1
e	$e \sim N(0,0.25)$	−0.01	0.03	−0.07	0.05	0.05	0.02	0.02	0.09
σ	$\sigma \sim Gamma(1,0.01)$	0.09	0.01	0.07	0.12	0.05	0.01	0.04	0.07
ξ	$\xi \sim N(900,100)$	873	91	697	1053	1023	67	898	1144
λ	$\lambda \sim Gamma(0.01,0.001)$	0.31	0.08	0.18	0.48	0.63	0.15	0.36	0.97

***Table 6**. Parameters of the statistical dynamical model in the (a) Château Jouan and (b) Avalanche des Pylônes paths. For each parameter, the marginal prior distribution used for Bayesian inference is provided, as well as the posterior mean, the posterior standard deviation and the lower and upper limits of the 95% credible interval.*

As discussed in Eckert et al. (2010c), an important point is the need of an informative prior on friction coefficient distributions to grant model identifiability. It is all the more true for our case studies where data quantity is too low to contain enough information to work with poorly informative priors. Many tries were carried out with different prior assumptions

resulting from expert knowledge and/or information transfer from other paths. Finally, "strongly" informative priors were found necessary to fit the data in both studied paths (Table 6). For instance, the sensitivity to the a priori distribution on σ, the standard deviation for μ, is very high. In both studied paths, fitting large runouts by combining data and prior information using Bayes theorem was possible only with an a priori little dispersed distribution for σ leading to realistic posterior probabilities for small μ values. Regarding ξ, prior influence is much lower so that prior choice is less difficult. Obtained posterior estimates are, in both paths, relatively close to the prior mean (900), i.e. higher than values proposed in other avalanche simulation studies performed in forested terrain (Bartelt and Stöckli, 2001; Feistl et al., 2012), but lower than those generally used in open grass terrain, in good agreement with the interpretation of ξ in terms of path roughness (Appendix 1.1).

3.3 Dendrogeomorphic analysis and avalanche event reconstruction

In this study, the area sampled with dendrogeomorphic techniques was restricted to the lower track of the path and its runout zone, as the main goal was to maximize the likelihood of identifying the maximum reach of avalanche events. Sampling was carried out in 2010 and 2011. A total of 438 samples (375 increment cores and 63 cross-sections) were taken from 210 trees at *Château Jouan* and 187 samples (161 increment cores and 26 cross-sections) were selected from 87 trees at *Avalanche des Pylônes* (Figure 19, Table 7). Sampling was restricted to *L. decidua* and *P. abies*. Characteristic growth disturbances (GD) used to calendar-date the occurrence of past snow avalanches included impact scars (Corona et al., 2013; Stoffel and Perret, 2006; Trappmann and Stoffel, 2013), callus tissue (Schneuwly et al., 2009a; Stoffel et al., 2010) and tangential rows of traumatic resin ducts (TRD; Bollschweiler et al., 2008; Schneuwly et al., 2009b; Stoffel and Hitz, 2008), the initiation of compression wood (Butler et al., 2010; Timell, 1986) and abrupt growth reductions (Butler and Malanson, 1985; Corona et al., 2012a; Kogelnig-Mayer et al., 2013; Stoffel et al., 2013). Selection of trees, sampling design as well as sample preparation and analysis followed the procedures described in Stoffel and Bollschweiler (2008) and Stoffel et al. (2013).

In a subsequent step, intensities were assigned to GDs in order to emphasize features that are clearly associated with avalanche activity and to discriminate these from

disturbances possibly induced by other factors (Corona et al., 2012a; Stoffel et al., 2013). GDs were classified based on the visual quality of the evidence of reactions within each sample according to the intensity scale presented in Table 2. GD data from individual trees were then summarized in a geographic information system with ArcGIS (ESRI, 2014). For each year derived from the tree-ring series, trees that were living (i.e. trees present in a given year considering their age as obtained from sample analysis) were plotted according to their geographic coordinates. The determination of snow avalanche years was based on a visual evaluation of the resulting maps and followed the procedure described by Schläppy et al. (2013). Basically, each map (one per chronology year) was assessed separately by analyzing simultaneously the number of disturbed trees present, the proportion of strong intensity GDs compared to intermediate ones as well as their distribution within the path. Weaker reactions were also considered in the yearly assessment and could be helpful in cases where only few disturbed trees were observed. Note that here an avalanche year is related to a winter, with the year 1999 corresponding, for example, to winter 1998–9.

The age structure of the stand was approximated by counting the number of tree rings in all sampled trees and visualized after interpolation. However, as trees were not sampled at the stem base and as their piths as well as the innermost rings were sometimes rotten, the obtained age structure is biased and does neither reflect inception nor germination dates (Corona et al., 2010; Stoffel et al., 2006). Nevertheless, it may provide valuable data on major disturbance events at the study site with reasonable precision, as *L. decidua* has been shown repeatedly to recolonize surfaces cleared by snow avalanches and other mass-movement processes in the years following an event (Stoffel et al., 2006; Van der Burght et al., 2012).

	Château Jouan		Avalanche des Pylônes	
Sample analysis	Number	Percentage	Number	Percentage
Sampled trees	**210**	**-**	**87**	**-**
Sample type	**438**	**100%**	**187**	**100%**
Cross section	63	14%	26	14%
Increment core	375	86%	161	86%
Growth disturbances	**491**	**100%**	**222**	**100%**
a Impact scars	35	7%	29	13%
TRD	229	46.5%	106	48%
Compression wood	156	32%	36	16%
Growth reduction	63	13%	51	23%
Callus tissue	8	1.5%	0	0%
b Intensity class 5	49	10%	40	18%
Intensity class 4	183	36.5%	138	62%
Intensity class 3	66	13%	5	2%
Intensity class 2	110	22%	19	9%
Intensity class 1	83	18.5%	20	9%

Table 7*. Sample size, (a) types, and (b) intensity of growth disturbances in the Château Jouan and Avalanche des Pylônes paths. TRD = tangential rows of traumatic resin ducts.*

3.4 Evaluation of avalanche runout distances from field data

In a first step, we determined runout distances for all historical events based on information contained in the EPA database. We used the minimum runout elevation reported in the EPA to obtain a first idea of the reach of individual avalanches. In a second step, runout distances were estimated for all avalanches identified with dendrogeomorphic techniques, and based on the position of impacted trees within the path. The reach of avalanches in a given year was defined by the location of the lowermost cluster (≥ 2) of trees showing strong or moderate reactions as a result of avalanche disturbance. Reactions in trees scattered below the lowest tree cluster were disregarded to avoid overestimation of runout distances. Noteworthy, trees may record several impacts during the same winter, so

the maximum reach obtained with tree-ring records will therefore represent the largest reach and/or extent of all potential events in a given winter.

3.5 Evaluation of return periods

A return period $T_{x_{stop}}$ corresponding to the runout distance x_{stop} (i.e. the T year return level) can be evaluated by combining the annual avalanche rate f (the mathematical expectation of the random variable $a_t, t \in [1, T_{obs}]$), and $F(x_{stop}) = P(X_{stop} \leq x_{stop})$, the cumulative distribution function (cdf) of runout distances:

$$T_{x_{stop}} = \frac{1}{f\left(1 - F\left(x_{stop}\right)\right)} \tag{5}$$

Hence, for both model outputs and field data, estimates $\hat{f}$ and $\hat{F}(x_{stop})$ must be derived. In the Poisson frequency model with single parameter $\theta_F = \lambda$ used in this paper (Appendix 1.1), the mean frequency estimate $\hat{f}$ is simply$\hat{\lambda}$. For field data, rather than considering only the ratio between the total number of avalanche events observed and the related number of years considered in the chronology (i.e. mean frequency), we retained the median of all possible values. The possible values were determined considering the time period for which data quality was considered acceptable and data quantity sufficient to obtain robust estimates of avalanche occurrence rates (see Determination of event frequencies and Discussion and conclusion for details). This procedure was applied to both the historical and the dendrogeomorphic records.

On the other hand, $\hat{F}(x_{stop})$, the estimated cumulative distribution function (cdf) of runout distances was approximated using a variation of the Hazen formula (Hazen, 1914), common in hydrology:

$$\hat{F}\left(x_{stop}\right) = \frac{j\left(x_{stop}\right) + 0.5}{n + 1} \tag{6}$$

where $j(x_{stop})$ is the number of events which stopped before the distance x_{stop}, and n the total number of events observed in a path. This was applied to the historical and tree-ring runout distance datasets, but also to a sample of 20,000 simulations of $p(x_{stop}|\hat{\theta}_M)$, the estimated distribution of runout distances (see Figure 20c for *Château Jouan*).

As a result of the limited number of observations, the estimation of return periods was subject to a considerable level of uncertainty affecting both $\hat{f}$ and $\hat{F}(x_{stop})$. To evaluate and take into account these uncertainties, we (i) as said before computed all possible values of $\hat{f}$ and performed a sensitivity study, and (ii) computed asymptotic non-parametric confidence intervals CI_F for $\hat{F}(x_{stop})$ as follows:

$$CI_F = \hat{F}_{x_{stop}} \pm \frac{q_{N\alpha}}{\sqrt{n}} \times \sqrt{\hat{F}_{x_{stop}} \times \left(1 - \hat{F}_{x_{stop}}\right)} \quad (7)$$

with $q_{N\alpha}$ the quantile of the standard Gaussian distribution related to the confidence level α (classically 95%). This was done for tree-ring and historical records only, as for model simulations, samples large enough to lower the width of this interval to zero were considered.

For hazard zoning purposes, the inverse problem has to be solved, i.e. the annual exceedance probability is known, for example 0.01 for the centennial event, and the associated runout distance has to be found. Inverting Eq. (5) shows that the T year return level x_{stop_T} is provided by:

$$x_{stop_T} = \hat{F}^{-1}_{x_{stop}}\left(\frac{\hat{f}T - 1}{\hat{f}T}\right) \quad (8)$$

where $\hat{F}^{-1}_{x_{stop}}$ is the inverse cumulative distribution function of the considered runout sample. For the different samples, $\hat{F}^{-1}_{x_{stop}}$ was evaluated by kernel smoothing of the empirical inverse step function. This has the advantage to avoid using Hazen (Eq. (6)) or other similar approximations, and provides smoother runout distance–return period relations as compared to the direct use of Eq. (5). Note that Hazen formula was nevertheless used to

evaluate the maximum empirical return period for each event of the tree-ring and historical chronicles in the two studied paths, and to obtain bounds for computing the confidence interval around the runout distance–return period relationships.

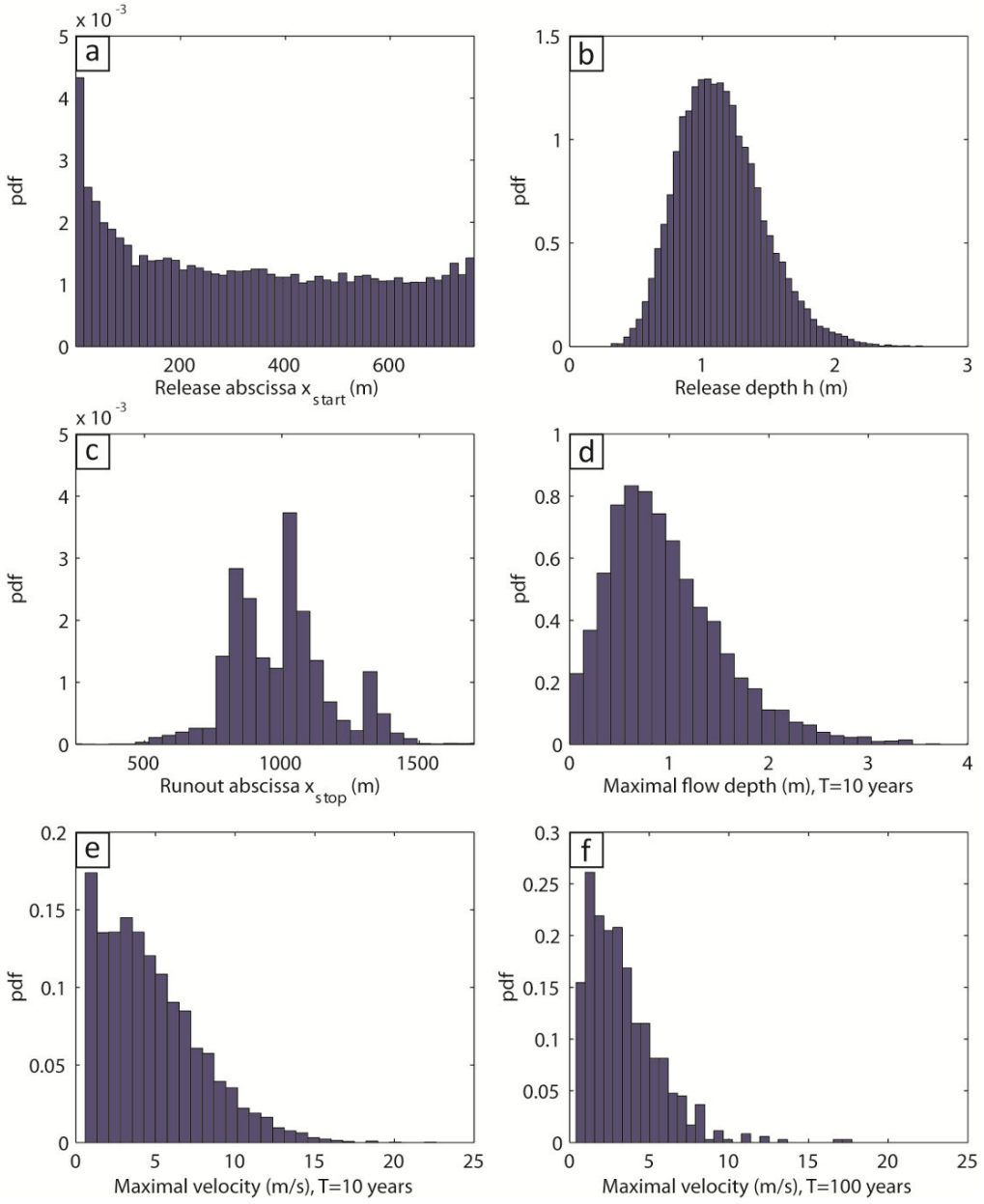

***Figure 20**. Multivariate statistical-dynamical avalanche model fitted on the Château Jouan EPA data. (a) release abscissa distribution. (b) release depth distribution. (c) runout distance distribution. (d) maximal flow depth distribution for avalanches whose runout distance exceeds the 10-yr return period abscissa. (e—f) maximal velocity distribution for avalanches whose runout distance exceed the (e) 10-yr and (f) 100-yr return period abscissas.*

Noteworthy, the joint distribution of the exceedance $p\left(y\middle|\hat{\theta}_M, x_{stop} > x_{stop_T}\right)$ provided by the statistical-dynamical model, summarizes the characteristics of all avalanche events at the abscissa x_{stop_T}. It can therefore be considered as the joint distribution of all reference scenarios corresponding to the return period T (Figure 20e–f for maximum flow depths and velocities at the 10-yr return period abscissa and maximum velocities at the 100-yr return period abscissa in the *Château Jouan* path, respectively).

3.6 Cross validation of model's simulations with independent dendrogeomorphic data

As summarized in Figure 21, the cross validation of model simulations and dendrogeomorphic chronicles is performed through the calculation of $\bar{\delta}$, the mean error, and $\bar{\delta}_2$, the (root) mean square error, between return levels derived from both methods:

$$\bar{\delta} = \frac{1}{(T_{max} - T_{min} + 1)} \times \sum_{T=T_{min}}^{T_{max}} \left(x_{stop_{model}}(T) - x_{stop_{dendro}}(T)\right) \quad (9)$$

$$\bar{\delta}_2 = \frac{1}{(T_{max} - T_{min} + 1)} \times \left[\sum_{T=T_{min}}^{T_{max}} \left(x_{stop_{model}}(T) - x_{stop_{dendro}}(T)\right)^2\right]^{1/2} \quad (10)$$

where $x_{stop_{model}}(T)$ and $x_{stop_{dendro}}(T)$ are the runout distances related to return period T derived from the model and tree-ring reconstruction, respectively, and $[T_{min}, T_{max}]$ the return period range on which the comparison is made.

The mean error on a given return period range corresponds to the mean value of the positive and negative errors on this range without considering its sign. In our case, a positive mean value implies that simulated runout distances are larger on average than empirical ones for the $[T_{min}, T_{max}]$ return period interval, and vice versa. However, independently from the sign, a low mean value can result from the compensation between overestimations and underestimations from the model. Consequently, a bias tending to zero provides no

information about the effective dispersion of errors around the mean value. For this reason, we also calculated the mean square error, which takes into account the average of the squares of the errors. In this case, a low value means that all observed bias were relatively low or tend to zero, indicating that simulations and observations are really similar on the $[T_{min}, T_{max}]$ range.

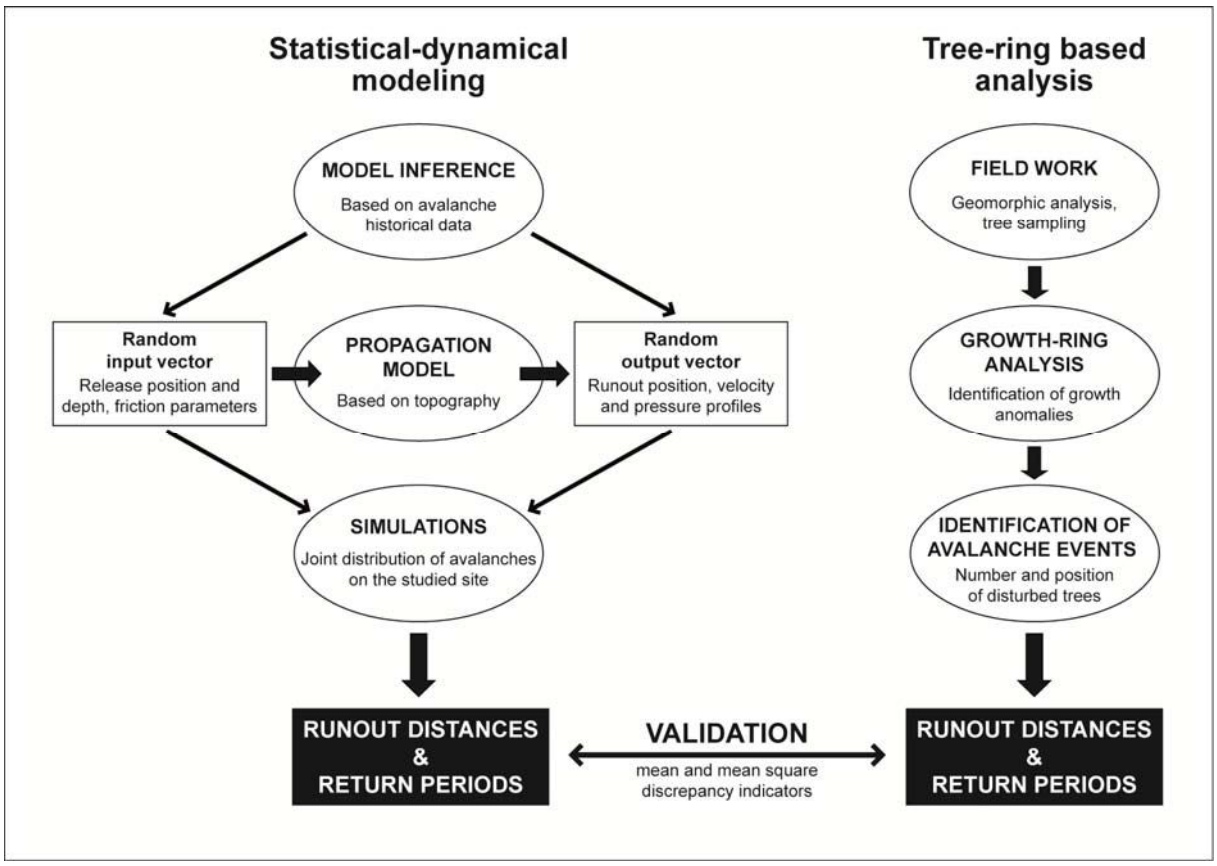

***Figure 21**. Flowchart of the principal steps leading to the cross validation of runout distance-return period relationships.*

4 Results

4.1 Tree-ring analysis and event reconstruction

4.1.1 Age structure of the forest stand

At *Château Jouan*, sampled trees have an average age of 160±70 yr at sampling height. The oldest tree reached sampling height in AD 1712 and the youngest one in 1992. A total of 92 trees were at least 200 yr old. Ages of trees tend to increase from the lower portions of the avalanche track to the lower segments of the runout zone (Figure 22a). In a similar way, tree ages gradually increase from the inner to the outer zones of the path. This spatially heterogeneous tree age distribution indicates that major parts of the stand might have been eliminated by large snow avalanches in the past.

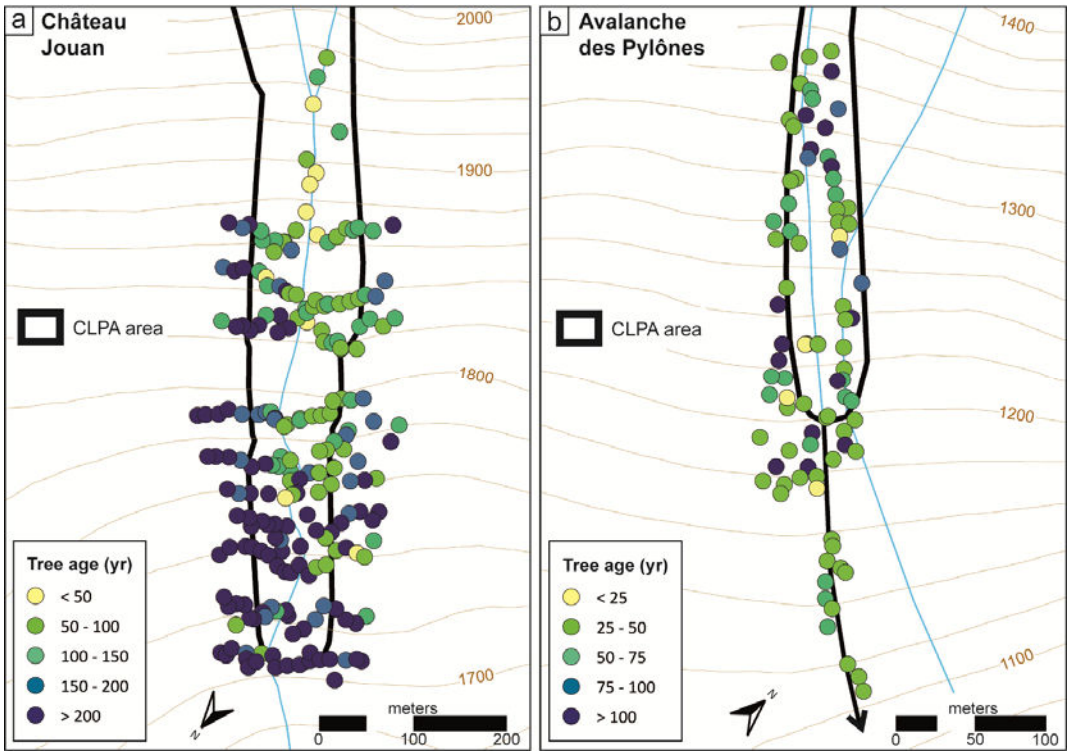

***Figure 22**. Age structure of the forest stand growing in the (a) Château Jouan and (b) Avalanche des Pylônes paths as obtained from tree-ring data. Tree ages were approximated by counting the number of tree rings present in the selected trees and at sampling height. The black arrow corresponds to the maximal reach of very shallow avalanche flows that have been recorded in the EPA data.*

In the *Avalanche des Pylônes* path, data on the pith age at sampling height indicates a mean age of trees of 65±52 yr. The oldest tree reached sampling height in AD 1770 and the youngest one in 1994. Figure 22b nicely illustrates that tree age distribution within the path is relatively homogeneous. As a consequence, we may assume that most avalanches remained confined to the inner part of the path and were not of sufficient magnitude to destroy major portions of the forest stand.

4.1.2 Growth disturbances and identification of avalanche events

Sample analysis permitted identification of 491 and 222 GD, respectively, in the *Château Jouan* and *Avalanche des Pylônes* paths (Table 7). The formation of TRD following cambium wounding and the onset of compression wood after tilting were commonly found in the samples, but abrupt growth reductions, impact scars as well as callus tissue were also present. Most of the GD are of moderate and strong intensities, but slightly less intense at *Château Jouan* (59.5%) than at *Avalanche des Pylônes* (82%; Table 7).

Based on the yearly distribution of reacting trees within the path, 13 avalanche events were identified in the *Château Jouan* path for the period 1799–2010 (Table 8). The temporal distribution of avalanche events was relatively homogeneous since 1910 with 1–3 avalanche winters per decade. Somewhat less activity is observed in the 1940s and 1990s. Only two avalanche winters can be dated prior to the 20th century, namely in 1873 and 1799. In the *Avalanche des Pylônes* path, 12 avalanche winters were identified for the period 1963–2011 (Table 8).

The temporal distribution of avalanche winters is quite homogeneous on this period, but small gaps exist for most of the 1970s and between 1999 and 2006.

Snow avalanche events					
Château Jouan			*Avalanche des Pylônes*		
Event year	Runout altitude (m)	Horizontal runout distance (m)	Event year	Runout altitude (m)	Horizontal runout distance (m)
2009	1840	1058	2006	1120	1136
2007	1790	1192	1999	1230	914
2004	1760	1271	1997	1200	968
1986	1740	1339	1992	1200	968
1977	1760	1271	1990	1270	830
1963	1830	1085	1986	1270	830
1960	1780	1218	1982	1180	1005
1951	1770	1243	1980	1200	968
1934	1790	1192	1979	1340	719
1930	1820	1111	1970	1270	830
1919	1750	1302	1966	1190	986
1873	1780	1218	1963	1190	986
1799	1710	1444			

***Table 8**. Tree-ring based snow avalanche events, minimum runout altitudes and related horizontal runout distances in the Château Jouan and Avalanche des Pylônes paths.*

4.2 Determination of event frequencies

Mean event frequencies in both paths are relatively constant over long time periods (Figure 23). In the *Château Jouan* (*Avalanche des Pylônes*) path, the median of all possible values amounted to 0.09 (0.22) for the tree-ring based event chronology and to 0.32 (0.59) for the historical archives (Figure 23, Table 9).

Figure 23d and Figure 23h also indicate the upper and lower plausible values (2.5 and 97.5% of the histograms) which will be used later to evaluate the influence of value choices on the comparison between empirical and simulated return periods.

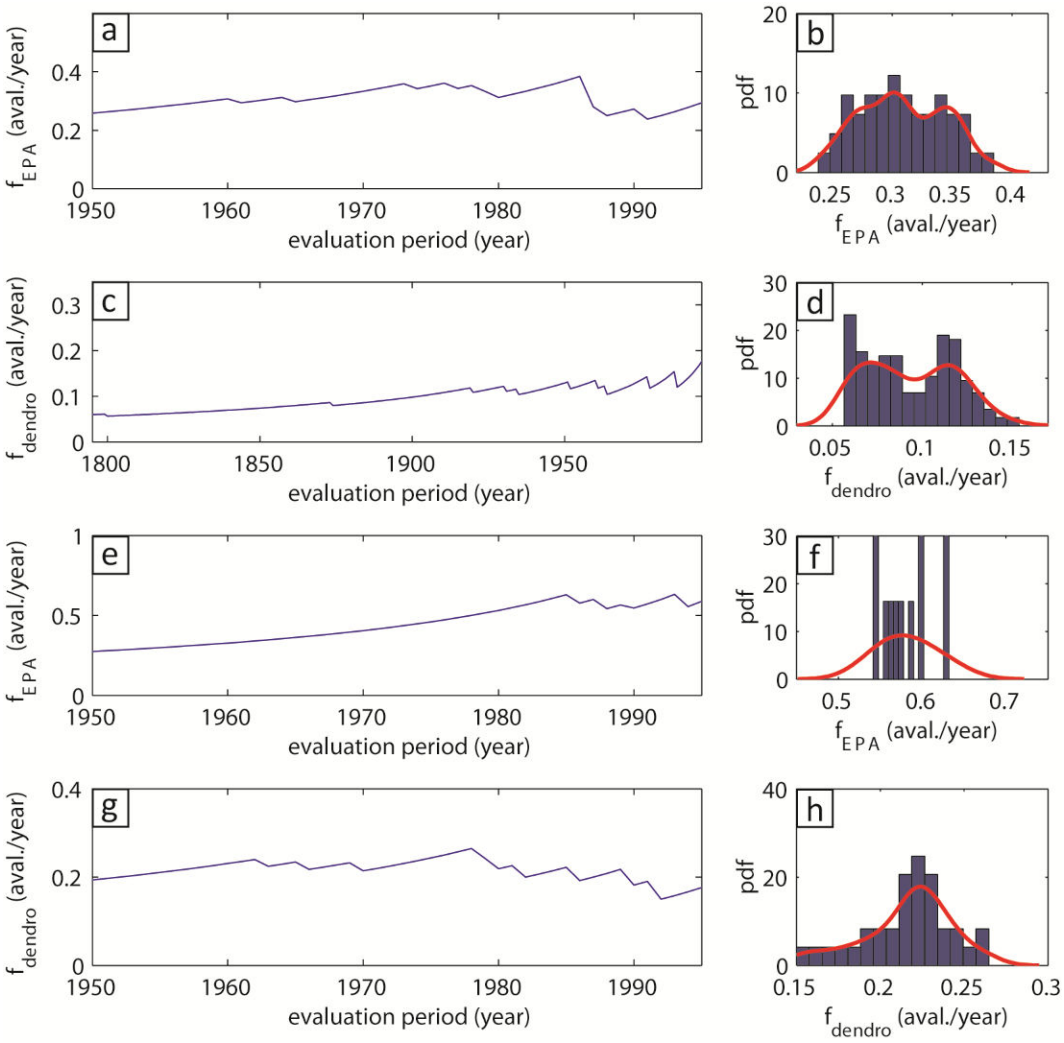

Figure 23. *Evaluation of annual mean frequency in the (a—d) Château Jouan and (e—h) Avalanche des Pylônes paths: (a, e) annual frequency for historical events as a function of the considered time window. (b, f) related probability distribution. (c, g) annual frequency for dendrogeomorphic events as a function of the considered time window. (d, h) related probability distribution. In this work, for the historical and tree-ring based chronicles, the median of histograms 23b, 23f, 23d, and 23h were primarily considered (Table 9).*

4.3 Runout distance distribution along the path

At *Château Jouan*, runout altitudes existed for 16 avalanches recorded accurately in the EPA database and ranged from 2100 to 1750 m asl. Runout altitudes estimated for the 13 avalanches reconstructed with tree-ring records ranged from 1840 to 1710 m asl (Table 10). At *Avalanche des Pylônes*, runout altitudes from 15 EPA events varied between 1450 and 1100 m asl, whereas the values derived from dendrogeomorphic data ranged from 1340 to

1120 m asl (Table 10). Based on the runout altitude data, we estimated runout distances and represented related empirical cumulative distribution functions (cdf) graphically. Figure 24 illustrates runout distances and indicates that the data obtained from the EPA principally informs about small to medium avalanche events, whereas the information derived from dendrogeomorphic reconstructions rather focuses on avalanches with larger spatial extent. This was particularly well illustrated in the *Château Jouan* path where 50% of the avalanche events reported in the EPA archives stopped before the first event identified in the tree-ring reconstruction (Figure 24a).

Path name	Chronology type	Annual frequency 2.5%	Annual frequency median	Annual frequency 97.5%
Château Jouan	Historical archives	0.26	**0.32**	0.38
	Tree-ring data	0.06	**0.09**	0.14
Avalanche des Pylônes	Historical archives	0.54	**0.59**	0.7
	Tree-ring data	0.18	**0.22**	0.26

***Table 9**. Historical and tree-ring based annual event frequencies. Considered median annual frequency and related 2.5%, and 97.5% were derived from Figure 23.*

Due to the fact that model calibration was based on avalanche data as reported in the EPA, cdfs derived from the simulations are quite similar to those derived from the database of historical events for small and intermediate runout distances (Figure 24). Conversely, for larger events, model output tends to look more like runout distances derived from dendrogeomorphic records, and thus confirms the appropriateness of tree-ring records to test extreme predictions.

4.4 Cross validation between simulated and empirical high return periods

Based on mean event frequencies $\hat{f}$ and estimated cumulative distribution functions $\hat{F}(x_{stop})$, return periods corresponding to all historical and tree-ring based events were then

evaluated using Eqs. (5)(6). At *Château Jouan*, return periods related to historical events ranged from 3 to 100 yr (Figure 25a). By contrast, runout distances derived from dendrogeomorphic data corresponded rather to large extent events with return periods $>$ 300 yr ($T_{max} = 311$ yr). Conversely, less information was obtained for small events, since the minimum return period that could be derived from the tree-ring record was $>$ 10 yr ($T_{min} = 12$ yr). At *Avalanche des Pylônes*, return periods obtained from the EPA database varied between 2 and 54 yr (Figure 25b), whereas dendrogeomorphic records informed about return periods trespassing 100 yr ($T_{max} = 118$ yr).

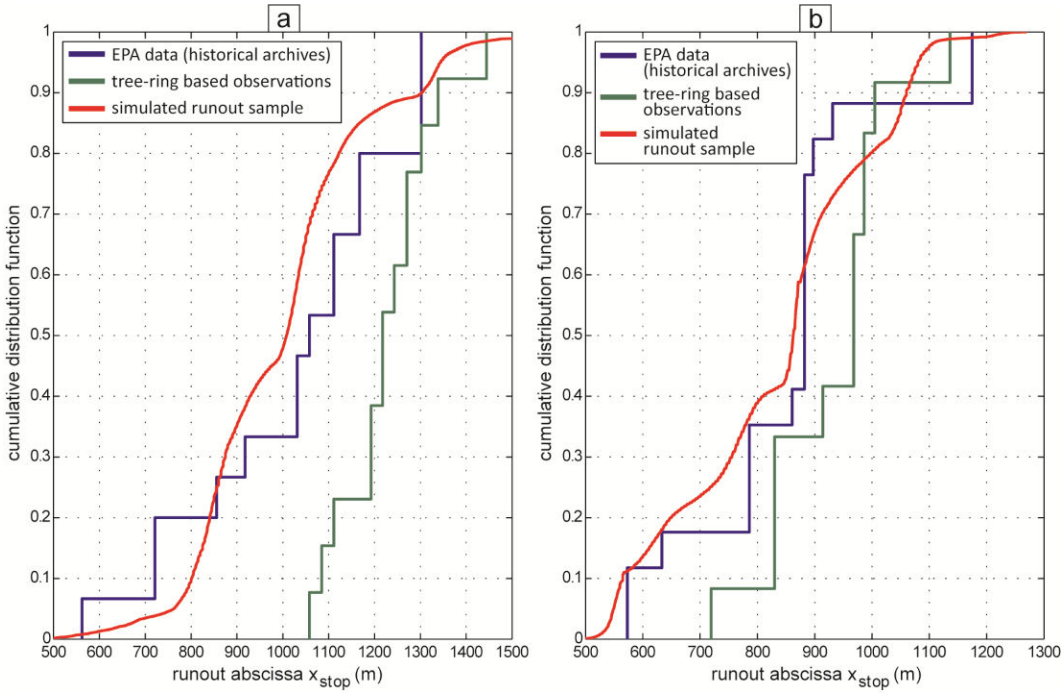

***Figure 24**. Empirical and simulated cumulative distribution functions (cdfs) of runout distances in the (a) Château Jouan and (b) Avalanche des Pylônes paths.*

However, although these discrete values may give an approximate idea of empirical return period distributions along the paths under investigation, it must be stressed that the related uncertainty level remains high due to the limited number of available data, as is illustrated by the 95% confidence intervals represented in Figure 26. This explains why, even if the true runout distance–return period relationship in one given path is unique, at a given

position along the path, corresponding return period from historical EPA archives may differ slightly from the one derived from tree-ring data. In that sense, uncertainty increases rapidly with runout distance for both the historical (EPA) and dendrogeomorphic records in both paths. At *Château Jouan*, for example, runout distances related to 30-yr and 100-yr return periods derived from tree-ring data are between 1200–1352 m and 1271 m and $+\infty$ m, respectively.

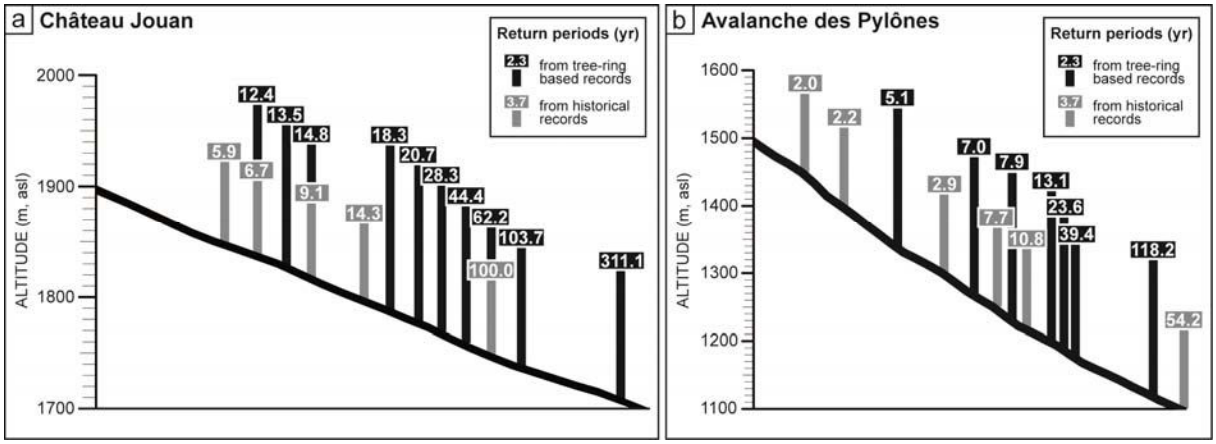

***Figure 25**. Return periods (in yr) for each of the historical (grey) and tree-ring based (black) events in the (a) Château Jouan and (b) Avalanche des Pylônes runout zones. Return periods were evaluated based on mean event frequencies (Table 9) and the estimated cumulative distribution function (cdf) of runout distances (Eq. (6)). Note that very small return periods ($<$ 5.9 yr) are not represented to simplify display.*

Noteworthy also, the maximum runout distance related to EPA events was reached twice during the period of observation in both studied paths. Consequently, the corresponding return period is somewhat undetermined, leading to a vertical ending of the corresponding runout distance–return period relationships and to even higher uncertainty levels for high return periods evaluated with historical archives.

Because the return periods reported above were evaluated with the Hazen approximation, introducing an additional source of uncertainty for very high return periods, we rather compared runout distance–return period relations as derived with the model simulations and dendrogeomorphic data using the inverse cumulative distribution function

(cdf) of the considered runout sample (Eq. (8)). Analysis included the mean and mean square errors for both paths and different return period ranges, according to data availability.

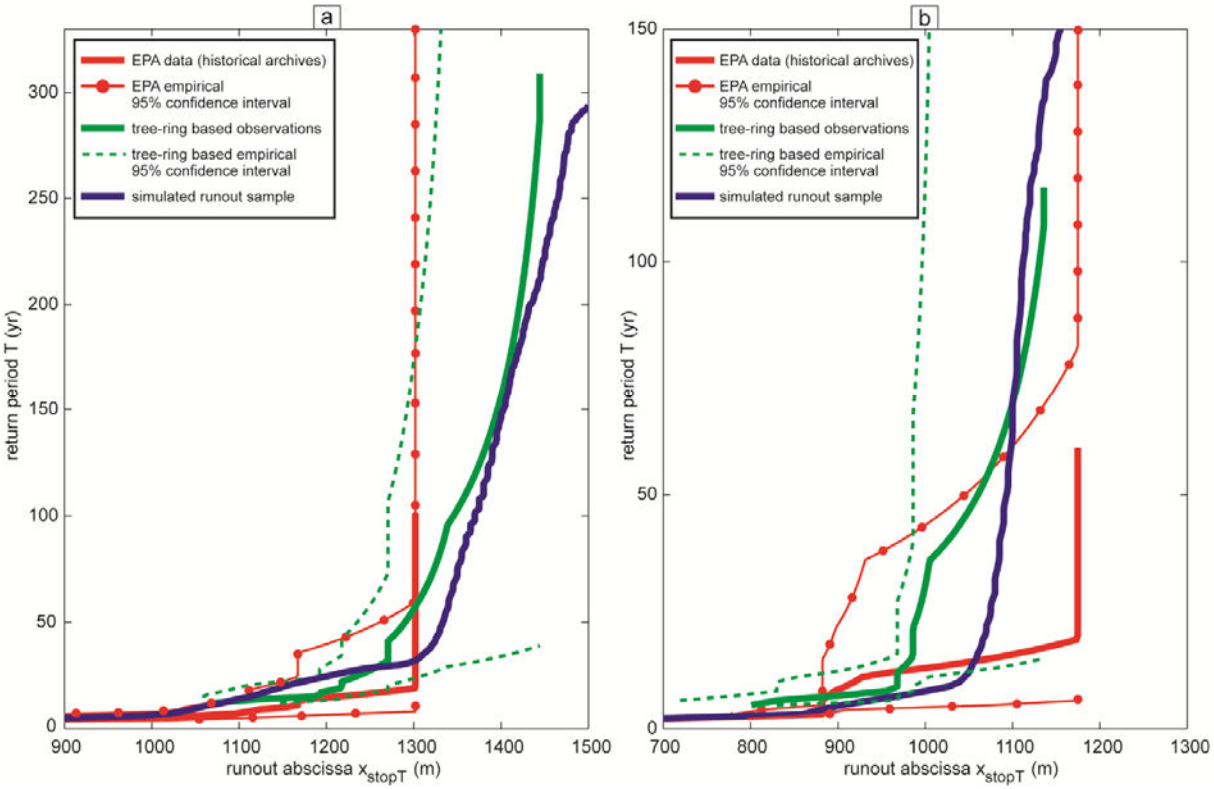

***Figure 26**. One-to-one relation between runout distance and return period. Empirical relations and associated 95% confidence intervals derived from historical archives and tree-ring reconstructions are compared to the ones derived from the statistical-dynamical simulations. (a) At Château Jouan, return periods derived from dendrogeomorphic analysis tend to approximate very well modeled data, especially for return periods ranging from 30 to 300 yr. (b) At Avalanche des Pylônes, tree-ring based return periods ranging from 50 to 110 yr correspond roughly to those simulated by the model.*

In the *Château Jouan* path, such a comparison was possible for return periods ranging roughly from 10 to 300 yr, corresponding to the classical interval used in hazard zoning (Figure 26, Table 10). Mean and mean square errors amounted to 19.7 and 28.9 m, respectively, which can be considered satisfying considering the different uncertainty sources that exist in this kind of analysis regarding data or model and with respect to the context of avalanche zoning problems. The best fit is observed for the range of 100–300 yr, for which the mean error amounted to only 20.0 m and the mean square error to 23.8 m

(Table 10). Larger discrepancies were found for the range of 10−30 yr with a negative value obtained for the mean error (–36.2 m), reflecting the fact that runout distances derived from tree-ring records are larger for this range of return period than the one derived from the model. Results for the 10–1000 yr return period range were similar to the range of 10–300 yr, given that only nine additional return periods were available for the tree-ring based runout distance–return period relationship ($T_{max} = 309$ yr).

Path name	T_{max}	T_{min}	δ runout distance	δ_2 runout distance	number of years with a tree-ring based estimate on the $[T_{min},T_{max}]$ interval
Château Jouan	10	300	19.7	28.9	289
	10	30	−36.2	46.2	19
	30	100	34.0	35.1	71
	100	300	20.0	23.8	201
	10	1000	21.7	32.2	298
Avalanche des Pylônes	10	300	23.5	45.8	107
	10	30	79.6	79.7	21
	30	100	17.1	36.1	71
	100	300	−18.0	18.1	17
	10	1000	23.5	45.8	107

Table 10*. Mean and mean square errors between tree-ring based runout distance–return period relations and model simulations as functions of time windows. For each time window, the number of years for which the tree-ring based estimation could be evaluated is provided.*

In the *Avalanche des Pylônes* path, comparison was mostly limited to return periods ranging from 10–100 yr, given the empirical $T_{max} = 118$ yr. However, for the purpose of comparison, we also calculated mean and mean square errors over the same intervals as in the *Château Jouan* path. As a consequence, mean and mean square errors are the same for the 10–300 and 10–1000-yr return period intervals, amounting to 23.5 and 45.8 m, respectively (Table 10). In more detail, for the return period interval 10–30 yr, errors amount to roughly 80 m, indicating that the model and tree-ring data are not in good agreement. Errors start to decrease with increasing ranges of return periods: for the interval 30–100 yr,

errors are 17.1 and 36.1 m, respectively. The best fit was found for the interval 100–300 yr, with mean and mean squared errors equal to −18.0 and 18.1 m, respectively. However, these values should be interpreted cautiously as they only reflect discrepancies between simulated and tree-ring data for the interval 100–118 yr, according to T_{max}.

5 Discussion and conclusion

Specification of expected runout distances and related return periods in the runout zone has been defined as the first and most important step for zoning in snow avalanche prone terrain (McClung, 2000). As a consequence, runout distances of extreme events have often been evaluated using physically based numerical models in the past. More precisely, the rationales of Salm et al. (1990) were thereby largely used by practitioners to evaluate "high magnitude" runout distances, in a rather efficient way but without an explicit statistical framework (Ancey et al., 2004). More recently, statistical-dynamical modeling approaches have been put forward as an alternative approach, where calibration is based on local data reported in historical archives – EPA in the present case – and where probabilistic simulations enable local evaluation of return period at any point along a given path (Eckert et al., 2008b, 2010c).

In this study, a statistical-dynamical approach has been used to analyze runout distances at two avalanche sites in the French Alps, *Château Jouan* and *Avalanche des Pylônes*. According to historical data available in the EPA, the model was capable to simulate current events with relatively small return periods (i.e. $\leq$ 30-yr return interval). As validation of simulated data could not be realized for higher return periods with EPA data, we reconstructed runout distances of larger, and less frequent, avalanches in both paths with dendrogeomorphic techniques (e.g., Corona et al., 2012a; Schläppy et al., 2013; Stoffel and Bollschweiler, 2008). The dendrogeomorphic record of snow avalanches yielded runout information for 25 avalanche winters in the paths (Table 8), and thus allowed reconstruction of local event chronologies of high-magnitude events as well as estimation of return periods for each of the 25 events using the local runout distance distribution and event frequency as estimated from the tree-ring samples. Comparison of runout distance–return period relations between the simulated data and dendrogeomorphic records showed good agreement on return period ranges for which tree-ring information was available, i.e. for return periods from 10–300 yr and 30–100 yr for the *Château Jouan* and *Avalanche des Pylônes* paths, respectively. At both sites, results clearly illustrate the interest and added value of the combined use of statistical-dynamical simulations and tree-ring reconstructions,

in particular, for return period ranges which are of interest for avalanche engineering, but not usually covered in historical (EPA) archives. However, we are aware that many sources of uncertainty were involved in the approach used in this paper and should thus be taken into account during the evaluation of the main outcomes. We tried to take them into account as much as possible by using non-parametric confidence intervals and sensitivity analysis to the mean event frequency determination. However, because of the inherent difficulty of working with extreme events and old (historical chronicles) or indirect (tree-ring reconstruction) data, all sources of uncertainty could not fully be assessed in a quantitative way.

First of all, uncertainties may result from the physical and probabilistic modeling assumptions, as partially discussed in Statistical-dynamical model (interpretation of the Voellmy' equation), and, in more details, by Eckert et al. (2010c). Among these, subjectivity introduced into analysis by the friction coefficients prior choice should be kept in mind while considering the interest of our results for avalanche hazard mapping purposes. For instance, to fit our data to the paths under investigation, imposing an a priori low dispersed distribution for σ (the standard deviation of μ) could not be avoided because of the small size of the available historical chronicles, which will obviously reduce the strength of our results in view of a possible application of statistical-dynamical models on poorly documented sites. At the same time, however, the same prior choice yielded the best results among numerous trials (not presented in this paper) on both paths. Furthermore, the necessity of its use may reflect nothing more that the so-called Weibull (bounded) attraction domain of extreme avalanches that has been documented for the few datasets where it could be estimated (Ancey, 2012; Keylock, 2005). Hence, the strongly informative prior put forward in this study may well be a robust choice for a first approximation in various other paths.

Second, determination of a mean event frequency represents a crucial analytical step as it influences the evaluation of empirical return periods and, consequently, their comparison with model simulations. The sensitivity of the comparison was performed for the *Château Jouan* path, where the tree-ring chronology is much longer as compared to *Avalanche des*

Pylônes. On the range $f = 0.06-0.14$ (Figure 23c−d), the bias between methods tends to become increasingly negative with increasing values of f (Figure 27a) which "mechanically" increase tree-ring based runout distance corresponding to given return periods. The tree-ring event frequency value which minimizes the mean square error with model simulations is $f = 0.102$, and thus similar to the value selected for this path ($f = 0.09$, the median over all possible values). Furthermore, fluctuations between the tree-ring based runout distance–return period relations, where f varied between 0.09 and 0.102, and modeled data were inferior to 10 m on average (Figure 27). Consequently, using the median of all possible values as a mean event frequency does not only seem relevant but also yields fairly robust results.

The evaluation of empirical return periods also depends on the cumulative distribution function (cdf) of observed runout distances. Rather than using the classical Hazen formula or other techniques used for the estimation of empirical exceedance probabilities, we calculated x_{stop_T} using the inverse cdf of the considered runout sample (Eq. (8)) so as to minimize the uncertainty level related to the limited number of available data.

This study did not, by contrast, quantify the influence of the quality of the historical and dendrogeomorphic event chronologies. These could have been addressed as well, as recent studies highlighted that tree-ring reconstructions tend to underestimate the number of years with natural avalanche activity by up to 60% (Corona et al., 2010, 2012a; Schläppy et al., 2013), and that avalanche chronicles, such as the EPA, may have observational gaps or records of limited quality. As a matter of fact, both the historical and dendrogeomorphic mean event frequencies might have been underestimated, which, in turn, may affect the evaluation of empirical return periods. At the same time, however, and as high return period events tend to cause significant damage to infrastructure and/or forest, the likelihood that they have been missed in historical archives or not been recorded by the trees is unlikely. As a consequence, and as reported by Corona et al. (2012a), Stoffel and Bollschweiler (2009) and Stoffel et al. (2013), the resulting bias is supposed to influence preferentially small return periods (≤ 30 yr) which typically correspond to current events. Indeed, the agreement between model and tree-ring data has been shown to be somewhat limited for this return period range, but much more conclusive for larger ranges. In consequence, we

assume that this source of uncertainty will be rather limited for return periods varying between 30 and 300 yr, i.e. for the interval which is of much more relevance for long-term avalanche forecasting.

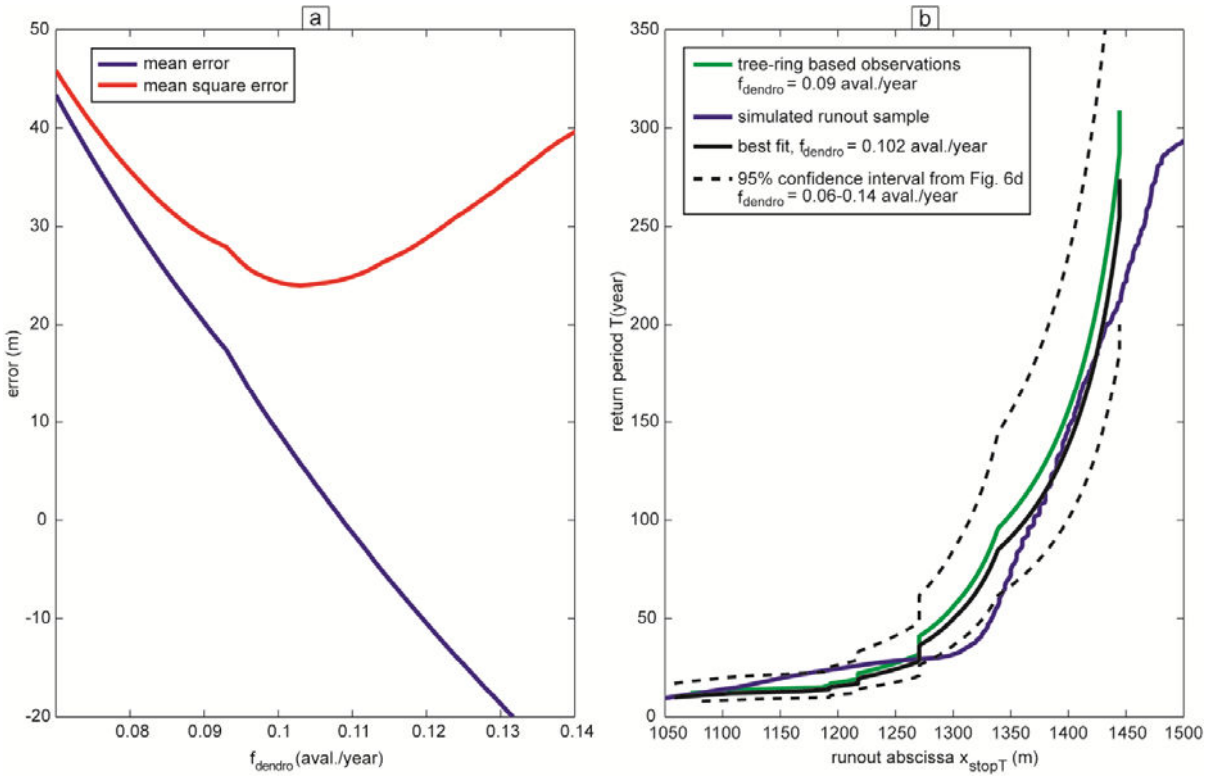

***Figure 27**. Influence of the tree-ring based event frequency on the comparison for the Château Jouan path: (a) mean and mean square errors as functions of the tree-ring event frequency. (b) tree-ring based runout distance–return period relations versus model simulations for the range of possible mean event frequencies from Figure 23c—d.*

Another source of uncertainty results from the estimation of runout distances based on the position of impacted trees within a path, as dendrogeomorphic reconstructions have been reported to possibly underestimate runout distances in some cases (Corona et al., 2012a). This underestimation is mainly due to changes in path geometry (steepness, curvature) as well as to the presence of a forest stand in the runout zone that can induce rapid avalanche deceleration (McClung, 1990; McClung and Schaerer, 1985). As a consequence, snow pressures may be insufficient in these zones to damage trees and thereby cause reactions in the tree-ring record, particularly at the front of the deposit. In

addition, the sampling strategy can also influence the accuracy of runout distance estimation. Given that the sampled trees are generally selected along transects across the slope (Figure 22a), one might underestimate runout distances of avalanches stopped between two transects and possibly explains the negative bias observed between runout distances for return periods of 30–300 yr (Figure 26a) derived from tree-ring records and those obtained with simulations in the *Château Jouan* path.

We also assumed in this study that an underlying stationary process would generate high-magnitude snow avalanche events, as, despite of a clear climate control of avalanche occurrences (Castebrunet et al., 2012), long-term changes in avalanche activity could not been found in most observational records (Laternser and Schneebeli, 2002). We did not, therefore, include the findings of Eckert et al. (2013) who observed, based on EPA data, a recent and accelerated reduction of high return period avalanches in the French Alps which could possibly be linked with a decrease of snow cover and changes in preferred avalanche types under climate warming (Martin et al., 2001). In addition, climate change since the end of the Little Ice Age as well as changes in land use are likely to have had considerable impacts on both forest cover and avalanche activity on the longer term as well (Jomelli and Pech, 2004), but have not been considered in the context of this study either. As a consequence, the frequency and magnitude of destructive forest avalanches may have been larger or smaller in the past, but signs of such changes are not obvious in the investigated paths where the total number of events reconstructed with tree-ring records was only large enough to see that the number of recorded events decreases with time and at a pace similar to the decrease of the sample size of trees available for dendrogeomorphic analyses (Stoffel et al., 2013). We call for future work where non-stationary statistical-dynamical simulations are implemented and, if possible, confronted with longer and more abundant tree-ring chronicles to take climate and land-use change effects into account as well (Corona et al., 2012b).

All in all, despite the various sources of uncertainty, we are convinced that this contribution is of high value as it provides, for the first time, a rather conclusive cross-validation of runout distance–return period relations derived from a statistical-dynamical

model with data derived from independent, natural archives. Hence, dendrogeomorphic data can be seen as an extremely valuable data pool for the assessment of runout distances and return periods of extreme avalanche events, and in particular for the hazard zoning on forested paths with limited or no historical data. At the same time, we illustrate that the statistical-dynamical model presented here can be used with reasonable confidence to predetermine high return period avalanches and associated information on avalanche velocity, snow pressure and snow depth. Furthermore, it is hoped that the information contained in tree-ring records could be used in the future to evaluate the various modeling assumptions related to weight and sensitivity for high return periods as well as velocity and/or pressure distributions within the statistical-dynamical set-up, and to propose subsequent model improvements.

Acknowledgements

The authors gratefully acknowledge Louis Manière and Matthieu Schläppy for their assistance in the field. They also want to thank the Office National des Forêts (ONF) for sampling permissions. This study has been realized within the framework of the MOPERA (MOdélisation Probabiliste pour l'Evaluation du Risque d'Avalanche) program funded by the French National Research Agency (ANR-09-RISK-007-01). R.S. acknowledges support from the Swiss National Science Foundation (project P1SKP2_148492). Finally, the authors are grateful to J. Schweizer, P. Gauer and two anonymous referees whose constructive comments helped to improve the paper.

CHAPTER D

ASSESSMENT OF AVALANCHE-CLIMATE RELATIONS

ASSESSMENT OF AVALANCHE-CLIMATE RELATIONS

Romain Schläppy[1], Vincent Jomelli[1], Nicolas Eckert[2], Markus Stoffel[3,4], Delphine Grancher[1], Daniel Brunstein[1], Christophe Corona[3,5], Michaël Deschatres[2]

"About the assessment of avalanche-climate relations using tree-ring data – case studies in the French Alps"

[1] Laboratoire de Géographie Physique, Université Paris 1 Panthéon-Sorbonne, UMR 8591 CNRS
[2] Irstea, UR ETGR Érosion Torrentielle Neige et Avalanches / Université Grenoble Alpes
[3] Dendrolab.ch, University of Berne, Institute of Geological Sciences
[4] Climatic Change and Climate Impacts, University of Geneva, Institute for Environmental Sciences
[5] Laboratoire de Géographie Physique et Environnementale, Université Blaise Pascal Clermont-Ferrand 2, UMR 6042 CNRS

Submitted in *Regional Environmental Change*
Submission: February 2014

Abstract
Dendrogeomorphology has been recognized as a powerful tool to reconstruct past avalanche activity with annual resolution and for risk assessment. This technique has also been repeatedly used to identify relationships of snow and weather variables with avalanche activity, especially in areas where information on historical events is insufficient or largely absent. However, given that reconstructions may also miss a significant number of avalanches, it seems necessary to evaluate the relevance of climate-avalanche relationships inferred from tree-ring chronologies. Avalanche activity was reconstructed in five paths of the French Alps for which a reasonable database of historical information was available. Based on daily snow and weather data covering the period 1959–2009, we derived a comprehensive set of 120 climatic and composite variables on a monthly basis. The variables which best explained avalanche activity as recorded in the tree-ring records were highlighted with an original variable selection procedure implemented within a logistic regression framework. The same approach was then used for the avalanche chronologies derived from historical archives as well as with a third data set composed of a combination of both chronologies. Results show clear statistical relations between snow and weather variables and tree-ring or historical avalanche event chronologies at the path scale. However, the logistic regression models also suggest that tree rings preferentially record avalanches triggered during cold winter storms with heavy precipitation. Conversely, historical avalanche data seem to contain a majority of events that were released later in the season and during episodes of strong positive temperature anomalies. These discrepancies suggest that dendrogeomorphic records only allow capturing the relations between snow or climate and avalanche occurrences to a certain extent. We illustrate that composite chronologies built from tree-ring and historical records can be very useful, but that their interpretation with respect to climate variables remains difficult. Future work should be performed at the regional scale to eliminate stationarity and to further evaluate the ability of tree-ring data to document the impact of climate change on avalanche activity.

Keywords
Dendrogeomorphology, snow avalanche, avalanche-climate relations, logistic regression, French Alps

1 Introduction

Snow avalanche activity depends on the interactions between terrain variables and meteorological conditions. More specifically, five key factors have been identified to contribute to avalanche formation, namely terrain, precipitation, wind, temperature, and snow pack stratigraphy (Schweizer et al. 2003). In this sense, statistical analyses including classification trees can help the understanding of physical processes inducing avalanche release (e.g., McClung, 2003; Smith and McClung, 1997a, 1997b), as a first step in any attempt to forecasting (e.g., Gassner and Brabec, 2002; Pozdnoukhov et al., 2011). If consistent avalanche occurrence data are available, analyses can be done quantitatively by relating these factors to snow and weather data at the time of release (Jomelli et al., 2007; McClung and Tweedy, 1993). On larger spatio-temporal scales, links with atmospheric circulation patterns can then be established (García et al., 2009; Keylock, 2003; McClung, 2013). In general, however, long and continuous historical observations are relatively scarce, so that climate-avalanche studies have remained restricted to a few areas in the world.

Dendrogeomorphology (Alestalo, 1971; Stoffel et al., 2010) has been demonstrated to represent a powerful tool to reconstruct past activity of avalanches with annual resolution and for periods covering past decades to centuries (Butler and Sawyer, 2008). The approach is based on the fact that trees form one increment ring per year in temperate climates and that trees affected by mass movements record the evidence of geomorphic disturbance in their growth-ring series (Stoffel and Bollschweiler, 2008; Stoffel and Corona, 2014; Stoffel et al., 2013). Reactions of trees to snow avalanches are driven by the forces of the avalanche and the mechanical impact of debris (i.e. rocks and boulder or broken trees) transported by the snow as well as by the size and flexibility of the tree itself (Bebi et al., 2009).

In that context, dendrogeomorphology has been used repeatedly to examine relations between snow and weather variables and avalanche activity at locations where little or no historical avalanche data was available. For example, the probability of major avalanche years was associated with mean January snowfall in the western United States (Hebertson and Jenkins, 2003) and the French Alps (Corona et al., 2010). High-magnitude avalanche

years were significantly correlated to positive snowpack anomalies in the U.S. (Reardon et al., 2008) or snowy winters, with total snowfall well above average in Canada (Dubé et al., 2004). Similarly, Casteller et al. (2011) found a significant correlation between years with large avalanche activity and abundant precipitation during austral winters (May to October) in Argentina. All these studies have helped to better understand the main drivers of avalanche activity at the local scale.

On the other hand, several studies recently demonstrated that dendrogeomorphic reconstructions tend to underestimate years with natural avalanche activity by roughly 60% (Corona et al., 2012a; Schläppy et al., 2013; Stoffel et al., 2013). Consequently, the relevance of climate–avalanche relationships inferred from tree-ring data may be questioned, and, at least, may need more precise evaluation. This relevance is tested in this contribution so as to explore the link between avalanche occurrences and climate patterns in areas where little historical information is available. *Climate* is used here in its classical sense of *statistical average of snow and weather conditions*, so as to be in agreement with the limited temporal resolution of tree-ring data.

In general, evaluating avalanche-climate relationship derived from tree rings may seem difficult because of the amount of information required. In France, however, a rather favorable context exists: Comprehensive avalanche data are available for an exceptionally long period, as systematic surveys of avalanches have been initiated by foresters in the early 20th century (Mougin, 1922). On the other hand, the SAFRAN-CROCUS model chain (hereafter referred to as SC model chain; more details are provided in Modeled weather and snow data) from Météo-France provides valuable reanalyzed daily snow and weather data at various elevations, aspects, and slopes for the 23 French massifs (Durand et al., 1999) and for the period 1958/9−2008/9.

The aim of this study is therefore to (i) reconstruct past snow avalanche activity in five paths distributed throughout the French Alps using dendrogeomorphic techniques; (ii) define a large set of potential variables from the SC simulations that could explain avalanche activity; (iii) pick the most pertinent variables using a variable selection procedure implemented within a logistic regression framework so as to (iv) assess statistical relations

between snow and weather data and avalanche years derived from tree-ring data and/or historical archives in the different paths; (v) discuss the results and draw conclusions regarding the ability of tree-ring data to capture avalanche-climate relations.

2 Study sites

Study site selection was based on the presence of old-growth forest signs with clear signs of snow avalanche disturbance, easy accessibility, the apparent absence of other mass wasting processes (e.g., landslides, rockfalls, fire), and the presence of avalanche stopping zones within the forest. We strived to find distant avalanche paths with various geomorphic characteristics (Table 11) to assure reasonable spatial representation. Five snow avalanche paths were selected in the northern and central parts of the French Alps, namely the *Avalanche des Pylônes* and *Pèlerins* paths near Chamonix-Mont-Blanc (Mont-Blanc massif), the *Ressec* path near Lanslevillard (Haute-Maurienne region), the Château Jouan path near Montgenèvre (Thabor massif) and the *Ourcière* path near La Grave (Oisans region; Figure 28).

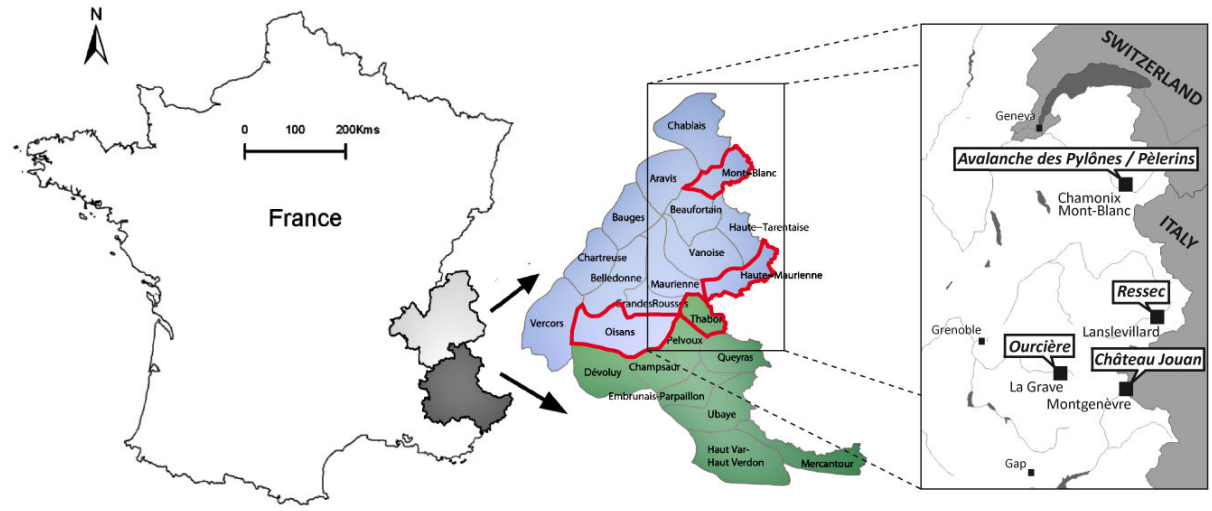

Figure 28. *Location of the five avalanche paths in the French Alps. The French Alps are divided into 23 massifs. The Northern French Alps and Southern French Alps are represented in blue and green, respectively. The massifs where the studied paths are located are surrounded in red (adapted from Castebrunet et al., 2012).*

2.1 *Avalanche des Pylônes* path

The *Avalanche des Pylônes* path (45°56’ N, 6°51’ E) is located on the S-facing slope of the Arve Valley and ends immediately above the uppermost houses of downtown Chamonix-Mont-Blanc. Snow avalanches are generally triggered from a starting zone at 1850–1700 m asl (Table 11). Once released, they pass through an incised path before reaching the runout extending from 1450 m to 1100 m asl. Forest vegetation is mainly comprised of *P. abies* with sparse *P. sylvestris*, *L. decidua*, *B. pendula*, *A. alba*, *A. viridis* and *A. alnobetula* (Bergue, 2000).

Path name	Starting zone (m)	Runout zone (m)	Altitudinal drop (m)	Mean slope angle (degree)	Aspect	Dominant tree species
Avalanche des Pylônes	1850−1700	1450−1100	750	45	S	*Picea abies* (L.) Karst.
Pèlerins	3600−2750	1500−1100	2400	35	NW	*Larix decidua* Mill., *Picea abies* (L.) Karst.
Ressec	3000−2300	2100−1700	1300	30	NW	*Picea abies* (L.) Karst., *Larix decidua* Mill.,
Château Jouan	2500−2000	1900−1700	800	30	N	*Larix decidua* Mill., *Pinus mugo* subsp. *mugo*
Ourcière	2900−1900	1800−1250	1650	35	N	*Larix decidua*

***Table 11**. Principal site-related characteristics in the different avalanche paths.*

2.2 *Pèlerins* path

The *Pèlerins* avalanche path (45°53’ N, 6°52’ E) on the NW-facing slope of the Arve Valley dominates the hamlet of *Les Pèlerins*, located 2 km southwest of downtown Chamonix. Snow avalanches are commonly triggered from a starting zone located between 3600 and 2750 m asl where an orthogneissic rockwall is partly covered by the *Pèlerins*

glacier. Most of the avalanches stop in the runout zone at 1500—1100 m asl (Table 11). Located in the upper mountain stage, the runout zone is covered by a dense forest dominated by *L. decidua* and *P. abies*.

2.3 *Ressec* path

The *Ressec* avalanche path (45°17’ N, 6°57’ E) on the NW-facing slope of the Arc Valley dominates the hamlet of Chantelouve, located 3 km northeast of downtown Lanslevillard. Snow avalanches are released from a starting zone located between 3000 and 2300 m asl and generally stop in the runout zone which extends between 2100 and 1700 m asl (Table 11). The runout zone is covered by a dense forest dominated by *P. abies* and *L. decidua* with exceptional *A. alba*.

2.4 *Château Jouan* path

The *Château Jouan* path (44°55’ N, 6°42’ E) is located on the N-facing slope of the Durance Valley, 2 km SW of Montgenèvre. Snow avalanches are commonly released from a starting zone located at 2500–2000 m asl (Table 11). Avalanches pass a short track before reaching the runout zone that extends between 1900—1700 m asl. The upper part of the runout zone is colonized by shrubs and invasive trees species (e.g., *P. mugo*), but *L. decidua* starts to dominate at 1800–1700 m asl.

2.5 *Ourcière* path

The *Ourcière* path (45°02’ N, 6°15’ E) is located on the N-facing slope of the Romanche Valley, 4 km W of La Grave. Most snow avalanches are released from a starting zone located at 2900–1900 m asl (Table 11). The lower part of the starting zone as well as the track are incised in a gneissic rockwall. Avalanches commonly reach the runout zone between 1800—1250 m asl. The talus deposits are covered by an open forest built of *L. decidua*.

3 Data and methods

3.1 Dendrogeomorphic analysis and avalanche event identification

In this study, the area sampled with dendrogeomorphic techniques was restricted to the lower portions of avalanche paths and their runout zones, as the main goal was to maximize the likelihood of identifying medium and large sized avalanche events. Following the recommendations of Corona et al. (2012) and Stoffel et al. (2013), at least 100 trees were sampled at each of the five selected paths (Table 12), which corresponds to an optimal threshold needed to obtain the best match between reconstructed events and those documented in historical archives.

Sampling was restricted to *L. decidua*, *P. abies* and *A. alba*. Characteristic growth disturbances (hereafter referred to as GD) used to calendar-date the occurrence of past snow avalanches included impact scars (Corona et al., 2013; Stoffel and Perret, 2006; Trappmann and Stoffel, 2013), callus tissue (Schneuwly et al., 2009a; Stoffel et al., 2010) and tangential rows of traumatic resin ducts (TRD; Bollschweiler et al., 2008; Schneuwly et al., 2009a; Stoffel and Hitz, 2008; Stoffel, 2008), the initiation of compression wood (Butler et al., 2010; Timell, 1986) and abrupt growth reductions (Butler and Malanson, 1985; Corona et al., 2012a; Kogelnig-Mayer et al., 2013; Stoffel et al., 2013). Selection of trees, sampling design as well as sample preparation and analysis followed the procedures described in Stoffel and Bollschweiler (2008), Stoffel et al. (2013) and Stoffel and Corona (2014).

In a subsequent step, intensities were assigned to GDs in order to emphasize features that are clearly associated with avalanche activity and to discriminate these from disturbances possibly induced by other factors (Corona et al., 2012a; Stoffel et al., 2013). GDs were classified based on the visual quality of the evidence of reactions within each sample according to the intensity scale presented in Table 2 (Schläppy et al., 2013). GD data from individual trees were then summarized in a geographic information system with ArcGIS (ESRI, 2014). For each year derived from the tree-ring series, trees that were living (i.e. trees present in a given year considering their age as obtained from sample analysis) were plotted according to their geographic coordinates.

	Avalanche des Pylônes		*Pèlerins*		*Ressec*		*Château Jouan*		*Ourcière*	
Sample analysis	Number	Rate	Number	Rate	Number	Rate	Number	Rate	Number	Rate
Sampled trees	**148**	**-**	**209**	**-**	**168**	**-**	**210**	**-**	**232**	**-**
Sample type	**311**	**100%**	**452**	**100%**	**401**	**100%**	**438**	**100%**	**374**	**100%**
Cross section	61	20%	0	0%	59	15%	63	14%	150	40%
Increment core	250	80%	452	100%	342	85%	375	86%	224	60%
Growth disturbances	**468**	**100%**	**660**	**100%**	**591**	**100%**	**491**	**100%**	**901**	**100%**
a Impact scars	66	14%	0	0%	28	5%	35	7%	0	0%
TRD	246	53%	115	17%	251	42.5%	229	46.5%	361	40%
Compression wood	106	23%	150	23%	155	26%	156	32%	342	38%
Growth reduction	50	11%	368	56%	155	26%	63	13%	90	10%
Callus tissue	0	0%	27	4%	2	0.5%	8	1.5%	108	12%
b Intensity class 5	76	16%	142	22%	69	11.5%	49	10.0%	154	17%
Intensity class 4	206	44%	219	33%	140	23.5%	183	36.5%	354	39%
Intensity class 3	19	4%	50	8%	105	18%	66	13.0%	267	30%
Intensity class 2	59	13%	240	36%	195	33%	110	22.0%	101	11%
Intensity class 1	108	23%	9	1%	82	14%	83	18.5%	25	3%

***Table 12**. Sample depth, (a) types, and (b) intensity of growth disturbances in the five paths.*

The determination of snow avalanche years was based on a visual evaluation of the resulting maps and followed the procedure described by Schläppy et al. (2013). Basically, each map (one per chronology year) was assessed separately by analyzing simultaneously the number of disturbed trees, the proportion of strong intensity GDs compared to intermediate ones as well as their distribution within the path. Weaker reactions were also considered in the assessment and could be helpful in cases where only few disturbed trees were observed. An avalanche year was always related to a winter, with the year 1999 corresponding, for example, to the "full" winter 1998–9 (roughly from November/December 1998 to April/May 1999).

3.2 Historical avalanche data

In France, the systematic survey of avalanches was initiated by foresters in the early 20th century (Mougin, 1922) in the *"Enquête Permanente sur les Avalanches"* (hereafter referred to as EPA). This chronicle contains ~80,000 avalanche events in approximately 3900 recognized paths in the French Alps and the Pyrenees. Event occurrence dates as well as various quantitative (e.g., runout altitudes, deposit volumes) and qualitative (e.g., flow regime, snow quality) data (Jamard et al., 2002) complemented with data regarding meteorological conditions during the days preceding the release are stored in this database maintained by Irstea. For each surveyed path, EPA data is usually complemented with the maximal extent of past observations, plotted on a map (*Carte de Localisation des Phénomènes Avalancheux* or CLPA; Bonnefoy et al., 2010).

Locally, the quality of EPA records depends to a large extent on the rangers' careful data recording which renders certain series poor, at least for the period of the ranger's career. In addition, in forested terrain, avalanches are sometimes badly documented as events stopping in forests are not of key importance in terms of hazards as compared to large destructive avalanches threatening settlements, infrastructure, and human lives in open terrain (Teich et al., 2012). More generally, the quality of observations in the different paths is strongly influenced by the potential threat to existing or projected infrastructure and by the ease of observation (Jamard et al., 2002). Nevertheless, the EPA has repeatedly been found to represent a valuable source of information for local scale risk evaluation (Eckert et

al., 2007b, 2009), the design of defense structures (Naaim et al., 2010), and for larger-scale investigations of avalanche activity and related snow and weather drivers (Eckert et al., 2010b; Jomelli et al., 2007; Naaim et al., 2013). As a result of the criteria used for sample site selection, historical records corresponding to the five studied paths are by far not the most complete in the EPA chronicle. Nevertheless, we assume that the quality of information reported for all events is reliable enough to be compared and/or merged with tree-ring chronologies. Note that for all the historical data, an avalanche year is considered as a year ("winter") during which at least one avalanche event was reported, as the main objective of this study is to compare avalanche–climate relations derived from dendrogeomorphic and historical data.

3.3 Modeled weather and snow data

The Météo-France observation network provides snow and weather data for France. However, the spatial coverage of this network is insufficient to characterize snow and weather conditions at very specific locations in the French Alps, such as for starting zones of avalanche paths. Consequently, the primary dataset used for the five sites analyzed in this study consisted of daily modeled snow and weather data from the SAFRAN-CROCUS model: SAFRAN (Durand et al., 1993) is a meteorological application that performs an objective analysis of weather data available from human and automatic meteorological networks over the elevations and aspects considered for the different massifs. SAFRAN combines the data observed with a preliminary estimation generally provided by large-scale weather forecasting models. CROCUS (Brun et al., 1989, 1992) is a numerical snow model used to calculate changes in energy, mass, and stratigraphy of the different layers in the snow cover. It uses only the meteorological data provided by SAFRAN as input and simulates temperature, density, liquid water content profiles, and snowpack layering at different elevations, slopes, and aspects, including the internal metamorphism processes.

The SC model chain has been used for retrospective snow and weather climate analyses (Durand et al., 2009a, 2009b). Specifically, using 44 yr of newly analyzed atmospheric model data from the 40-yr European Centre for Medium-Range Weather Forecast (ECMWF) reanalysis (ERA-40) project (Uppala et al., 2005), and complemented by datasets extracted

from the operational database of Météo-France, the SC model chain has been run on an hourly basis for a period starting in winter 1958/9. For more detail about the simulation setup and validation procedures, see Durand et al. (2009a, 2009b). The modelled data were successfully used in Castebrunet et al. (2012) to highlight snow and weather climatic control on snow avalanche occurrence fluctuations over the past 50 yr and at different regional scales in the French Alps.

In this study we use various daily outputs of these simulations for the four alpine massifs related to the paths studied (i.e. Mont-Blanc, Haute-Maurienne, Thabor, and Oisans massifs; Figure 28) over the period 1958/9 to 2008/9. Modeled data is available for three different elevations (1800, 2400, and 3000 m asl). The following weather and snowpack parameters were used:

- daily precipitation, temperature (minimum, maximum, and mean), maximum wind speed (SAFRAN output);
- for the main aspect (northern, eastern, southern, and western) and a 40° slope, the thickness of surface wet snow and the thickness of surface recent dry snow. These variables are derived from the standard CROCUS outputs: the thickness of surface wet snow is taken as the sum of the contiguous wet snow layers thermally characterized by a liquid water content greater than 0.01%, from the surface, and the thickness of the surface recent dry snow as the depth of the deeper recent snow layer characterized by a dendricity greater than 0.25.

In a given path, we considered only the variables corresponding to the main aspect and mean elevation of the starting zone. For example, in the *Avalanche des Pylônes* path, variables retained were those modeled for the northern aspect at 1800 m asl (Table 11). Note that the altitude 2400 m asl was considered as the starting zone mean elevation in the *Ressec* path, but an elevation of 3000 m asl could have been another reasonable choice, with presumably little influence on the final results.

3.4 Monthly standardized data

As dendrogeomorphic methods provide data on the year during which an avalanche event occurred, mean monthly climate values were thought to provide an appropriate level of resolution for comparison, as also emphasized by Hebertson and Jenkins (2003). Consequently, we calculated monthly values for December through May based on the daily outputs of the SAFRAN and CROCUS models. This was justified by the fact that all avalanche events recorded in the historical archives of the five paths were released within these six months. Precipitation values were summed, while temperature, wind and snow pack values were averaged. In addition to these variables directly derived from the models, several composite variables were calculated with the objective to raise particular anomalies resulting from extreme meteorological situations. A detailed list of the twenty variables calculated on a monthly basis is provided in Appendix 2.

The different variables X_{jt}, where j denotes the (monthly) variable and t the year, were standardized to produce yearly anomaly series as:

$$X_{jt}^{norm}(t) = \frac{X_{jt} - \mu_j}{\sigma_j} \tag{11}$$

where μ_j and σ_j are the interannual mean and standard deviation of X_{jt}, respectively. The goal of this standardization procedure is to facilitate inter-variable comparison and graphical visualizations, and to interpret the respective contribution of each covariate to the interannual fluctuations of avalanche activity. Another advantage is that it avoids numerical traps for numerical likelihood maximization in logistic regression models (see below).

3.5 Variable selection in logistic regression

Logistic regression is a special case of a formal generalization of linear regression concepts commonly summarized under the term *Generalized Linear Models* -GLMs. It was used to investigate the relationship between the dichotomous response variable, i.e., the occurrence or non-occurrence of avalanche events the year *t*, and a set of explanatory variables as:

$$logit(p_t) = \beta_0 + \beta_1 X_{1,t} + \ldots + \beta_k X_{K,t} \quad (12)$$

where p_t is the probability of an avalanche for the year t, $X_{j,J} \in [1, K]$ represents the K climatic factors used as regressors, β_0 the intercept and β_j the regression coefficients. The *logit* is simply the log odds ratio:

$$logit(p_t) = \ln\left(\frac{p_t}{1 - p_t}\right) \quad (13)$$

with an equivalent formulation:

$$p_t = \frac{1}{1 + e^{-(\beta_0 + \beta_1 X_{1,t} + \ldots + \beta_k X_{K,t})}} \quad (14)$$

Our calculations were performed under the glm package of the software R (R Development Core Team, 2011).

A specific difficulty was that the total number of potential explanatory variables amounted to 120, as each of the 20 snow and weather variables (Appendix 2) were calculated over the six months from December to May. To choose the best explanatory covariates of avalanche activity, we therefore carried out an original selection procedure in several steps within the logistic regression framework.

In the first step, we tested all covariates for marginal statistical significance in the logistic regression, considering p-values of $p \leq 0.2$ as small enough to keep a covariate. This relatively low significance threshold was retained so as to keep enough potential variables for the following steps (see below). Spearman's rank correlation coefficient $r$was then calculated for all possible pairs of remaining variables. This step was necessary as correlation between explanatory variables can lead to masking effects in an automatic variable selection procedure. For example, fresh snow depth data undoubtedly contain information already given by precipitation. At this stage, among the strongly correlated variables ($r > 0.5$), we kept only the one with the highest marginal significance.

A stepwise regression (e.g. Saporta, 2011) was then undertaken with the remaining covariates. This is a variable selection procedure originally designed for linear models but that can also be applied to certain classes of GLMs. With a stepwise procedure, the set of predictive variables retained is selected by an automatic sequence of Fisher F-tests. Starting from an initial *logit* model with no covariates and then comparing the explanatory power of incrementally larger and smaller models, it combines forward selection and backward elimination. Forward selection tests the variables one by one and includes them if they are statistically significant based on the p-value of the F-statistics, while backward elimination starts with all candidate variables and tests them one by one for statistical significance, deleting any of them that are not significant on the basis of the p-value of the F-statistics.

The stepwise selection generally led to multiple logistic regression models including less than five covariates, as expected. In some cases (depending on the chronology and path, see below), however, models obtained still had more variables. As our goal was to get a good compromise between a nearly maximal explanatory power and a restricted number of covariates, we finally kept only models with a maximum of four covariates, and with each covariate marginally significant at the 10% level. This has the advantage to allow a better interpretation of the retained models in terms of physics.

Such multivariate logistic regression models have been established for the three chronology types (dendrogeomorphic and historical datasets, as well as combined dataset) in the five studied paths.

Model performance was evaluated with several indicators. First, we checked if a given model provided a better fit to the data than the null model, i.e. the intercept-only model, by calculating the likelihood ratio test. Then, we tested the statistical significance of individual regression coefficients (i.e. the βs) using the Wald chi-square statistic. According to the selection procedure used, they are all significant at the 0.1 significance level, but this allowed checking the exact p-value for each of them. The test was also performed for the intercept, i.e. the constant term, to check if it should be included in the model (Peng et al., 2002). In addition, we considered the R^2 determination coefficient defined by Nagelkerke (1991), which is a variation of the R^2 concept defined for linear models to assess the fit of a

logistic model against the actual outcomes, i.e. avalanche occurrence/non-occurrence in our case.

Finally, we checked if modeled high probabilities p_t were indeed associated with events and low probabilities with nonevents. With a 0.5 probability threshold, this turns into calculating the sensitivity, measuring the proportion of correctly classified events, and the specificity, measuring the proportion of correctly classified nonevents. In a more qualitative investigation, we considered a 80% threshold to identify years corresponding to the highest snow and weather anomalies and confront them to the actual avalanche observations. This was done at the level of the linear regression, meaning that the considered 80^{th} percentile was the one of the model interannual distribution. In other words, 20% of the annual values of the $logit(p_t)$ series are, by definition, above the threshold, indicating the years for which the retained combination of snow and weather variables is the most favorable to avalanche occurrence.

4 Results

4.1 Avalanche event chronologies derived from dendrogeomorphic and/or historical data

The focus of this study is limited to the period 1959−2009, for which snow and weather data is available. Tree-ring analysis allowed identification of hundreds of GD related to snow avalanche impacts in the trees sampled at the five study sites. A detailed presentation of all growth anomalies recorded in the tree-ring records in each path are given in Table 12. Based on the yearly distribution of reacting trees within the runout zone, a total of 19, 8, 12, 7, and 9 avalanche events are identified in the *Avalanche des Pylônes*, *Pèlerins*, *Ressec*, *Château Jouan*, and *Ourcière* paths, respectively (Figure 29).

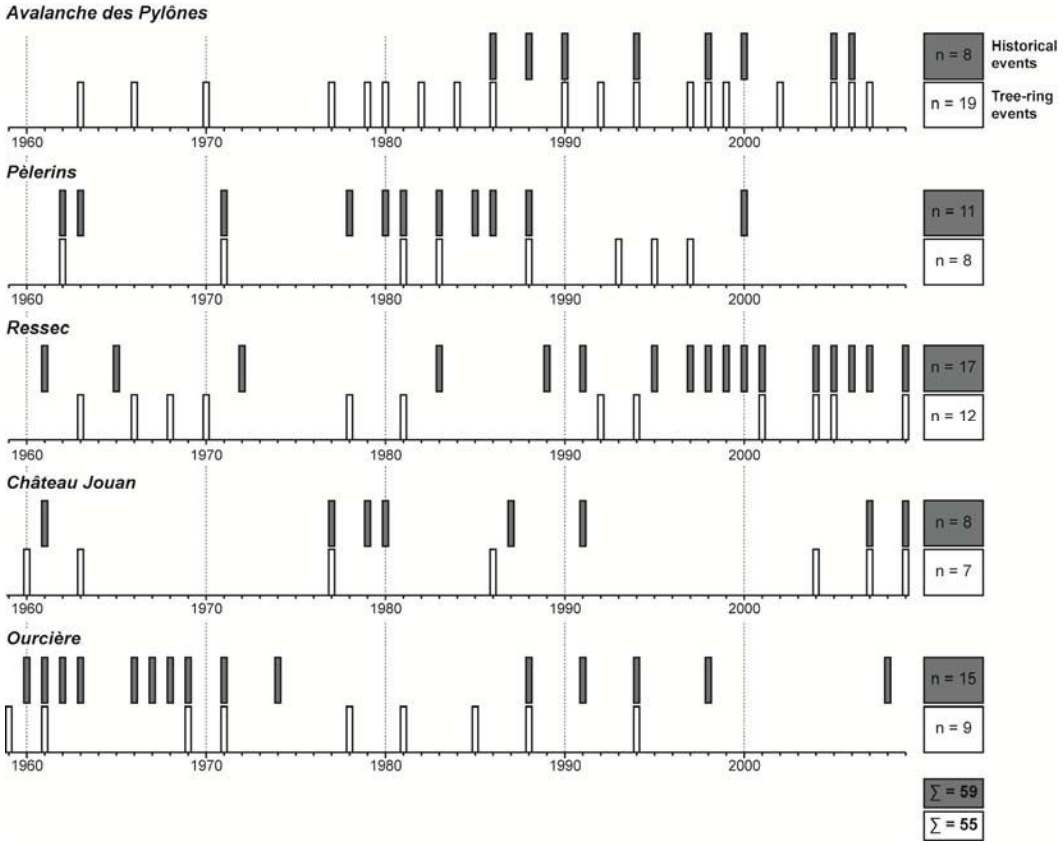

***Figure 29**. Snow avalanche years in the five paths. Grey and white features correspond to avalanche events derived from historical and dendrogeomorphic data, respectively.*

Historical data on avalanches (EPA) cover the period investigated in all but one of the studied paths. In the *Avalanche des Pylônes* path, the avalanche survey started only during winter 1985–6. In the five paths, the EPA reports between 8 to 17 years with avalanche activity over the period 1959−2009 (Figure 29). Note that only those events which reached the areas analyzed with dendrogeomorphic techniques have been considered as the main goal of this study was to compare results obtained with dendrogeomorphic records and historical data.

By combining the dendrogeomorphic and historical chronologies, the total number of events per path increased to 21, 14, 25, 12, and 19 avalanches in the *Avalanche des Pylônes*, *Pèlerins*, *Ressec*, *Château Jouan* and *Ourcière* paths, respectively (Figure 29).

4.2 Statistical relationships between snow/climate variables and avalanche activity

4.2.1 Snow and weather explanatory factors of avalanche events recorded in dendrogeomorphic data

Based on dendrogeomorphic data, logistic regression models related to the five paths use significant explanatory covariates, all at least above the 10% significance level (p-value < 0.1; Table 13), but often largely higher (i.e. with much smaller p-values). The likelihood ratio test is always highly significant ($p < 0.001$), suggesting that the different logistic models are better than a null model. This is reinforced by relatively good R^2 indices, ranging from 0.38 to 0.61. The models' specificity is high with rates varying between 87.5 and 97.7%. On the other hand, the models' sensitivity is somewhat lower and varies between 42.9 and 78.9%. This means that the models are generally more effective to characterize years with no avalanche event. However, most event years correspond well to strong anomalies in the selected combination of covariates. Indeed, 39 out of 55 events (71%) recorded in the five paths occurred in years for which the respective model exceeds the 80th percentile of its interannual distribution (Figure 30).

Each model uses between 2 to 4 covariates, and mainly consists in a combination of precipitation and temperature variables (Table 13, Figure 30). Note that the models for the *Avalanche des Pylônes* and *Ressec* paths also include snowpack variables. All except one variable have a positive contribution ($\beta_j > 0$), indicating that higher values imply higher probability of an avalanche year which seems intuitive, at least for precipitation and snowpack variables. Conversely, the temperature variable included in the model related to the *Ourcière* path (*Tmax_(*Jan*)*) has a negative contribution, indicating that high probabilities of avalanche years are more likely associated with low temperatures in that path, another meaningful result.

According to the weighting coefficients (β_j) and marginal correlation coefficients between models and covariates (ρ_j), precipitation and snow pack variables contribute more to the models than temperature variables (Table 13, Figure 30).

Path name	Explanatory variables X_j	$p-$ value	β_j	ρ_j	R^2	Sensitivity	Specificity	Overall prediction correction
Avalanche des Pylônes	Intercept	0.04	−0.91		0.58	78.9%	87.5%	84.3%
	*P_(*Feb*)*	0.00	1.56	0.53				
	*FreshSnow(*Dec*)*	0.01	1.91	0.50				
	*Tmoy_(*Dec*)*$_{>mean+2SD}$	0.01	1.13	0.37				
	*FreshSnow(*Jan*)*$_{>q90}$	0.02	1.21	0.42				
Pèlerins	Intercept	0.00	−2.84		0.59	62.5%	97.7%	92.2%
	*Pmoy3j_(*Apr*)*$_{>mean+2SD}$	0.01	1.42	0.60				
	*Tmin_(*Mar*)*$_{<mean-2SD}$	0.02	1.19	0.61				
	*Tmax_(*Dec*)*$_{>mean+2SD}$	0.06	0.77	0.45				
Ressec	Intercept	0.00	−1.45		0.38	50.0%	97.4%	86.3%
	*FreshSnow(*Jan*)*$_{>q95}$	0.01	1.28	0.80				
	*Tmax_(*May*)*$_{>mean+2SD}$	0.03	0.91	0.54				
Château Jouan	Intercept	0.00	−4.06		0.61	42.9%	97.7%	90.2%
	*Pmoy3j_(*Jan*)*$_{>mean+SD}$	0.03	2.05	0.60				
	*Pmoy3j_(*Apr*)*$_{>mean+2SD}$	0.04	1.98	0.58				
	*Tmin_(*Apr*)*	0.03	2.21	0.51				
Ourcière	Intercept	0.00	−1.99		0.53	66.7%	95.2%	90.2%
	*P_(*Mar*)*$_{>75}$	0.01	2.53	0.91				
	*P_(*Apr*)*$_{>75}$	0.06	0.61	0.18				
	*Tmax_(*Jan*)*	0.06	−1.04	−0.47				

***Table 13**. Logistic regression models $p_t = \sum_{j=1}^{K} X_{jt}^{norm} \beta_j$ at the path scale for the annual avalanche/non avalanche years derived from dendrogeomorphic data. For each explanatory variable retained, X_{jt}, β_j is the weighting coefficient, ρ_j the marginal correlation coefficient between X_{jt}^{norm} and p_t (the regression model seen as a time series), and R^2 the determination coefficient of the logistic regression (Nagelkerke, 1991).*

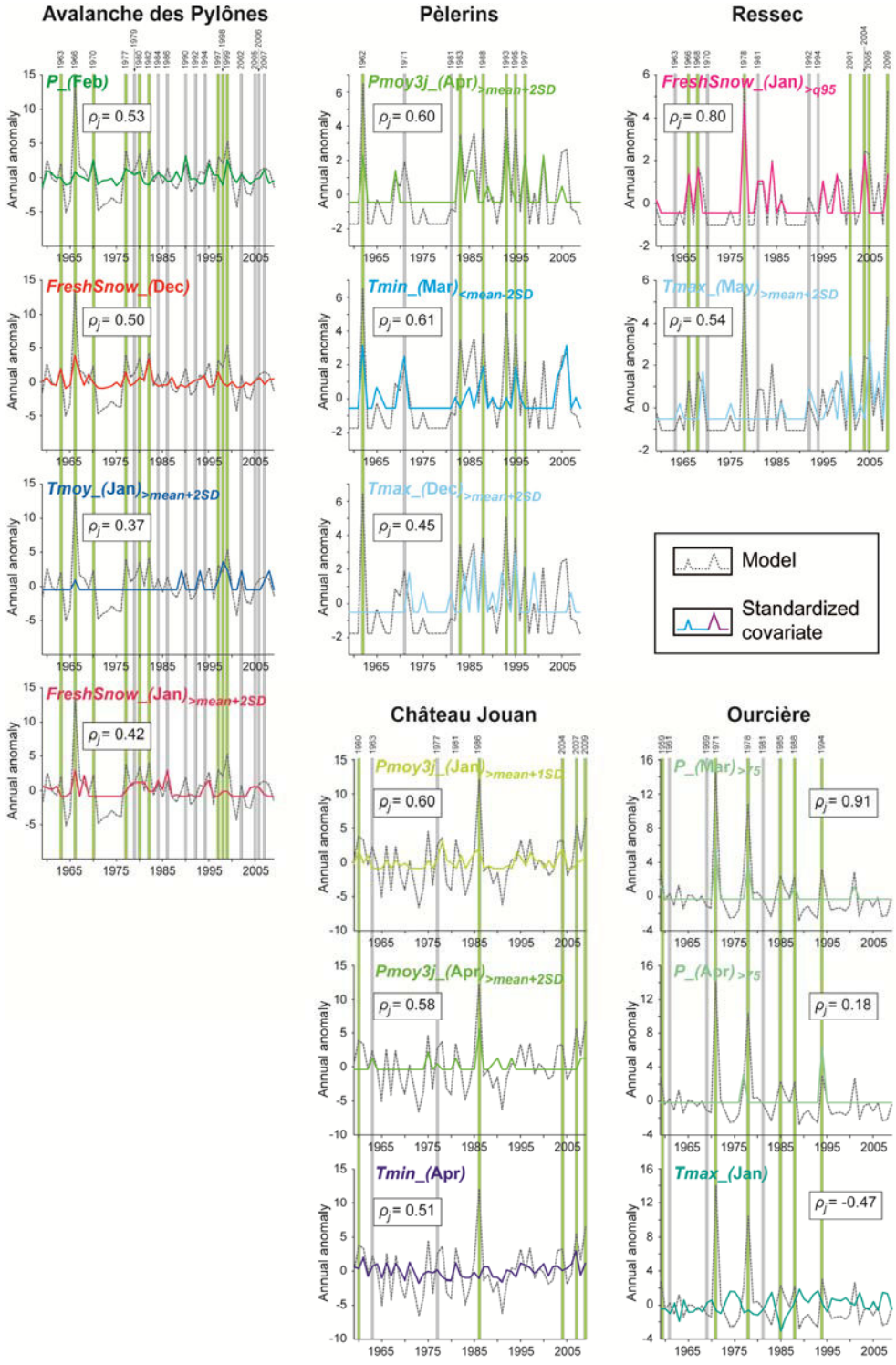

Figure 30. *Interannual anomalies in the covariates retained in the regression models related to avalanche activity derived from dendrogeomorphic data in the five paths.* ρ_j *is the marginal correlation coefficient between each covariate and the regression model seen as a time series. Green bands correspond to avalanche years for which the regression model is above its 80*th *percentile. Grey bands correspond to avalanche years for which the model does not exceed the threshold.*

4.2.2 Snow and weather explanatory factors of avalanche events reported in historical data

The five models related to historical data are based on a small number of covariates, all of them at least significant at the 10% significance level (Table 14). Note, however, that the intercept in the model related to the *Avalanche des Pylônes* path is insignificant ($p = 0.35$), suggesting that the alternative model without the intercept might be applied to the data as well.

The five models are better than the null model given the high significance of the likelihood ratio test ($p < 0.004$ in all cases) as well as the good R^2 indices (> 0.5). Cross-validation classification probabilities indicate that specificity is more than 90% in all models, while sensitivities range from 53.3 to 64.7% (Table 14). As for models related to dendrogeomorphic data, models better fit avalanche activity in nonevent years. Nevertheless, the 80th percentile is well exceeded in 58% of all event years (34 out of 59 events), meaning that most of the events eventually occurred during years with "strong" combinations of snow and weather anomalies (Figure 31).

Models related to historical data include 2 to 4 explanatory variables. Strikingly, most of them represent temperature variables. Snowpack factors are also included in three models, but no precipitation variable is retained (Figure 31). Note that the model related to the *Ourcière* path also uses an additional variable related to wind speed in March (*Vmax_(*Mar*)*).

Except for the model for the *Ressec* path, variables related to anomalies in maximum air temperature have a highly negative contribution. Hence, high peaks in the model generally correspond well to sharp "anti-peaks" in these negatively correlated variables, indicating that most of the events were recorded during years where abnormally cold episodes occurred. Noteworthy, marginal correlations (ρ_j) illustrate the preponderant role of temperature variables in comparison with those related to snowpack and wind speed variables.

Path name	Explanatory variables $_j$	p-value	β_j	ρ_j	R^2	Sensitivity	Specificity	Overall prediction correction
Avalanche des Pylônes	Intercept	0.35	−0.55		0.52	62.5%	93.8%	83.3%
	*Tmax_(*Apr*)*$_{>mean+1SD}$	0.05	−2.10	−0.72				
	*Tmax_(*Jan*)*$_{>mean+1SD}$	0.08	−1.41	−0.61				
Pèlerins	Intercept	0.00	−2.38		0.52	54.5%	92.5%	84.3%
	*Tmax_(*Jan*)*	0.01	−2.51	−0.77				
	*FreshSnow(*Apr*)*$_{>q95}$	0.01	1.65	0.46				
Ressec	Intercept	0.02	−1.07		0.58	64.7%	97.1%	86.3%
	*Tmin_(*Feb*)*$_{<mean-2SD}$	0.00	1.73	0.42				
	*Tmax_(*Mar*)*$_{>mean+2SD}$	0.04	1.22	0.34				
	*Tmax_(*Feb*)*$_{>mean+1SD}$	0.03	1.07	0.31				
	*Tmax_(*Apr*)*	0.04	1.38	0.51				
Château Jouan	Intercept	0.00	−3.43		0.54	62.5%	97.7%	92.2%
	*Tmin_(*May*)*$_{<mean-1SD}$	0.02	1.25	0.57				
	*WetSnow_(*Apr*)*	0.02	1.39	0.38				
	*Tmax_(*Jan*)*$_{>mean+1SD}$	0.07	−2.08	−0.77				
Ourcière	Intercept	0.00	−1.61		0.56	53.3%	91.7%	80.4%
	*Tmax_(*Dec*)*	0.00	−1.50	−0.62				
	*Vmax_(*Mar*)*	0.01	1.35	0.57				
	*Tmax_(*Feb*)*$_{>mean+2SD}$	0.08	0.94	0.22				
	*WetSnow_(*Dec*)*	0.01	1.44	0.10				

***Table 14**. Logistic regression models $p_t = \sum_{j=1}^{P} X_{jt}^{norm} \beta_j$ at the path scale for the annual avalanche/non avalanche years derived from historical data. For each explanatory variable retained, X_{jt}, β_j is the weighting coefficient, ρ_j the marginal correlation coefficient between X_{jt}^{norm} and p_t (the regression model seen as a time series), and R^2 the determination coefficient of the logistic regression (Nagelkerke, 1991).*

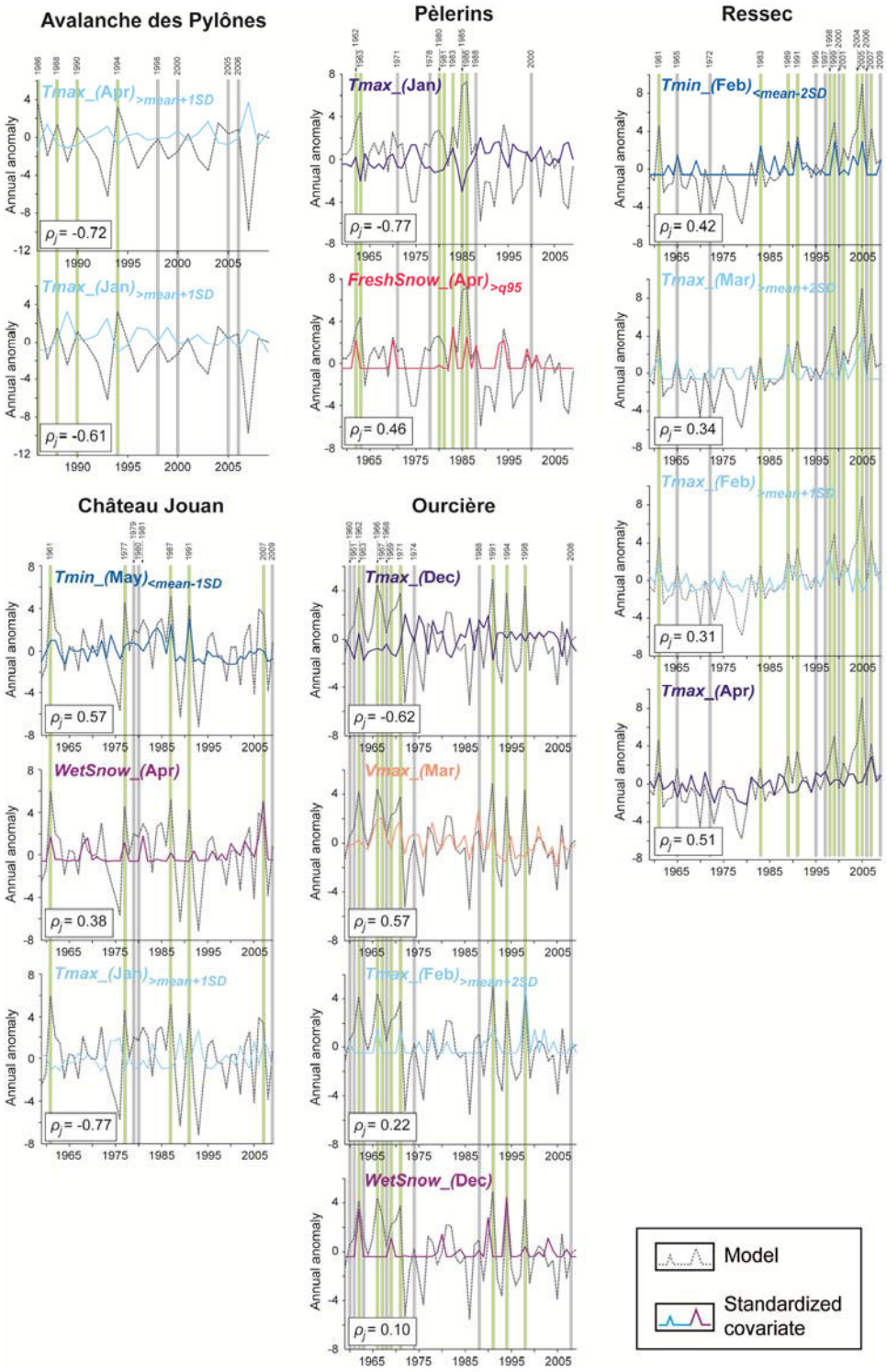

Figure 31. *Interannual anomalies in the covariates retained in the regression models related to avalanche activity derived from historical data in the five paths.* ρ_j *is the marginal correlation coefficient between each covariate and the regression model seen as a time series. Green bands correspond to avalanche years for which the regression model is above its* 80^{th} *percentile. Grey bands correspond to avalanche years for which the model does not exceed the threshold.*

4.2.3 Snow and weather explanatory factors of events derived from both datasets

While exploring statistical relations between snow/weather data and the chronology containing dendrogeomorphic and historical data, all models retain 2 to 4 significant ($p < 0.1$) explanatory factors (Table 15). In the models related to the *Avalanche des Pylônes* and *Ressec* paths, the intercept might not be considered given that it is far from the 10% significance level. According to the likelihood ratio test ($p < 0.003$ in all cases) and relatively satisfying R^2 indices ranging from 0.27 to 0.58, all models are better than the null model. Specificity is more than 90% in all but one model (the proportion of correctly classified nonevents derived from the model related to the *Ressec* path equals 76.9%, Table 15). On the other hand, sensitivity ranged from 41.7 to 80%.

These models are globally less accurate to fit avalanche activity in comparison with the models derived for the dendrogeomorphic or historical chronologies, as illustrated by overall prediction corrections (Table 15). Nevertheless, one in two events occurred in years with "strong" combinations of snow and climatic anomalies according to the fact that models exceed the 80th percentile of their interannual distribution in 45 out of 91 events.

Models are composed of a "composite" combination of precipitation, temperature and snowpack variables; they are more complex than the models composed solely of tree-ring or historical data. However, in a similar way as in the models related to dendrogeomorphic data, all but one variable have a positive contribution ($\beta_j > 0$). Only one variable, related to temperature (*Tmax_(*Jan*)*), shows a negative contribution in the model associated to the *Château Jouan* path (Table 15).

Path name	Explanatory variables $_j$	p-value	β_j	ρ_j	R^2	Sensitivity	Specificity	Overall prediction correction
Avalanche des Pylônes	Intercept	0.35	−0.35		0.52	71.4%	90.0%	82.4%
	*Pmoy3j_(*Feb*)*$_{>mean+1SD}$	0.01	1.10	0.65				
	*FreshSnow(*Dec*)*	0.01	1.48	0.39				
	*Tmax_(*Dec*)*$_{>mean+2SD}$	0.02	1.34	0.41				
Pèlerins	Intercept	0.00	−1.54		0.58	64.3%	91.9%	84.3%
	*Pmoy3j_(*Apr*)*$_{>mean+2SD}$	0.00	1.46	0.48				
	*FreshSnow(*Mar*)*$_{>q90}$	0.01	1.11	0.48				
	*FreshSnow(*May*)*	0.05	1.22	0.47				
	*Tmax_(*Dec*)*$_{>mean+2SD}$	0.07	0.75	0.30				
Ressec	Intercept	0.97	−0.02		0.50	80.0%	76.9%	78.4%
	*Tmax_(*Mar*)*$_{>mean+1SD}$	0.00	1.28	0.71				
	*Tmin_(*Dec*)*$_{<mean-1SD}$	0.02	0.94	0.53				
	*FreshSnow(*Jan*)*$_{>q95}$	0.04	1.08	0.37				
Château Jouan	Intercept	0.00	−1.53		0.36	41.7%	97.4%	84.3%
	*Tmax_(*Jan*)*	0.03	−1.04	−0.86				
	*Tmin_(*May*)*$_{<mean-2SD}$	0.04	0.93	0.63				
Ourcière	Intercept	0.08	−0.59		0.27	57.9%	93.8%	80.4%
	*FreshSnow(*Jan*)*	0.01	0.88	0.86				
	*Tmax_(*Feb*)*$_{>mean+2SD}$	0.08	0.81	0.45				

***Table 15**. Logistic regression models $p_t = \sum_{j=1}^{P} X_{jt}^{norm} \beta_j$ at the path scale for the annual avalanche/non avalanche years derived from both dendrogeomorphic and historical data. For each explanatory variable retained, X_{jt}, β_j is the weighting coefficient, ρ_j the marginal correlation coefficient between X_{jt}^{norm} and p_t (the regression model seen as a time series), and R^2 the determination coefficient of the logistic regression (Nagelkerke, 1991).*

5 Discussion

In the last decades, dendrogeomorphology has been increasingly used for the identification of snow avalanche activity worldwide (e.g., Butler and Malanson, 1985; Casteller et al., 2008; Corona et al., 2010; Germain et al., 2009). Although recent studies highlighted that tree-ring reconstructions tend to underestimate years with natural activity by roughly 60% (Corona et al., 2012a; Schläppy et al., 2013), dendrogeomorphic data represents a valuable data pool for the assessment of runout distances and return periods of extreme avalanche events on forested paths with limited or no historical data (Schläppy et al., 2014; Stoffel et al., 2006).

Several studies also explored the link between climate and avalanche activity derived from tree rings and were able to emphasize various explanatory factors (Corona et al., 2010; Dubé et al., 2004; Germain et al., 2009; Hebertson and Jenkins, 2003; Reardon et al., 2008). However, given the fact that tree-ring reconstructions miss a certain number of avalanche events and due to their poor temporal (annual or at best seasonal) resolution, it seems necessary to evaluate the relevance of using dendrogeomorphic data to explore such climate-avalanche relations.

With this end in view, we first reconstructed avalanche activity in five paths distributed across the French Alps and with differing site-related characteristics (Table 11). Based on refined daily snow and weather data over 51 yr, we derived a comprehensive set of 120 climatic and composite variables potentially related to avalanche occurrences on a monthly basis (Appendix 2Description of snow and weather variables). The best of them to explain avalanche activity recorded in tree-ring chronologies were highlighted, and a similar approach was used with event chronologies derived from historical archives as well as with a third data set composed of a combination of both chronology types.

We have used modeled snow and weather data instead of actual observations. These data result from assimilation of all available information and reliable physical rules regarding the snow metamorphism, snowmelt, etc. Furthermore, they have been extensively validated with comparison to point measurements (Durand et al., 2009b). On the other hand, the

relevance of using regional (massif scale) snow and weather data may be questioned as the present study focused on the path scale. This choice was primarily driven by the fact that no long-term series of observation was available at the direct vicinity of the studied paths. Daily modeled data derived from the SC model chain have the advantage of having spatial significance and, in turn, of better reflecting the actual meteorological conditions in the starting zone compared to observations from distant stations.

Because of the very large number of variables involved in the analysis, it was necessary to implement an original variable selection procedure within the logistic regression framework. Starting from a rather non-constraining criteria (i.e. statistical significance > 0.2), different steps including a stepwise procedure led to models able to represent avalanche year occurrence/non-occurrence with relative confidence, highlighting significant statistical relations between avalanche activity and anomalies in reasonably small sets (two to four) of snow/climate variables (Table 13—Table 15). This procedure constitutes the methodological outcome of this work, which could be used in the future for other similar problems.

For the different chronologies/paths, specificities were found to be higher than sensitivities, meaning that nonevent years are more effectively identified by the models than event years in average. This probably results from the relatively weak proportion of years with avalanche occurrence. Nevertheless, according to the 0.5 probability threshold and the model 80^{th} percentile threshold, almost all events correspond to anomalies in the selected combinations of covariates, with more than one in two events (55%) related to exceedances of the 80% threshold (Figure 30 & Figure 31). Furthermore, the retained variables generally make sense, influencing avalanche release probabilities in rather intuitive ways.

The global evaluation of the different models yielded satisfactory results. However, one should keep in mind that statistical models do not demonstrate causality but only highlight a coherent interannual evolution of avalanche activity indicators and selected covariates. As a consequence, it seems natural that models resulting from a variable selection procedure are not always fully interpretable. This is, for instance, well illustrated by the model related to historical data in the *Ressec* path, where three covariates related to monthly maximum

temperature anomalies have been retained to contribute positively to avalanche occurrences (Table 14). Such a relationship may be relatively difficult (if not impossible) to interpret in terms of physical processes.

Discrepancies between the models obtained for different types of chronology are sometimes striking and may help to understand the initial question of how informative dendrogeomorphic data are for the assessment of avalanche-climate relations. Indeed, as corroborated by most explanatory variables retained in the "tree-ring models" (Table 13, Figure 30), our results seem to indicate that trees preferentially record events which occur during cold episodes accompanied by heavy precipitation. Such meteorological conditions are mainly observed during the coolest winter months. Similar results were found by Corona et al. (2010) who showed that avalanche activity registered in tree rings in a path of the French Alps was correlated to above-average snowfalls and abnormally low temperatures. On the other hand, EPA models indicate that avalanche events reported in historical archives are mainly related to temperature anomalies as well as, to a lesser extent, to wind and snowpack anomalies, and that these events occurred mostly in late winter.

These discrepancies may indicate that dendrogeomorphic data record the link between snow/climate and avalanche occurrences to a certain extent only, registering well certain types of avalanches, and less well other types of events. The symmetric conclusion is also true for medium-quality historical archives (the five studied paths are by far not the best documented in the EPA chronicle). As the interactions between snow and material transported in the avalanche flow and living trees are complex and have not been studied in detail so far, care must be taken to go further into the interpretation. Nevertheless, some qualitative insights can be gained.

During severe winter storms, visibility is often bad, and many avalanches occur simultaneously, so that an important proportion of them may be missed by human observation on remote paths or on paths were risk exposure is low. However, such "full" winter events may be large enough in terms of e.g., extent or snow volume to affect a significant number of trees, and may thus be registered in tree-ring records. On the other hand, during spring, visibility is often better and avalanches tend to be more sporadic. These

generally wet snow avalanches are therefore only rarely missed by less busy rangers in charge of observation, whereas their extent may be too small to affect a significant number of trees and may thus not be recorded in tree-ring chronologies. Somewhat similar conclusions were highlighted by Castebrunet et al. (2012) where high EPA avalanche counts have been shown to often correspond to years where strong temperature and wet snow anomalies occurred, whereas a classical instability index with high values has more often been described for cold and snowy winters.

The fact that both types of data tend to record avalanche events having occurred in different contexts, and thus presumably with very different characteristics (roughly speaking wet or dry snow avalanches, even if this is certainly not always true) is probably the reason why models resulting from the combined chronology are hard to interpret, and do not hive higher specificity, sensitivity, or predictive ability than the models for the separated EPA and tree ring chronologies.

Another issue is the strong variability between the five study paths, both in terms of mean activity (in terms of mean number of events per year) and retained generating factors (i.e. the variables in the regression models). Indeed, since weather conditions vary substantially according to path location, the triggering factors of avalanche can logically be very different from one path to another, as illustrated by the different covariates retained in the different models, independently of the type of chronology considered (Table 11). Moreover, terrain variables are known to influence avalanching since they control slope characteristics, strongly influencing mean activity. This was clearly illustrated in the *Avalanche des Pylônes* path which represents a singular situation in comparison with the other paths. Indeed, its very steep slope coupled with south-facing aspect seem to be responsible for more frequent avalanche releases as suggested by the high number of events ($n = 19$) recorded in the tree-ring series (Figure 29). Nevertheless, possible explicative terrain variables were not considered in this analysis as the main objective was to evaluate the contribution of dendrogeomorphic data to the understanding of avalanche-climate relations independently of the mean activity of each path.

6 Conclusion and outlook

This study highlights that clear statistical relations can be found between snow/climate variables and dendrogeomorphic or historical avalanche chronologies at the local scale. Our results confirm that dendrogeomorphic data may contribute to a better understanding of the link between snow/climate and avalanche activity, but only to a certain extent, and for avalanches occurring in “full” winter conditions. On the other hand, and for the sites investigated, historical archives tend to miss the winter events, whereas most spring avalanches seem to be recorded, by contrast, in the EPA database. Moreover, a combination of dendrogeomorphic and historical chronologies remains problematic in view of refining the study of climate-avalanche relations, whereas the combined use of both approaches has been shown to be helpful in the context of risk assessment (e.g., Schläppy et al., 2014). All analyses presented here, including the model fits and variable selection, have been realized under the assumption of stationarity. As a consequence, we did not consider the existing potential of dendrogeomorphic data to inform about long-term climatic evolution and its influence on avalanche activity. This choice was made because event chronologies were too diverse from one path to another, too short, and, more generally, presumably too lacunar (few “ones” among many “zeros”) to infer possible trends in relation to climate change at the scale of a single path.

However, a clear climate control of avalanche activity exists in the French Alps in the current context of global warming (Castebrunet et al., 2012, 2014; Eckert et al., 2010a, 2010c, 2013), and similar approaches as the one presented here should be performed at the regional scale and by pooling as many tree-ring chronologies as possible. The valuable information contained in the substantial EPA database could then allow evaluating the contribution of dendrogeomorphic data for the documentation of the response of avalanche activity to climate change.

Acknowledgements

The authors gratefully acknowledge Louis Manière and Matthieu Schläppy for their assistance in the field. They also want to thank the Office National des Forêts (ONF) for sampling permissions. This study has been realized within the framework of the MOPERA (MOdélisation Probabiliste pour l'Evaluation du Risque d'Avalanche) program funded by the French National Research Agency (ANR-09-RISK-007-01). SCM data have been provided by MétéoFrance within the framework of the ECANA (Etude Climatologique de l'Activité Avalancheuse NAturelle) project, and feedback/comments from S. Morin and G. Giraud are acknowledged. Finally, R.S. acknowledges financial support from the Swiss National Science Foundation (project P1SKP2_148492).

CHAPTER E

SYNTHESIS

1 Conclusions

Since the 1970s, dendrogeomorphology has been repeatedly used worldwide to reconstruct past activity of avalanches, especially on forested paths where there is little or no historical data available. In addition, several researchers have used this approach to find relationships between snow and weather variables and avalanche activity. Surprisingly, little attention has been paid so far to assess the accuracy and relevance of dendrogeomorphology for these particular uses in the field of snow avalanche science.

In this PhD thesis, snow avalanche activity was reconstructed in five paths of the French Alps using tree-ring techniques. The focus has been put on the assessment of the possibilities and limitations of tree-ring analyses in snow avalanche research. The main achievements of this thesis were developed in three papers presented in CHAPTER B, CHAPTER C and CHAPTER D. Here, we sum up the principal conclusions in regards to the different objectives stated initially.

1.1 An improved tool for the identification of snow avalanche events

In the first part of this PhD thesis (CHAPTER B), we presented a new tree-ring-based semi-quantitative approach for the identification of avalanche events. Based on the analysis of more than 500 disturbed conifers in three different avalanche paths, we were able to reconstruct a total of 75 avalanche events for the period 1799—2010. As the semi-quantitative approach relies on the assessment of the number and position of disturbed trees within avalanche paths as well as on the intensity of reactions in trees, the principal objective of this study was to demonstrate that no bias was induced by the dendrogeomorphic expert. Based on a statistical evaluation (Classification Trees, or CART) of the approach, we pointed out the consistency and replicability of the procedure. In addition, we emphasized that the approach is not restricted to the identification of high-magnitude avalanches and allows determination of relatively small events. Futhermore, we aimed at evaluating the quality and completeness of tree-ring records. Comparison between the avalanche years recorded in a substantial database in a well-documented path in Chamonix and those defined with dendrogeomorphic techniques showed that the avalanche record

reconstructed from tree-ring series contains 38% of the observed events. Despite the fact that dendrogeomorphic data miss a significant number of avalanches, the semi-quantitative approach can provide valuable information on past snow avalanche activity dating back to centuries, especially where there is little or no historical data available.

1.2 Tree-ring data contain valuable information to anticipate future extreme avalanche events

The second objective of this work (CHAPTER C) was to perform the first cross-validation of high return period avalanches derived from a locally calibrated statistical-dynamical model and the long-term, higher-return period information gathered from tree-ring records. We used dendrogeomorphic records from several hundreds of trees impacted by snow avalanches in their runout zone to reconstruct past activity in two avalanche paths of the French Alps. Based on the reconstructed distribution of runout distance of 25 events for the period 1799–2010 and mean event frequencies, we successfully derived runout values for events with return periods of $\leq$ 300 yr. Comparison of relations between runout distance and return periods between both approaches shows very good agreement. Indeed, within the classical intervals used in hazard zoning (i.e. 10–300 yr), mean and mean square errors amounted to $\sim$20 and 30–45 m, respectively. This showed that, despite various source of uncertainty related to both approaches, dendrogeomorphic data can be seen as a valuable data pool for the assessment of runout distances and return periods of extreme avalanche events in forested areas. At the same time, we illustrated that the statistical-dynamical model used in this study can be used with reasonable confidence to predetermine high return period avalanches, providing at the same time information on avalanche velocity, pressure and snow depth.

1.3 Trees may preferentially record avalanche events occurring in “full winter” conditions

The last objective of this PhD thesis (CHAPTER D) was to evaluate the relevance of climate-avalanche relationships inferred from tree-ring chronologies at the local scale, given the fact that dendrogeomorphic reconstructions miss a significant number of avalanches. To do so, we firstly reconstructed past avalanche activity in five scattered paths of the French

Alps with various site-related characteristics. Based on refined daily snow and weather data for the period 1959–2009, we defined a large set of potential variables that could explain avalanche activity and picked up the most pertinent of them using a variable selection procedure implemented within a logistic regression framework. A similar approach was then used with event chronologies derived from historical archives as well as with a third data set composed of a combination of both chronology types. Our study highlighted that clear statistical relations can be found between snow/climate variables and dendrogeomorphic or historical avalanche event chronologies at the local scale. In addition, we suggest that dendrogeomorphic data may contribute to a better understanding of the link between snow/climate and avalanche activity, but only up to a certain extent, specifically, for avalanche events occurring during strong winter storms. Conversely, an important proportion of such events may be missed by human observation on remote paths or on paths were risk exposure is low. Finally, it appeared that combining tree-ring data and historical archives for refining the study of climate-avalanche relations remains a difficult and open problem, while the combined use of both approaches has been shown to be helpful in the context of risk assessment (refer to previous section).

2 Further research

All studies included in this PhD thesis aimed at emphasizing the various contributions of dendrogeomorphology applied to snow avalanche science in the context of risk assessment. At the same time, an effort has been made to point out the limitations of this approach as objectively as possible.

Only five avalanche paths have been studied, as the different steps involved in tree-ring data collection and analysis are very time-consuming. For this reason, we call for further work in order to replicate procedures developed in this research. Specifically, the most relevant perspectives may be the followings:

- A new tree-ring-based, semi-quantitative approach for the identification of past snow avalanche events was presented. This approach has been demonstrated to be consistent and replicable, considering the very good results from the statistical validation that was implemented. However, since the datasets used in this study were quite small, the classification tree was rather sensitive. In the future, calibrating such a model using a larger dataset with more avalanche paths could help to standardize dendrogeomorphic procedures and therefore improve the determination of snow avalanche years.

- Dendrogeomorphic data may be useful for the validation of runout distance–return period relations derived from a statistical-dynamical model. Hence, it is hoped that the information contained in tree-ring records could be used in the future to evaluate in more details the various modeling assumptions required to simulate velocity and/or pressure fields distributions within the statistical-dynamical set-up, and to propose subsequent model improvements.

- Dendrogeomorphic data may contribute to a better understanding of the link between snow/climate and avalanche activity at the path scale. As recent studies emphasized a clear climate control of avalanche activity in the French Alps in the current context of warming, it might be of great interest to perform a similar

approach at the regional scale using as much tree-ring chronologies as possible together. The valuable information contained in the substantial EPA database could then make it possible to evaluate the contribution of dendrogeomorphic data for documenting the response of avalanche activity to climate change.

CHAPTER F

APPENDICES

1 Appendix to Chapter C

1.1 Statistical-dynamical model

Following Naaim et al. (2004), dense avalanche flow propagation is modeled with depth-averaged Saint Venant equations, but, to facilitate the specification of the input conditions corresponding to each simulation and to reduce computation times, snow incorporation and deposition are ignored. Variation in the momentum corresponds to the difference between gravity g and the robust (e.g., able to produce reasonable results in most occasions) Voellmy (1955) friction law. The equations of mass and momentum conservation in which v is the flow velocity, h is the flow depth, Φ is the local slope, and t is time are then:

$$\left.\begin{aligned} \frac{\partial h}{\partial t} + \frac{\partial (hv)}{\partial x} &= 0 \\ \frac{\partial (hv)}{\partial t} + \frac{\partial}{\partial x}\left(\alpha_{sv} h v^2 + k_{sv} g \frac{h^2}{2}\right) &= h\left(g \sin\Phi - \mu g \cos\Phi - \frac{g}{\xi h} v^2\right) \end{aligned}\right\} \quad (15)$$

k_{sv} represents the ratio between the stress normal to the slope and the stress parallel to the slope, and α_{sv} represents the shape of the vertical velocity profile. These equations are solved numerically using a finite volume scheme (Naaim, 1998). Classically, α_{sv} and k_{sv} were set to 1 for the entire study.

Traditionally (Salm et al., 1990), it is assumed that the coefficient μ summarizes snow properties as a function of e.g., altitude or exposure, whereas ξ is assimilated to a morphological parameter representing the roughness of the path. This interpretation of the Voellmy equation continues to be discussed (e.g., Ancey and Meunier, 2004), since it is not always fulfilled when calibration is undertaken on large data samples (Naaim et al., 2013). On the other hand, some theoretical justifications in its favor have been provided (Salm, 1993). We do not want to close the debate here, and adopt this simplification for a pragmatic reason: with regard to having two coefficients to estimate for each event, only

$n+1$ unknowns have to be estimated from the data. Hence, $\mu_1, i \in [1,n]$ are modeled as latent variables describing the random effects from one avalanche to another, and ξ as a parameter in the very statistical sense of the term.

Regarding probabilistic modeling of avalanche activity, avalanche frequency is assumed to be a Poisson distributed process (Eckert et al., 2007a), with its single parameter λ quantifying the mean annual avalanche number:

$$a|\lambda \sim P(\lambda) \tag{16}$$

The magnitude model embeds the propagation model within several probabilistic operators describing the variability of the different input–out quantities. First, the release abscissa x_{start} that corresponds to the beginning of the release zone is assumed to be purely random, and a Beta-distribution is a flexible choice to model various release zones behaviors (Meunier et al., 2001). However, since the Beta distribution is defined on the $]0,1[$ interval, a little restrictive normalization is necessary. The length of the release zone is used, so that the normalized release position x_{startn} is:

$$x_{startn}|\, a_1, a_2 = \frac{x_{start} - x_{min}}{x_{max} - x_{min}}\Big| a_1, a_2 \sim Beta(a_1, a_2) \tag{17}$$

where x_{max} and x_{min} are the maximal and minimal abscissas of the release zone that were estimated for the two case studies using simple topographical thresholds, and (a_1, a_2) the two parameters of the Beta distribution corresponding to each data set.

Given the normalized release abscissa x_{startn}, the mean release depth h_{start} is assumed to be gamma-distributed, with a parameterization reflecting the dependency of the snow depth on the release abscissa and a constant dispersion around the mean:

$$h_{start}|b_1, b_2, \sigma_h, x_{start} \sim Gamma\left(\frac{1}{\sigma_h^2}(b_1 + b_2 x_{startn})^2, \frac{1}{\sigma_h^2}(b_1 + b_2 x_{startn})^2\right) \tag{18}$$

This model is chosen to represent the skewness of a hydrological variable such as snow depth (where values much higher than the mean are plausible) as well as the possible variation of snow depth with altitude through the parameters (b_1, b_2, σ_h) of the Gamma mixture corresponding to each data set. For both case studies, release depths and other release dimensions corresponding to past observations were derived from deposit volumes of the EPA records as detailed in Eckert et al. (2010c), and/or from snow cover simulations (Durand et al., 2009b).

Given the normalized release abscissa and the flow depth, the latent friction coefficient μ is assumed to be normally distributed, with four parameters (c, d, e, σ) characterizing, for each case study, its dependency on the release abscissa and mean release depth and with a constant dispersion around the mean:

$$\mu|c, d, e, \sigma, x_{start}, h_{start} \sim N(c + dx_{startn} + eh_{start}, \sigma) \tag{19}$$

Small Gaussian differences between the observed runout distances $x_{stop_{data}}$ and the latent computed runout distances x_{stop} are postulated:

$$x_{stop_{data}}|\sigma_{num}, x_{stop} \sim N(x_{stop}, \sigma_{num}) \tag{20}$$

These differences can result from numerical errors due to the imperfection of the propagation model, and/or from observation errors. The standard deviation of these numerical errors σ_{num} is to be specified for model identifiability.

In summary, the proposed frequency model has only one parameter $\theta_F = \lambda$. Conversely, the magnitude model is relatively complex, with ten parameters $\theta_M = (a_1, a_2, b_1, b_2, \sigma_h, c, d, e, \sigma, \xi)$ and, for each avalanche, the latent friction coefficient μ and the computed runout distance x_{stop} measured on the horizontal axis starting at the top of the path. The different input variables and the latent friction coefficient μ are explicitly modeled as dependent variables, so as to take possible correlations into account that may affect extreme events. The joint probability of the magnitude observations given parameters and latent variables is obtained by combining the different conditional distributions:

$$p\left(x_{start}, h_{start}, x_{stop_{data}} \middle| \theta_M, \mu, x_{stop}, \sigma_{num}\right) = p(x_{start}|a_1, a_2)p(h_{start}|b_1, b_2, \sigma_h, x_{start})p\left(x_{stop_{data}} \middle| \sigma_{num}, x_{stop}\right) \quad (21)$$

μ appears in the right-hand side term only indirectly, by constraining the deterministic propagation and the runout distance x_{stop}.

1.2 Bayesian calibration on historical data and posterior sampling

Under the magnitude–frequency independence hypothesis, the frequency and the magnitude models can be inferred separately. As detailed in (Eckert et al., 2010c), it is straightforward for the frequency model. For the magnitude model, the joint posterior of all unknown is:

$$\begin{aligned} p\left(\theta_M, \mu, x_{stop} \middle| data, \sigma_{num}\right) & \\ & \propto \pi(\theta_M) \times p\left(x_{start}, h_{start}, x_{stop_{data}} \middle| \theta_M, \mu, x_{stop}, \sigma_{num}\right) \\ & \times p\left(\mu, x_{stop} \middle| \theta_M, x_{start}, h_{start}, x_{stop_{data}}, \sigma_{num}\right) \end{aligned} \quad (22)$$

where data denotes all observations $\left(x_{start_1}, h_{start_1}, x_{stop_{data_1}}, \dots, x_{start_N}, h_{start_N}, x_{stop_{data_N}}\right)$. $\pi(\theta_M)$ is the prior distribution detailed in text and Table 6. $\left(x_{start}, h_{start}, x_{stop_{data}} \middle| \theta_M, \mu, x_{stop}, \sigma_{num}\right) = \prod_{i=1}^{n}\left(p\left(x_{start_i}, h_{start_i, x_{stop_{data_i}}} \middle| \theta_M, \mu, x_{stop}, \sigma_{num}\right)\right)$ is the likelihood of the independent triplets $\left(x_{start_i}, h_{start_i}, x_{stop_{data_i}}\right), i \in [1, n]$. $p\left(\mu, x_{stop} \middle| \theta_M, x_{start}, h_{start}, x_{stop_{data}}, \sigma_{num}\right)$, the probability of the latent variables given parameters and observations, is given by the model specification (Eq. (19)) combined with the deterministic propagation.

Numerical implementation was carried out using Markov Chain Monte Carlo schemes. Specifically, the Metropolis-Hasting algorithm (Metropolis et al., 1953) fully detailed in

Eckert et al. (2010c) was used, and convergence was carefully tested and granted using different chains starting at different point of the parameter space.

From the *posterior* mean $(\hat{\theta}_M, \hat{\lambda})$, the Bayesian estimator of the parameters of our model under the classic hypothesis of a quadratic loss function, $p(y|\hat{\theta}_M)$ and $p(a|\hat{\theta}_F)$ were obtained for both case studies. These distributions quantify the randomness of the process studied given the data. For $p(y|\hat{\theta}_M)$ that includes the marginal distribution of some variables of interest for hazard zoning (runout distance, velocity, flow depth, see Figure 20 for the Château Jouan case), a statistical-dynamical Monte Carlo approach is needed to obtain the distribution of the outputs of the numerical avalanche propagation model given the distribution of its inputs. The specified conditional distributions have to be used to integrate over the distribution of the latent friction coefficient μ:

$$p(y|\hat{\theta}_M) = \int p(x_{start}|\hat{a}_1, \hat{a}_2) \times p(h_{start}|\hat{b}_1, \hat{b}_2, \hat{\sigma}_h, x_{start}) \times p(x_{stop}|x_{start}, h_{start}, \mu, \hat{\xi}) \times d\mu \quad (23)$$

This was easily carried out in the numerical Monte Carlo set-up by propagating each set of simulated input variables.

2 Appendix to Chapter D

2.1 Description of snow and weather variables

2.1.1 Variables that were tested on a monthly basis analysis

- *P_(*month*)*: sum of precipitation during a specific month.
- *Tmin_(*month*)*: mean of the minimum daily temperature during a specific month.
- *Tmoy_(*month*)*: mean of the mean daily temperature during a specific month.
- *Tmax_(*month*)*: mean of the maximum daily temperature during a specific month.
- *Vmax_(*month*)*: mean of the maximum daily wind speed during a specific month.
- *WetSnow_(*month*)*: mean of the daily thickness of surface wet snow during a specific month.
- *FreshSnow_(*month*)*: mean of the daily thickness of surface recent dry snow during a specific month.

2.1.2 Composite variables based on the daily outputs from SAFRAN and CROCUS simulations

- *Pmoy3j_(*month*)*$_{>mean+1SD}$: number of times with the mean of 3 consecutive days of precipitation more than 1 standard deviation above the mean of precipitation during a specific month calculated for the whole period (1958/9–2008/9).
- *Pmoy3j_(*month*)*$_{>mean+2SD}$: number of times with the mean of 3 consecutive days of precipitation more than 2 standard deviations above the mean of precipitation during a specific month calculated for the whole period (1958/9–2008/9).
- *P_(*month*)*$_{>50}$: number of times with the sum of 3 consecutive days of precipitation more than 50 cm.

- *P_(*month*)*$_{>75}$: number of times with the sum of 3 consecutive days of precipitation more than 75 cm.

- *P_(*month*)*$_{>100}$: number of times with the sum of 3 consecutive days of precipitation more than 100 cm.

- *Tmin_(*month*)*$_{<mean-1SD}$: number of times with the daily minimum temperature less than 1 standard deviation beneath the mean of the minimum temperature during a specific month calculated for the whole period (1958/9–2008/9).

- *Tmin_(*month*)*$_{<mean-2SD}$: number of times with the daily minimum temperature less than 2 standard deviation beneath the mean of the minimum temperature during a specific month calculated for the whole period (1958/9–2008/9).

- *Tmoy_(*month*)*$_{>mean+1SD}$: number of times with the daily mean temperature more than 1 standard deviation above the mean temperature during a specific month calculated for the whole period (1958/9–2008/9).

- *Tmoy_(*month*)*$_{>mean+2SD}$: number of times with the daily mean temperature more than 2 standard deviation above the mean temperature during a specific month calculated for the whole period (1958/9–2008/9).

- *Tmax_(*month*)*$_{>mean+1SD}$: number of times with the daily maximum temperature more than 1 standard deviation above the mean of the maximum temperature during a specific month calculated for the whole period (1958/9–2008/9).

- *Tmax_(*month*)*$_{>mean+2SD}$: number of times with the daily maximum temperature more than 2 standard deviation above the mean of the maximum temperature during a specific month calculated for the whole period (1958/9–2008/9).

- *FreshSnow(*month*)*$_{>q90}$: number of times with the daily thickness of surface recent dry snow more than the 90th percentile during a specific month calculated for the whole period 1958/9—2008/9.

- *FreshSnow(*month*)*$>_{q95}$: number of times with the daily thickness of surface recent dry snow more than the 95th percentile during a specific month calculated for the whole period 1958/9—2008/9.

3 Maps of snow avalanche years

3.1 *Avalanche des Pylônes* path

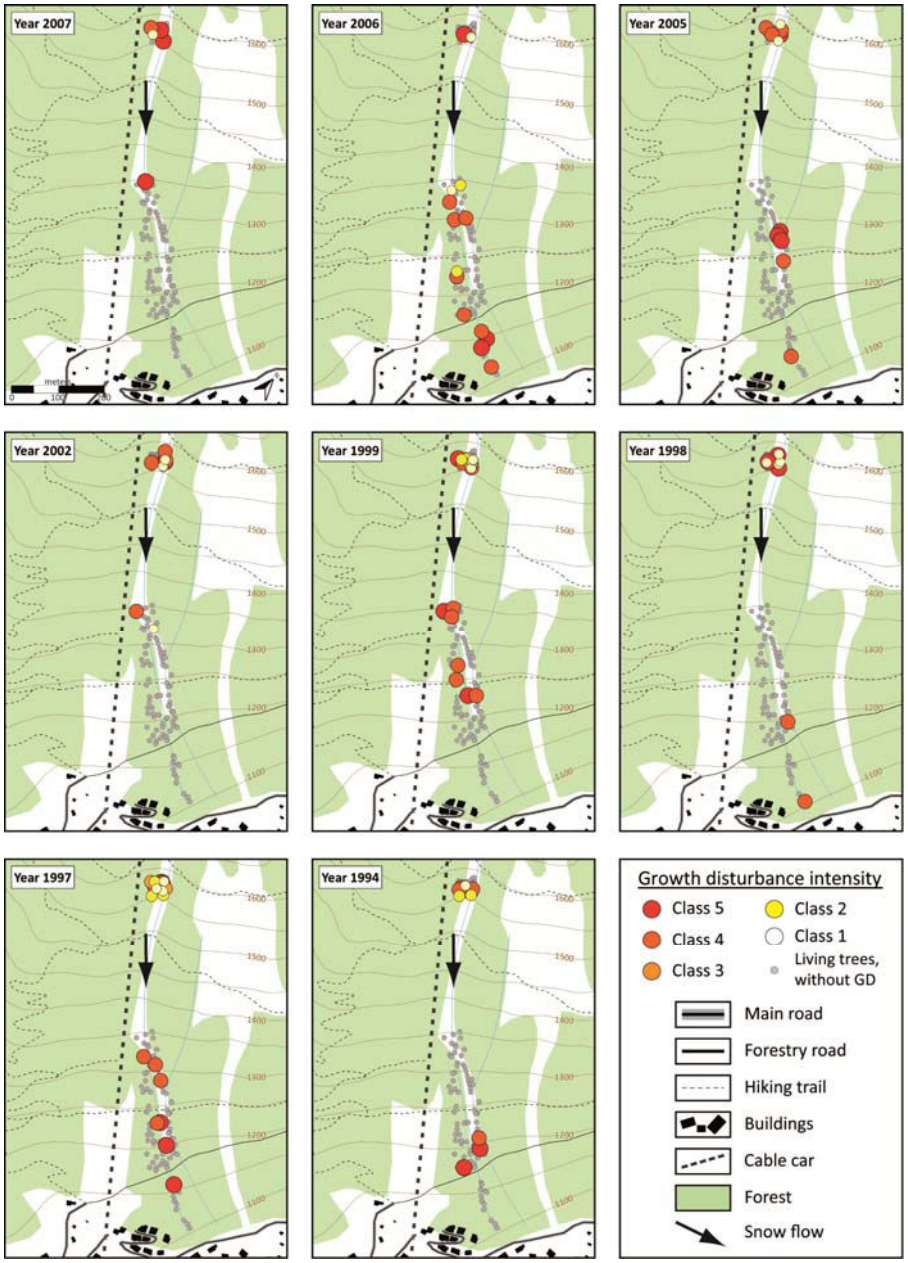

Spatial distribution of disturbed trees in the Avalanche des Pylônes path for the years identified as avalanche years – period 1994–2007.

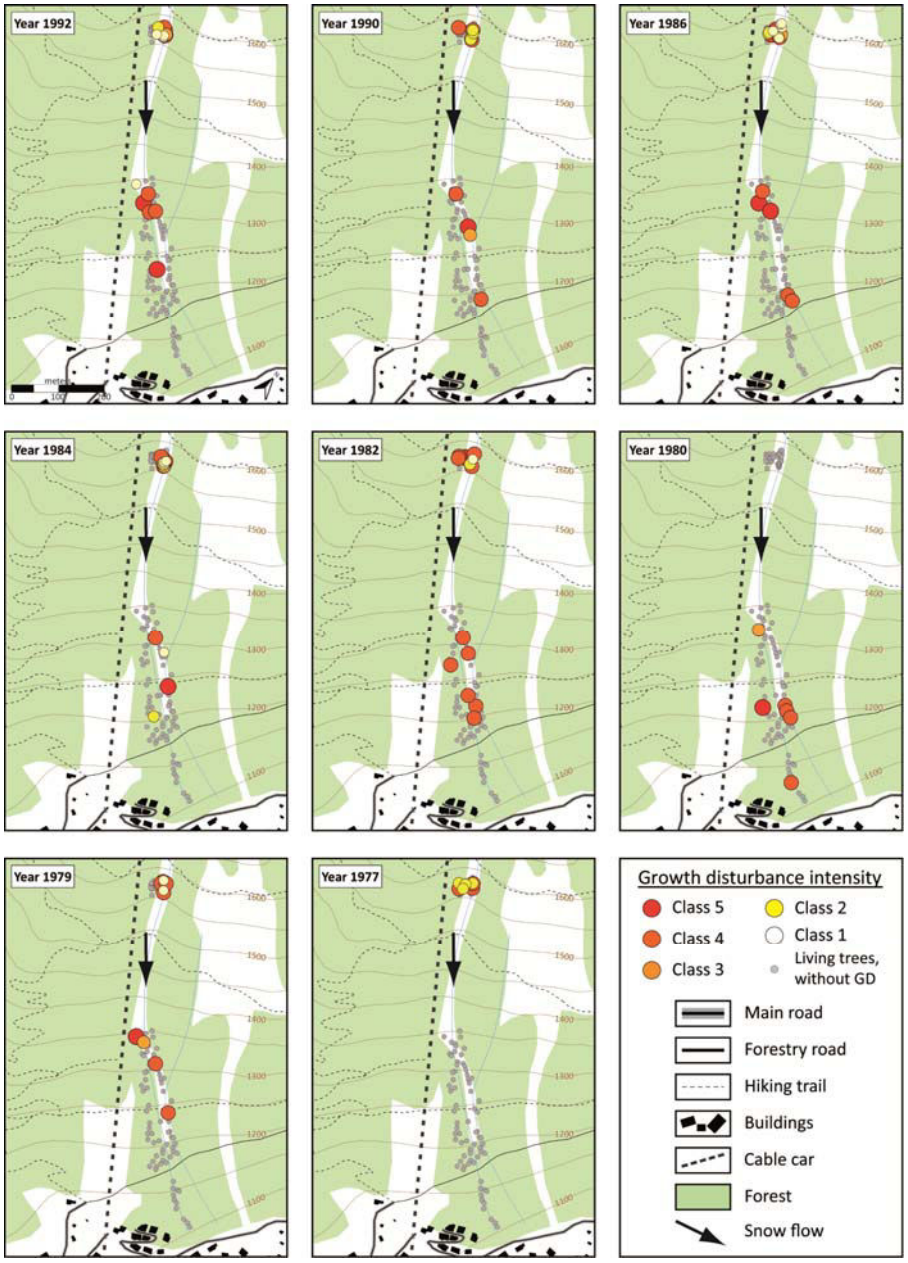

Spatial distribution of disturbed trees in the Avalanche des Pylônes path for the years identified as avalanche years – period 1977–1992.

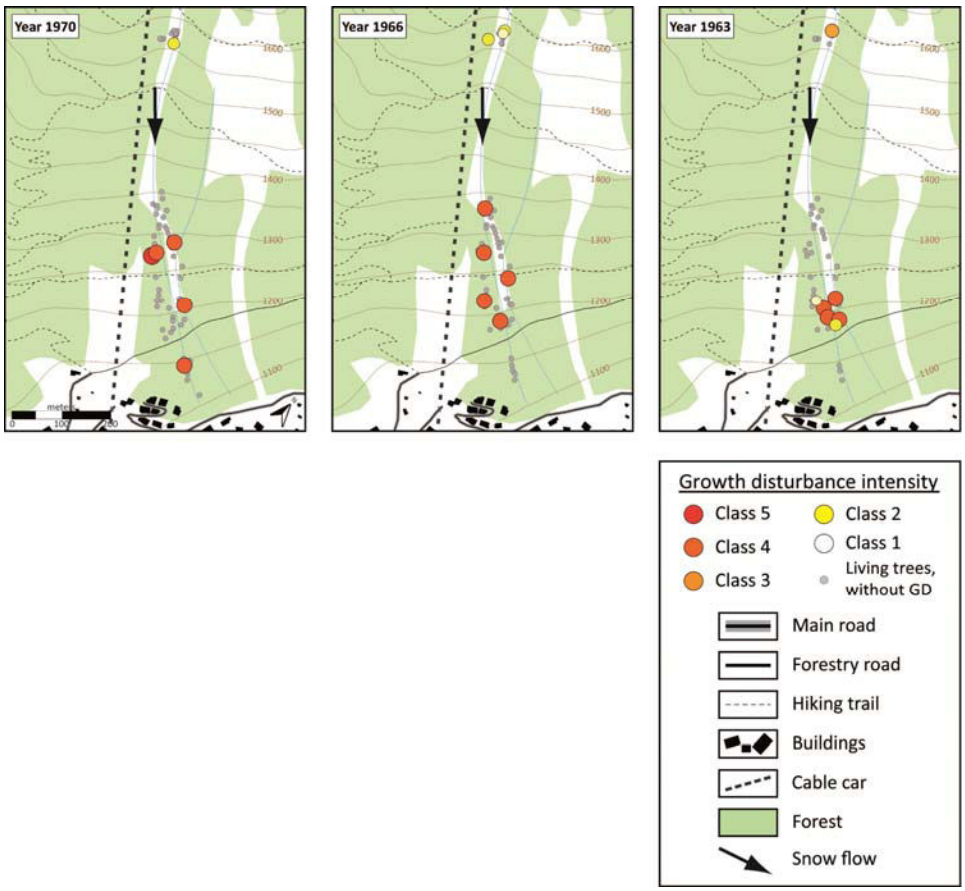

Spatial distribution of disturbed trees in the Avalanche des Pylônes path for the years identified as avalanche years – period 1963–1970.

3.2 *Pèlerins* path

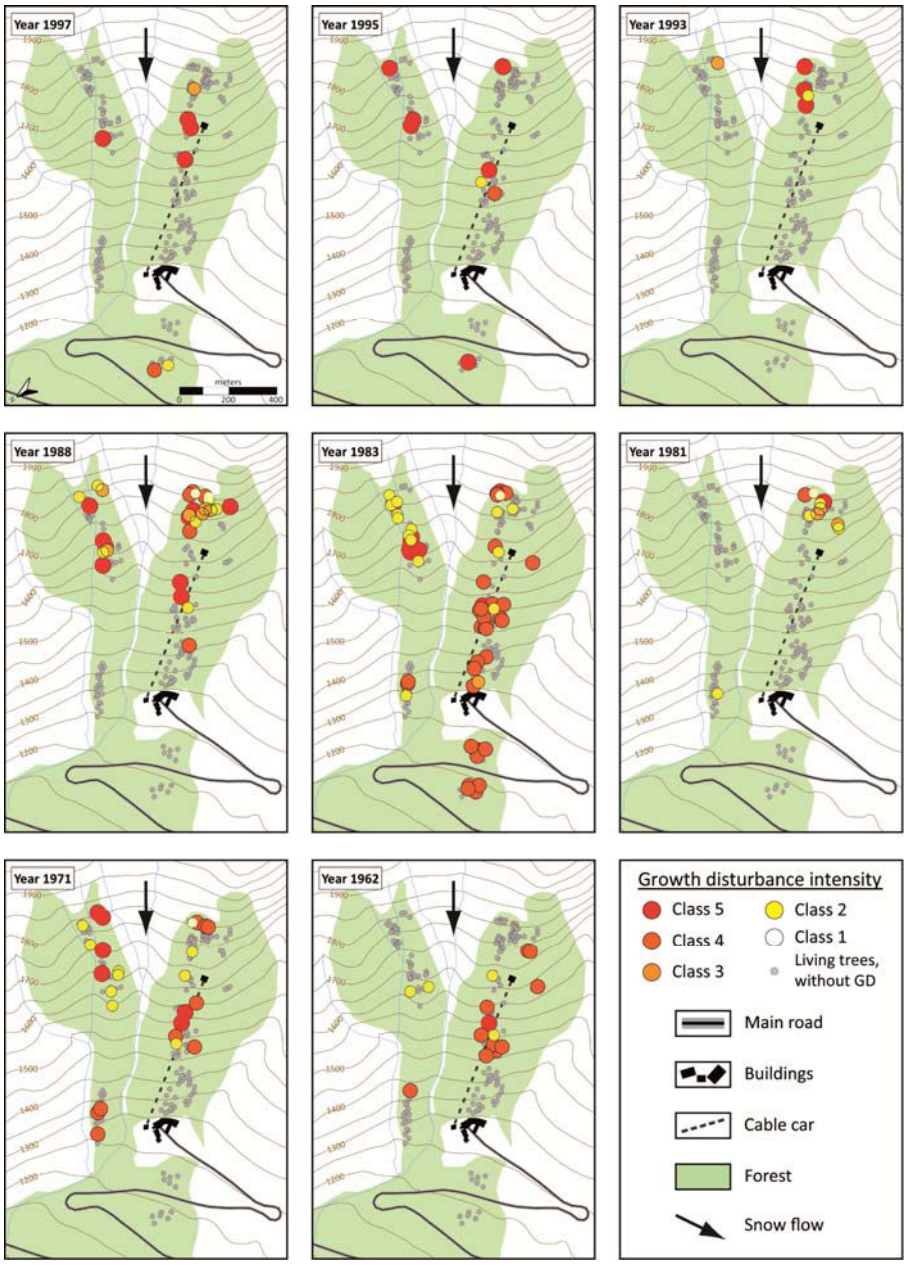

Spatial distribution of disturbed trees in the Pèlerins path for the years identified as avalanche years – period 1962–1997.

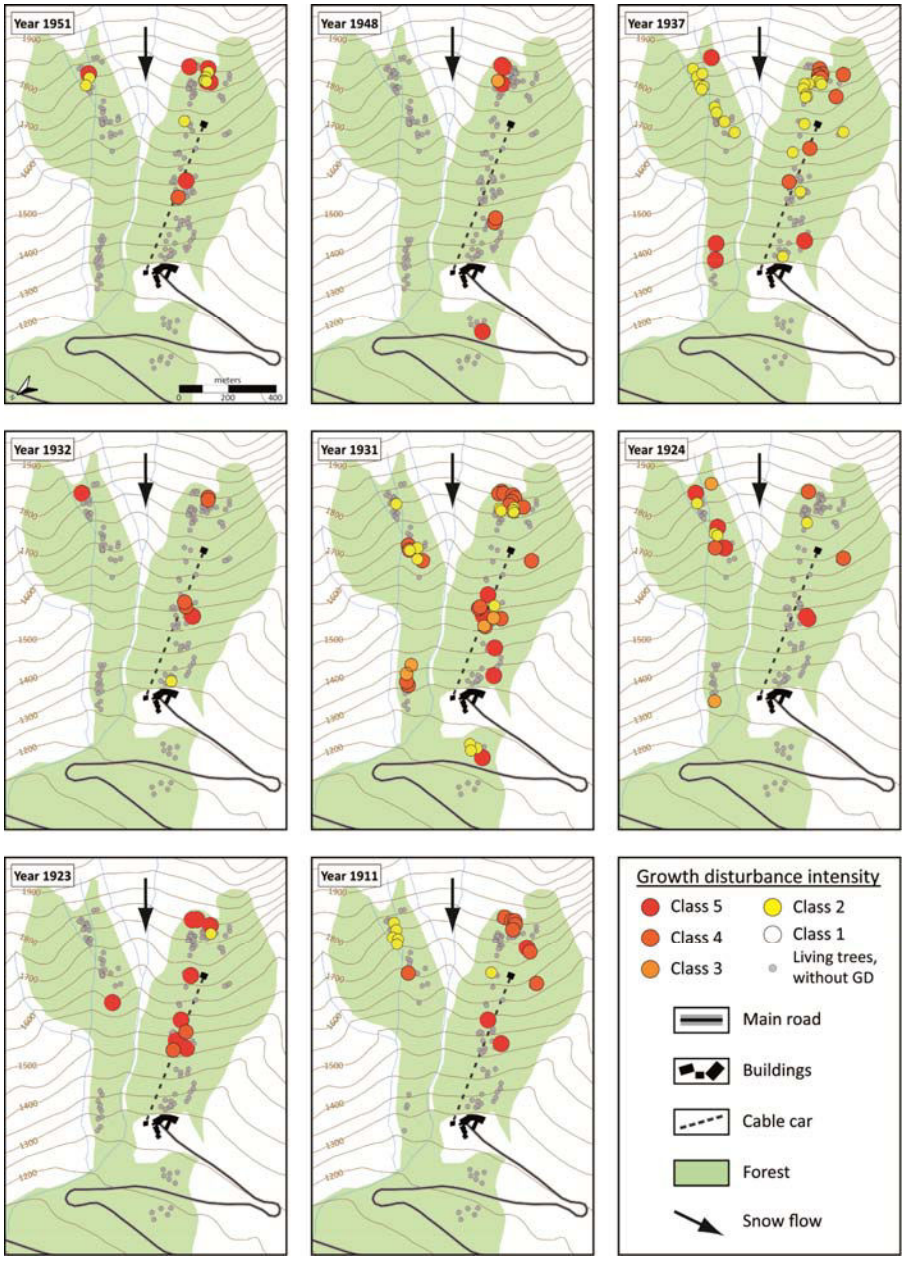

Spatial distribution of disturbed trees in the Pèlerins path for the years identified as avalanche years – period 1911–1951.

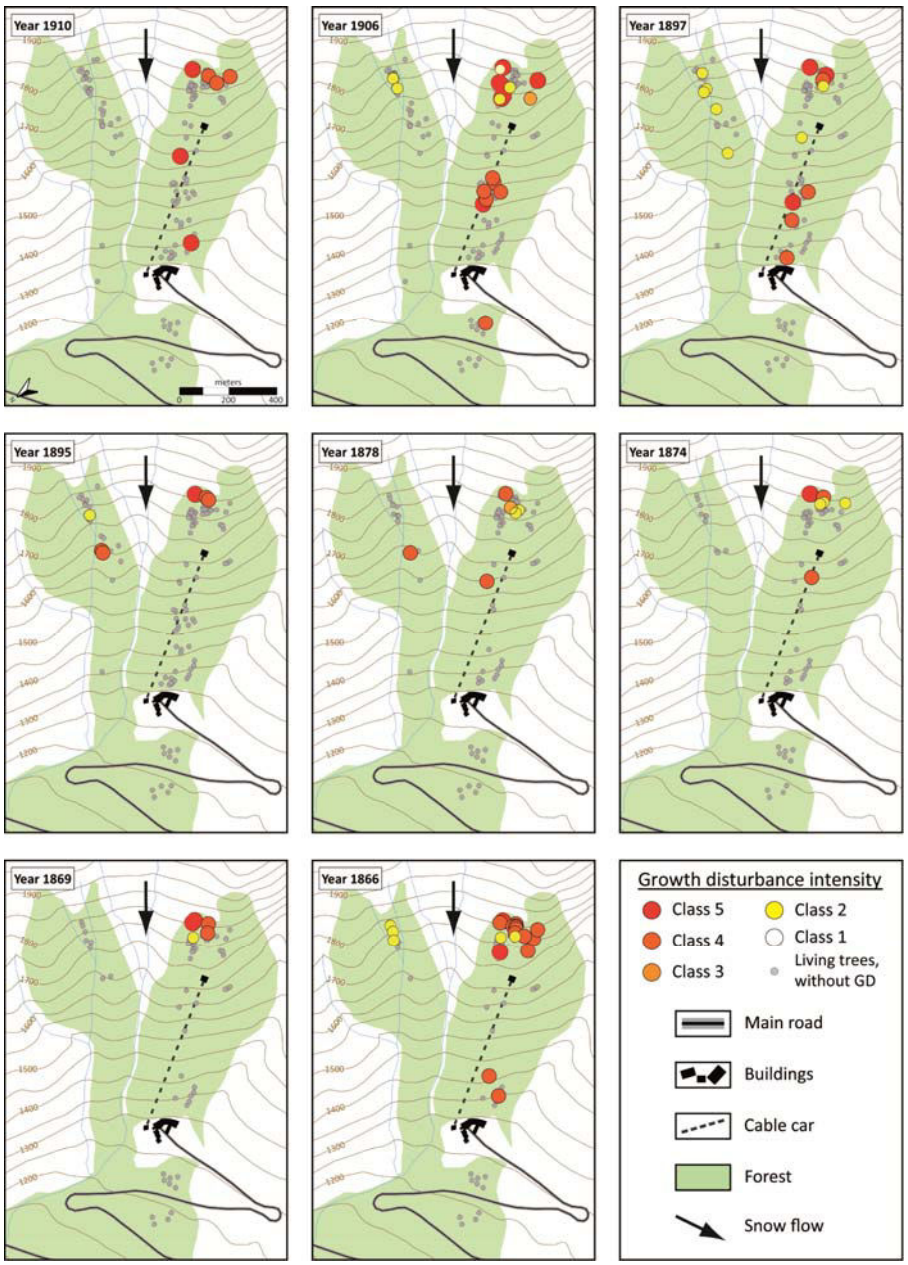

Spatial distribution of disturbed trees in the Pèlerins path for the years identified as avalanche years – period 1866–1910.

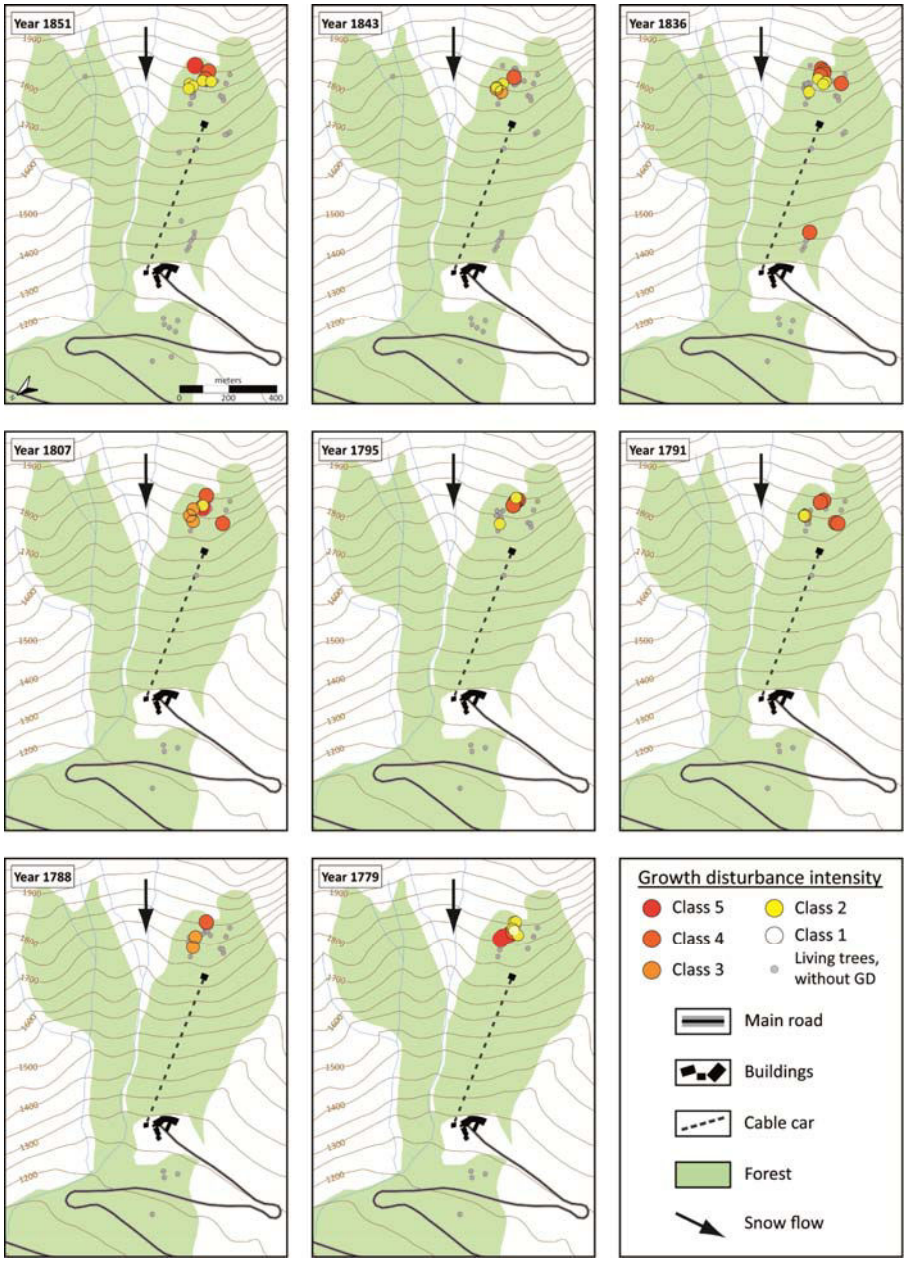

Spatial distribution of disturbed trees in the Pèlerins path for the years identified as avalanche years – period 1779–1851.

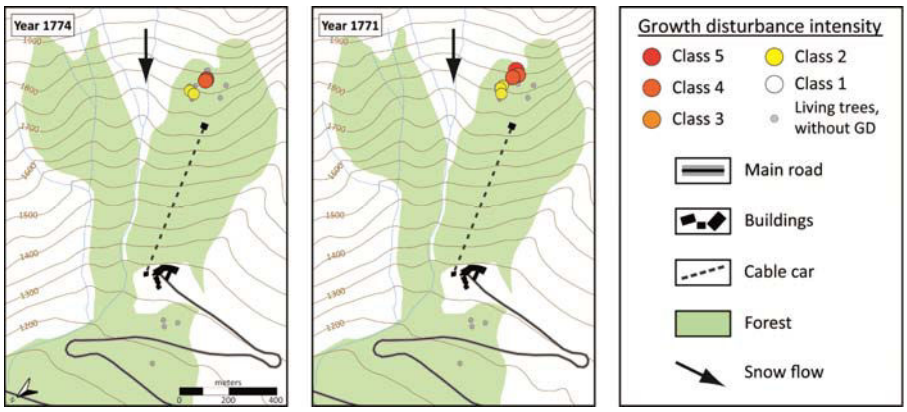

Spatial distribution of disturbed trees in the Pèlerins path for the years identified as avalanche years – period 1771–1774.

3.3 *Ressec* path

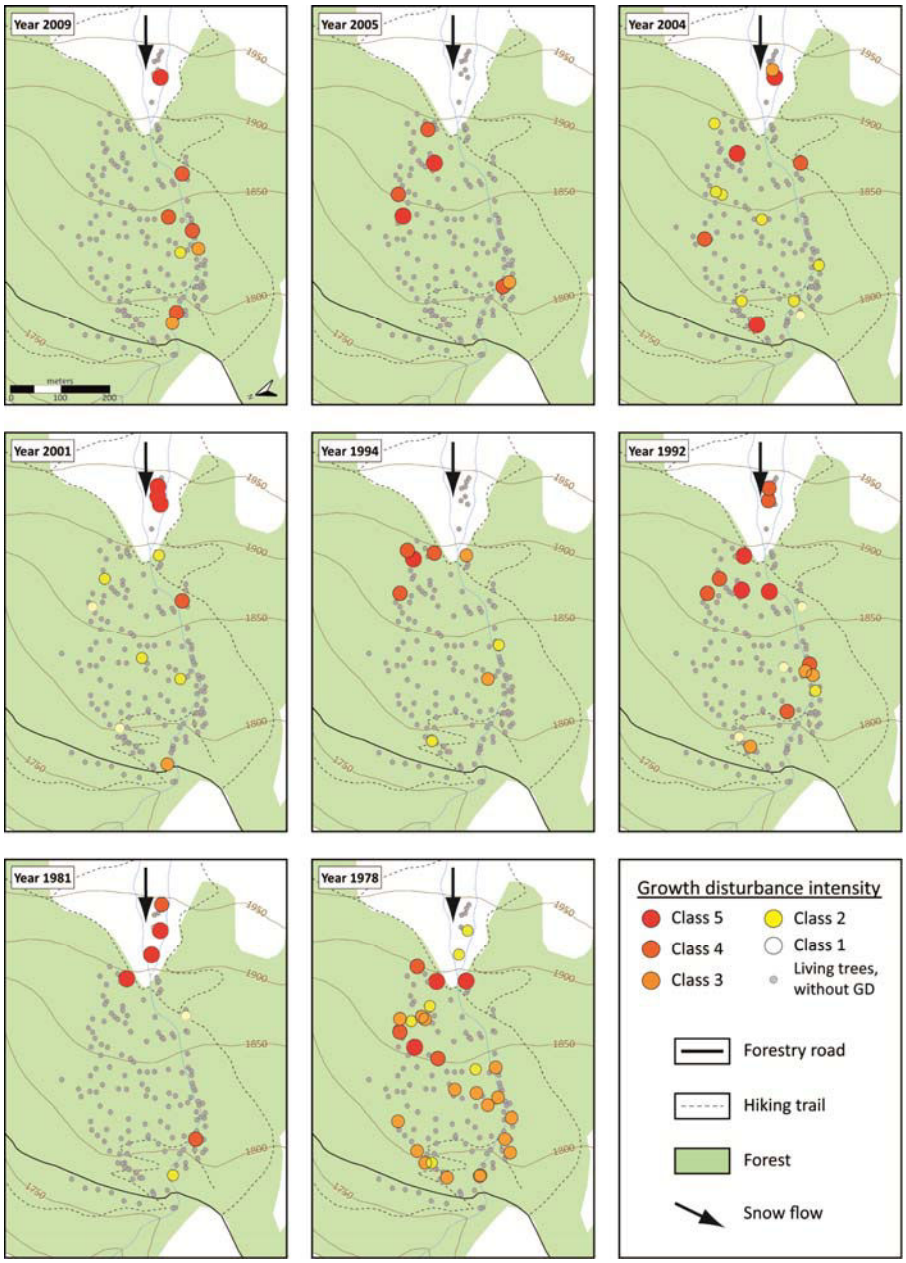

Spatial distribution of disturbed trees in the Ressec path for the years identified as avalanche years – period 1978–2009.

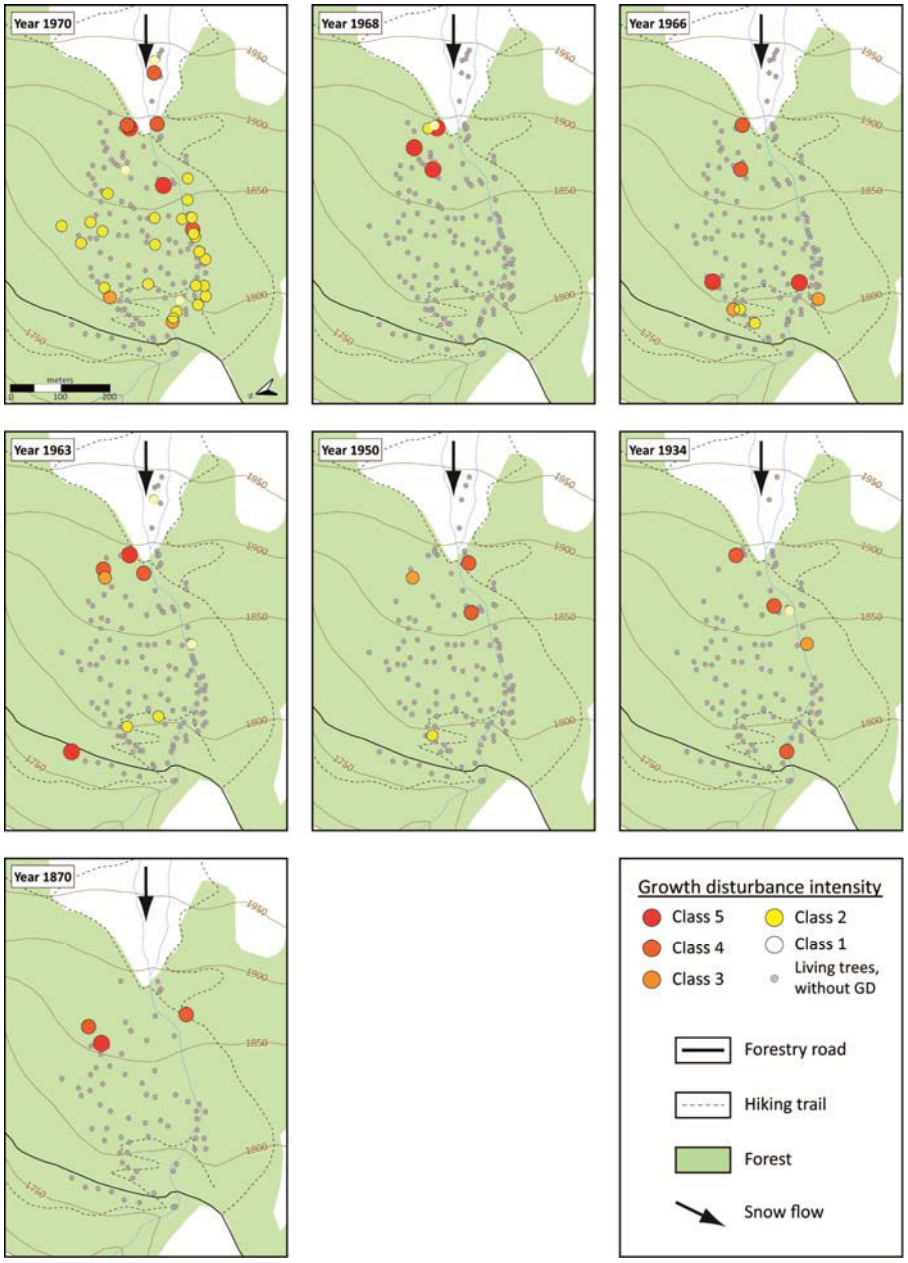

Spatial distribution of disturbed trees in the Ressec path for the years identified as avalanche years – period 1870–1970.

3.4 *Château Jouan* path

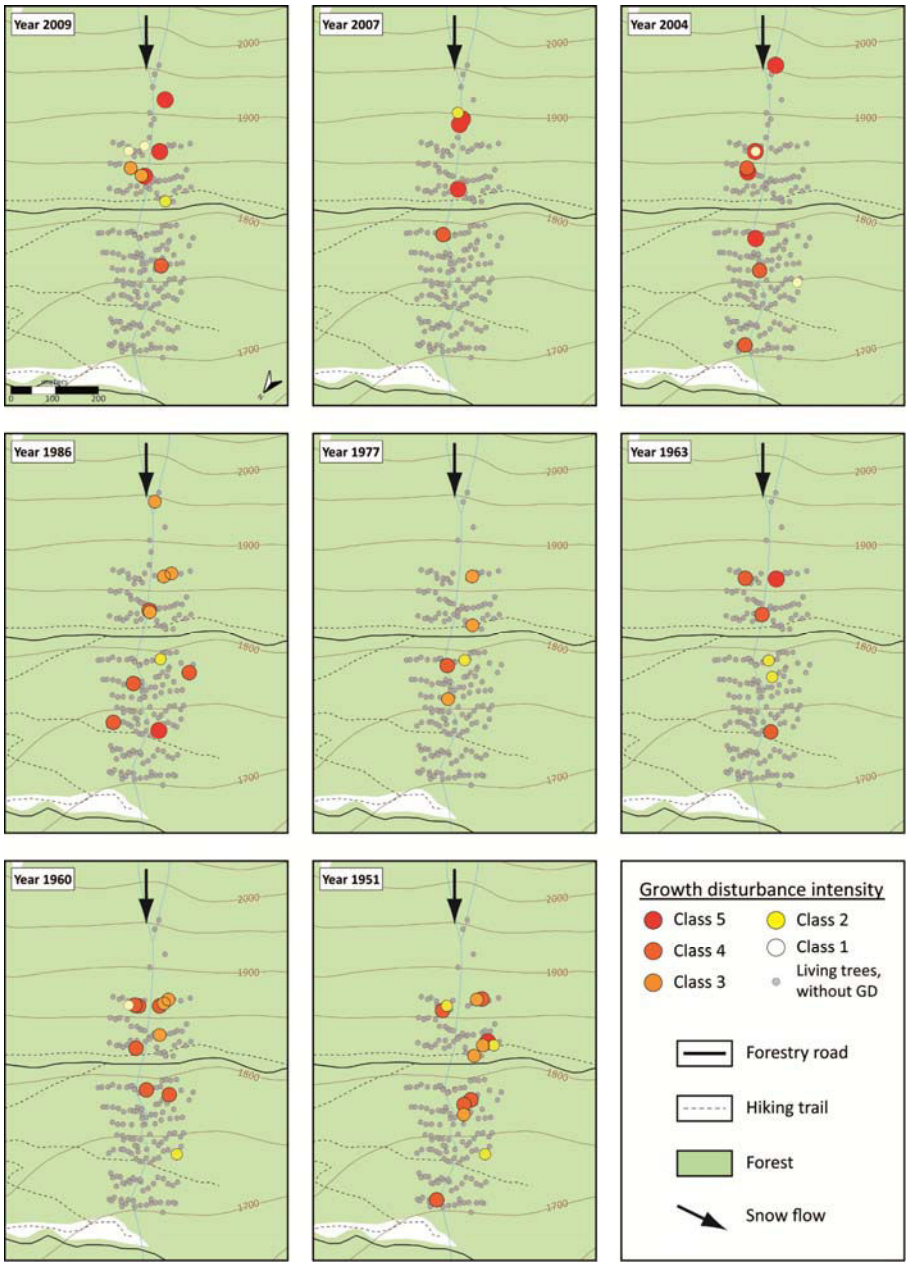

Spatial distribution of disturbed trees in the Château Jouan path for the years identified as avalanche years – period 1951–2009.

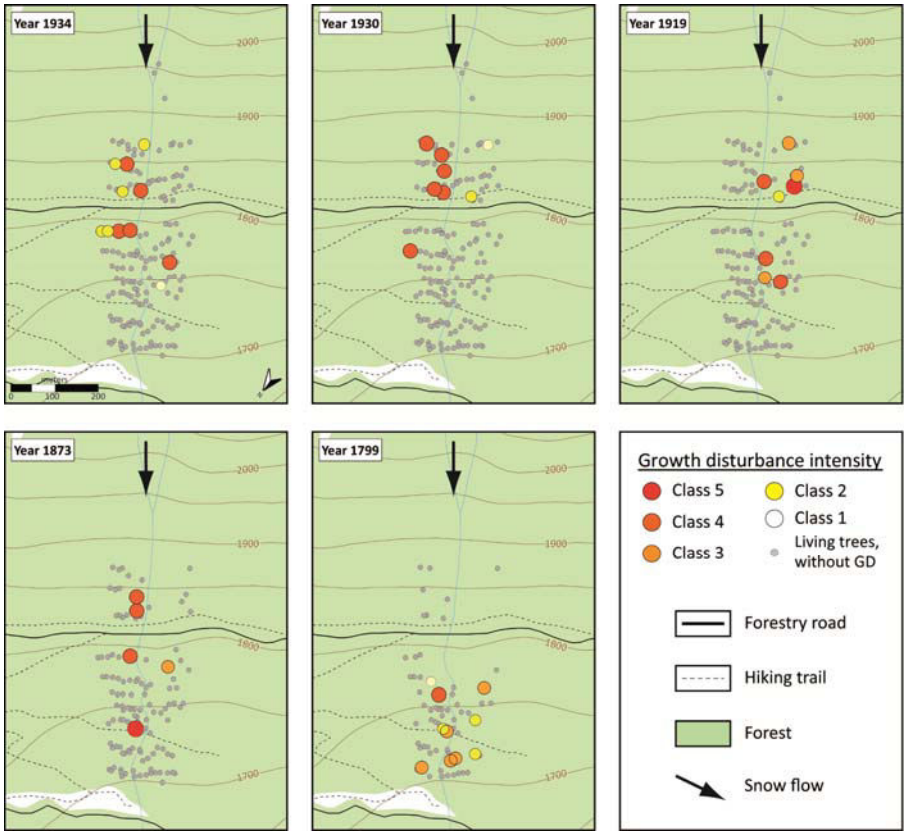

Spatial distribution of disturbed trees in the Château Jouan path for the years identified as avalanche years – period 1799–1934.

3.5 *Ourcière* path

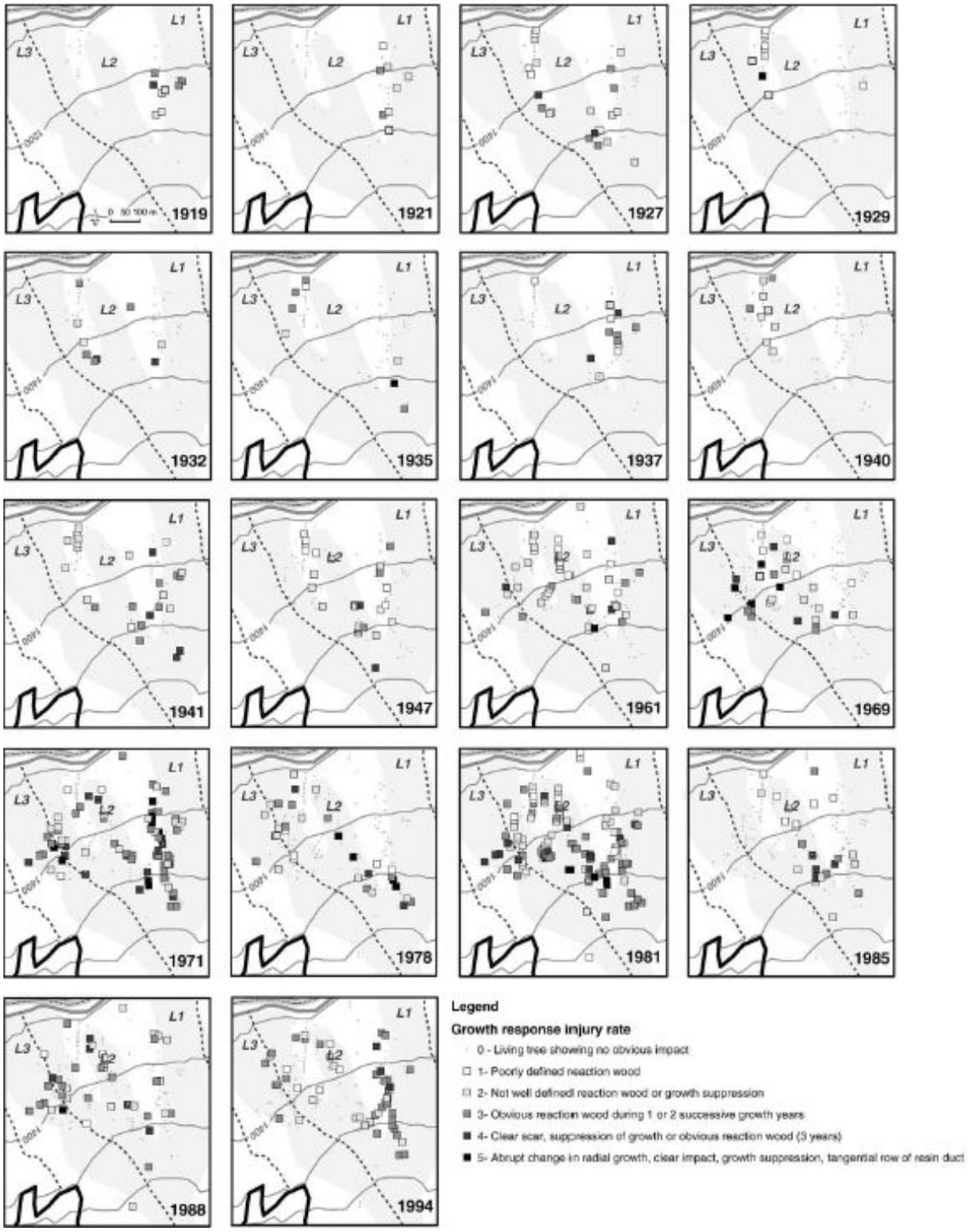

Spatial distribution of disturbed trees in the Ourcière path for the years identified as avalanche years – period 1919–2007 (Source: Corona et al., 2010).

Bibliography

A

Alestalo, J., 1971. Dendrochronological interpretation of geomorphic processes. Fennia 105, 1–139.

Ancey, C., 2005. Monte Carlo calibration of avalanches described as Coulomb fluid flows. Philos. Trans. R. Soc. 363(1832), 1529–1550.

Ancey, C., 2012. Are there “dragon-kings” events (i.e. genuine outliers) among extreme avalanches? Eur. Phys. J. Spec. Top. 205, 117–129.

Ancey, C., Gervasoni, C., Meunier, M., 2004. Computing extreme avalanches. Cold Reg. Sci. Technol. 39, 161–180.

Ancey, C., Meunier, M., 2004. Estimating bulk rheological properties of flowing snow avalanches from field data. J. Geophys. Res. 109.

Ancey, C., Meunier, M., Richard, D., 2003. Inverse problem in avalanche dynamics models. Water Resour. Res. 39.

Ancey, C., Rapin, F., Martin, E., Coleou, C., Naaim, M., Brunot, G., 2000. L’avalanche de Péclerey du 9 février 1999. La Houille Blanche, 45–53.

Arbellay, E., Stoffel, M., Decaulne, A., 2013. Dating of snow avalanches by means of wound-induced vessel anomalies in sub-arctic *Betula pubescens*. Boreas 42, 568–574.

B

Baltensweiler, W., Rubli, D., 1999. Dispersal: an important driving force of the cyclic population dynamics of the larch bud moth, *Zeiraphera diniana* Gn. For. Snow Landsc. Res. 74, 1–153.

Bannan, M.W., 1936. Vertical resin ducts in the secondary wood of the *Abietineae*. New Phytol. 35, 11–46.

Barbolini, M., Keylock, C.J., 2002. A new method for avalanche hazard mapping using a combination of statistical and deterministic models. Nat. Hazards Earth Syst. Sci. 2, 239–245.

Bartelt, P., Bühler, Y., Buser, O., Christen, M., Meier, L., 2012. Modeling mass-dependent flow regime transitions to predict the stopping and depositional behavior of snow avalanches. J. Geophys. Res. 117.

Bartelt, P., Stöckli, V., 2001. The influence of tree and branch fracture, overturning and debris entrainment on snow avalanche flow. Ann. Glaciol. 32, 209–216.

Bayes, M., Price, M., 1763. An essay towards solving a problem in the doctrine of chances. By the late rev. Mr. Bayes, F. R. S. Communicated by Mr. Price, in a letter to John Canton, A. M. F. R. S. Philos. Trans. R. Soc. London 53, 370–418.

Bebi, P., Kulakowski, D., Rixen, C., 2009. Snow avalanche disturbances in forest ecosystems—State of research and implications for management. For. Ecol. Manage. 257, 1883–1892.

Bergue, M., 2000. P.P.R, Révision partielle du plan de prévention des risques naturels prévisibles - Commune de Chamonix Mont-Blanc.

Bollschweiler, M., 2007. Spatial and temporal occurrence of past debris flows in the Valais Alps - results from tree-ring analysis. GeoFocus 20, 182 pp.

Bollschweiler, M., Stoffel, M., Schläppy, R., 2011. Debris-flood reconstruction in a pre-alpine catchment in Switzerland based on tree-ring records of coniferous and broadleaved trees. Geogr. Ann. A, 1–15.

Bollschweiler, M., Stoffel, M., Schneuwly, D.M., Bourqui, K., 2008. Traumatic resin ducts in *Larix decidua* stems impacted by debris flows. Tree Physiol. 28, 255–263.

Bonnefoy, M., Borrel, G., Richard, D., Bélanger, L., Naaim, M., 2010. La carte de localisation des phénomènes d'avalanche (CLPA): enjeux et perspectives. Sci. Eaux Territ., 6–14.

Boucher, D., Filion, L., Hétu, B., 2003. Reconstitution dendrochronologique et fréquence des grosses avalanches de neige dans un couloir subalpin du Mont Hog's Back, Gaspésie centrale (Québec). Géographie Phys. Quat. 57, 159–168.

Bovis, M.J., Mears, A.I., 1976. Statistical prediction of snow avalanche runout from terrain variables in Colorado. Arct. Alp. Res. 8, 115–120.

Bozhinskiy, A.N., Nazarov, A.N., Chernouss, P.A., 2001. Avalanches: a probabilistic approach to modelling. Ann. Glaciol. 32, 255–258.

Bräuning, A., 1995. Zur Anwendung der Dendrochronologie in den Geowissenschaften. Die Erde 126, 189–204.

Breiman, L., Friedman, J., Olshen, R., Stone, C., 1984. Classification and regression trees. Wadsworth & Brooks.

Brun, E., David, P., Sudul, M., Brunot, G., 1992. A numerical model to simulate snow-cover stratigraphy for operational avalanche forecasting. J. Glaciol. 38, 13–22.

Brun, E., Martin, E., Simon, V., Gendre, C., Coleou, C., 1989. An energy and mass model of snow cover suitable for operational avalanche forecasting. J. Glaciol. 35, 333–342.

Burrows, C.J., Burrows, V.L., 1976. Procedures of the study of snow avalanche chronology using growth layers of woody plants. Arct. Alp. Res.

Butler, D.R., Malanson, G.P., 1985. A history of high-magnitude snow avalanches, southern Glacier National Park, Montana, USA. Mt. Res. Dev. 5, 175–182.

Butler, D.R., Sawyer, C.F., 2008. Dendrogeomorphology and high-magnitude snow avalanches: A review and case study. Nat. Hazards Earth Syst. Sci. 8, 303–309.

Butler, D.R., Sawyer, C.F., Maas, J.A., 2010. Tree-ring dating of snow avalanches in Glacier National Park, Montana, USA, in: Stoffel, M., Bollschweiler, M., Butler, D.R., Luckman, B.H. (Eds.), Tree Rings and Natural Hazards. Springer Netherlands, Dordrecht, pp. 35–46.

C

Camarero, J.J., Guerrero-Campo, J., Gutiérrez, E., 1998. Tree-Ring Growth and Structure of *Pinus uncinata* and *Pinus sylvestris* in the Central Spanish Pyrenees. Arct. Alp. Res. 30, 1–10.

Carrara, P.E., 1979. The determination of snow avalanche frequency through tree-ring analysis and historical records at Ophir, Colorado. Geol. Soc. Am. Bull. 90.

Castebrunet, H., Eckert, N., Giraud, G., 2012. Snow and weather climatic control on snow avalanche occurrence fluctuations over 50 yr in the French Alps. Clim. Past 8, 855–875.

Castebrunet, H., Eckert, N., Giraud, G., Durand, Y., Morin, S., 2014. Projected changes of snow conditions and avalanche activity in a warming climate: a case study in the French Alps over the 2020–2050 and 2070–2100 periods. Cryosph. Discuss. 8, 581–640.

Casteller, A., Christen, M., Villalba, R., Martínez, H., Stöckli, V., Leiva, J.C., Bartelt, P., 2008. Validating numerical simulations of snow avalanches using dendrochronology: The Cerro Ventana event in Northern Patagonia, Argentina. Nat. Hazards Earth Syst. Sci. 8, 433–443.

Casteller, A., Stöckli, V., Villalba, R., Mayer, A.C., 2007. An Evaluation of Dendroecological Indicators of Snow Avalanches in the Swiss Alps. Arctic, Antarct. Alp. Res. 39, 218–228.

Casteller, A., Villalba, R., Araneo, D., Stöckli, V., 2011. Reconstructing temporal patterns of snow avalanches at Lago del Desierto, southern Patagonian Andes. Cold Reg. Sci. Technol. 67, 68–78.

Cook, E.R., Kairiukstis, L.A., 1990. Methods of Dendrochronology - Applications in the Environmental Sciences. Kluwer, London.

Corona, C., Lopez Saez, J., Stoffel, M., Bonnefoy, M., Richard, D., Astrade, L., Berger, F., 2012a. How much of the real avalanche activity can be captured with tree rings? An evaluation of classic dendrogeomorphic approaches and comparison with historical archives. Cold Reg. Sci. Technol. 74-75, 31–42.

Corona, C., Lopez Saez, J., Stoffel, M., Rovera, G., Edouard, J.-L., Berger, F., 2012b. Seven centuries of avalanche activity at Echalp (Queyras massif, southern French Alps) as inferred from tree rings. The Holocene 23, 292–304.

Corona, C., Rovéra, G., Lopez Saez, J., Stoffel, M., Perfettini, P., 2010. Spatio-temporal reconstruction of snow avalanche activity using tree rings: Pierres Jean Jeanne avalanche talus, Massif de l'Oisans, France. Catena 83, 107–118.

Corona, C., Trappmann, D., Stoffel, M., 2013. Parameterization of rockfall source areas and magnitudes with ecological recorders: When disturbances in trees serve the calibration and validation of simulation runs. Geomorphology 202, 33–42.

D

Decaulne, A., 2006. Snow-avalanche and debris-flow hazards in the fjords of north-western Iceland, mitigation and prevention. Nat. Hazards 41, 81–98.

Decaulne, A., Eggertsson, Ó., Laute, K., Beylich, A.A., 2013. Dendrogeomorphologic approach for snow-avalanche activity reconstruction in a maritime cold environment (upper Erdalen, Norway). Zeitschrift für Geomorphol. Suppl. Issues 57, 55–68.

Decaulne, A., Eggertsson, Ó., Laute, K., Beylich, A.A., 2014. A 100-year extreme snow-avalanche record based on tree-ring research in upper Bødalen, inner Nordfjord, western Norway. Geomorphology in press.

Decaulne, A., Eggertsson, Ó., Sæmundsson, Þ., 2012. A first dendrogeomorphologic approach of snow avalanche magnitude–frequency in Northern Iceland. Geomorphology 167-168, 35–44.

Decaulne, A., Sæmundsson, Þ., 2008. Dendrogeomorphology as a tool to unravel snow-avalanche activity: Preliminary results from the Fnjóskadalur test site, Northern Iceland. Nor. Geogr. Tidsskr. - Nor. J. Geogr. 62, 55–65.

Delparte, D., 2008. Avalanche terrain Modeling in Glacier National Park, Canada. University of Calgary.

Delparte, D., Jamieson, B., Waters, N., 2008. Statistical runout modeling of snow avalanches using GIS in Glacier National Park, Canada. Cold Reg. Sci. Technol. 54, 183–192.

Dorren, L., Berger, F., Jonsson, M., Krautblatter, M., Mölk, M., Stoffel, M., Wehrli, A., 2007. State of the art in rockfall – forest interactions. Schweizerische Zeitschrift fur Forstwes. 158, 128–141.

Du, S., Yamamoto, F., 2007. An overview of the biology of reaction wood formation. J. Integr. Plant Biol. 49, 131–143.

Dubé, S., Filion, L., Hétu, B., 2004. Tree-ring reconstruction of high-magnitude snow avalanches in the Northern Gaspé Peninsula, Québec, Canada. Arctic, Antarct. Alp. Res. 36, 555–564.

Durand, Y., Brun, E., Mérindol, L., Guyomarc'h, G., Lesaffre, B., Martin, E., 1993. A meteorological estimation of relevant parameters for snow models. Ann. Glaciol. 18, 65–71.

Durand, Y., Giraud, G., Brun, E., Mérindol, L., Martin, E., 1999. A computer-based system simulating snowpack structure as a tool for regional avalanche forecasting. J. Glaciol. 45, 469–484.

Durand, Y., Giraud, G., Laternser, M., Etchevers, P., Mérindol, L., Lesaffre, B., 2009a. Reanalysis of 47 years of climate in the French Alps (1958–2005): climatology and trends for snow cover. J. Appl. Meteorol. Climatol. 48, 2487–2512.

Durand, Y., Laternser, M., Giraud, G., Etchevers, P., Lesaffre, B., Mérindol, L., 2009b. Reanalysis of 44 yr of climate in the French Alps (1958–2002): methodology, model validation, climatology, and trends for air temperature and precipitation. J. Appl. Meteorol. Climatol. 48, 429–449.

E

Eckert, N., Baya, H., Deschatres, M., 2010a. Assessing the response of snow avalanche runout altitudes to climate fluctuations using hierarchical modeling: Application to 61 winters of data in France. J. Clim. 23, 3157–3180.

Eckert, N., Coleou, C., Castebrunet, H., Deschatres, M., Giraud, G., Gaume, J., 2010b. Cross-comparison of meteorological and avalanche data for characterising avalanche cycles: The example of December 2008 in the eastern part of the French Alps. Cold Reg. Sci. Technol. 64, 119–136.

Eckert, N., Keylock, C.J., Castebrunet, H., Lavigne, A., Naaim, M., 2013. Temporal trends in avalanche activity in the French Alps and subregions: from occurrences and runout altitudes to unsteady return periods. J. Glaciol. 59, 93–114.

Eckert, N., Naaim, M., Parent, E., 2010c. Long-term avalanche hazard assessment with a Bayesian depth-averaged propagation model. J. Glaciol. 56, 563–586.

Eckert, N., Parent, E., Bélanger, L., Garcia, S., 2007a. Hierarchical Bayesian modelling for spatial analysis of the number of avalanche occurrences at the scale of the township. Cold Reg. Sci. Technol. 50, 97–112.

Eckert, N., Parent, E., Faug, T., Naaim, M., 2008a. Optimal design under uncertainty of a passive defense structure against snow avalanches: from a general Bayesian framework to a simple analytical model. Nat. Hazards Earth Syst. Sci. 8, 1067–1081.

Eckert, N., Parent, E., Faug, T., Naaim, M., 2009. Bayesian optimal design of an avalanche dam using a multivariate numerical avalanche model. Stoch. Environ. Res. Risk Assess. 23, 1123–1141.

Eckert, N., Parent, E., Naaim, M., Richard, D., 2008b. Bayesian stochastic modelling for avalanche predetermination: From a general system framework to return period computations. Stoch. Environ. Res. Risk Assess. 22, 185–206.

Eckert, N., Parent, E., Richard, D., 2007b. Revisiting statistical–topographical methods for avalanche predetermination: Bayesian modelling for runout distance predictive distribution. Cold Reg. Sci. Technol. 49, 88–107.

ESRI, 2014. ArcGIS. URL: http://www.esri.com/software/arcgis/

F

Fantucci, R., Sorriso-Valvo, M., 1999. Dendrogeomorphological analysis of a slope near Lago, Calabria (Italy). Geomorphology 30, 165–174.

Feistl, T., Bebi, P., Bühler, Y., Christen, M., Teich, M., Bartelt, P., 2012. Stopping behavior of snow avalanches in forests, in: Proceedings of the International Snow Science Workshop ISSW. Anchorage, Alaska, pp. 420–426.

Fischer, J.-T., Fromm, R., Gauer, P., Sovilla, B., 2014. Evaluation of probabilistic snow avalanche simulation ensembles with Doppler radar observations. Cold Reg. Sci. Technol. 97, 151–158.

Frazer, G.W., 1985. Dendrogeomorphic evaluation of snow avalanche history at two sites in Banff National Park. University of Western Ontario.

Fritts, H.C., 1976. Tree rings and climate, Academic Press London.

G

Garavaglia, V., Pelfini, M., 2011. The role of border areas for dendrochronological investigations on catastrophic snow avalanches: A case study from the Italian Alps. Catena 87, 209–215.

García, C., Martí, G., Oller, P., Moner, I., Gavaldà, J., Martínez, P., Peña, J.C., 2009. Major avalanches occurrence at regional scale and related atmospheric circulation patterns in the Eastern Pyrenees. Cold Reg. Sci. Technol. 59, 106–118.

Gassner, M., Brabec, B., 2002. Nearest neighbour models for local and regional avalanche forecasting. Nat. Hazards Earth Syst. Sci. 2, 247–253.

Gauer, P., Medina-Cetina, Z., Lied, K., Kristensen, K., 2009. Optimization and probabilistic calibration of avalanche block models. Cold Reg. Sci. Technol. 59, 251–258.

Germain, D., Filion, L., Hétu, B., 2005. Snow avalanche activity after fire and logging disturbances, northern Gaspé Peninsula, Quebec, Canada. Can. J. Earth Sci. 42, 2103–2116.

Germain, D., Filion, L., Hétu, B., 2009. Snow avalanche regime and climatic conditions in the Chic-Choc Range, eastern Canada. Clim. Change 92, 141–167.

Germain, D., Hétu, B., Filion, L., 2010. Tree-ring based reconstruction of past snow avalanche events and risk assessment in Northern Gaspé Peninsula (Québec, Canada), in: Stoffel, M., Bollschweiler, M., Butler, D.R., Luckman, B.H. (Eds.), Tree Rings and Natural Hazards. Springer Netherlands, Dordrecht, pp. 51–73.

Grêt-Regamey, A., Straub, D., 2006. Spatially explicit avalanche risk assessment linking Bayesian networks to a GIS. Nat. Hazards Earth Syst. Sci. 6, 911–926.

Grissino-Mayer, H.D., 2003. A manual and tutorial for the proper use of an increment borer. TreeRing Res. 59, 63–79.

H

Hazen, A., 1914. Storage to be provided in impounding reservoirs for municipal water supply. Trans. Am. Assoc. Civ. Eng. 77.

Hebertson, E.G., Jenkins, M.J., 2003. Historic climate factors associated with major avalanche years on the Wasatch Plateau, Utah. Cold Reg. Sci. Technol. 37, 315–332.

I

Iseli, M., Schweingruber, F.H., 1989. Sichtbarmachen von Jahrringen für dendrochronologische Untersuchungen. Dendrochronologia 4, 145–147.

Issler, D., 1998. Modelling of snow entrainment and deposition in powder-snow avalanches. Ann. Glaciol. 26, 253–258.

J

Jamard, A.-L., Garcia, S., Bélanger, L., 2002. L'Enquête Permanente sur les Avalanches (EPA) - Statistique descriptive générale des événements et des sites.

Jomelli, V., Delval, C., Grancher, D., Escande, S., Brunstein, D., Hetu, B., Filion, L., Pech, P., 2007. Probabilistic analysis of recent snow avalanche activity and weather in the French Alps. Cold Reg. Sci. Technol. 47, 180–192.

Jomelli, V., Pech, P., 2004. Effects of the Little Ice Age on avalanche boulder tongues in the French Alps (Massif des Ecrins). Earth Surf. Process. Landforms 29, 553–564.

K

Kajimoto, T., Daimaru, H., Okamoto, T., Otani, T., Onodera, H., 2004. Effects of Snow Avalanche Disturbance on Regeneration of Subalpine *Abies mariesii* Forest, Northern Japan. Arctic, Antarct. Alp. Res. 36, 436–445.

Keylock, C.J., 2003. The North Atlantic Oscillation and snow avalanching in Iceland. Geophys. Res. Lett. 30.

Keylock, C.J., 2005. An alternative form for the statistical distribution of extreme avalanche runout distances. Cold Reg. Sci. Technol. 42, 185–193.

Keylock, C.J., McClung, D.M., Mar Magnússon, M., 1999. Avalanche risk mapping by simulation. J. Glaciol. 45, 303–314.

Kogelnig-Mayer, B., Stoffel, M., Schneuwly-Bollschweiler, M., 2013. Four-dimensional growth response of mature *Larix decidua* to stem burial under natural conditions. Trees 27, 1217–1223.

Kogelnig-Mayer, B., Stoffel, M., Schneuwly-Bollschweiler, M., Hübl, J., Rudolf-Miklau, F., 2011. Possibilities and Limitations of Dendrogeomorphic Time-Series Reconstructions on Sites Influenced by Debris Flows and Frequent Snow Avalanche Activity. Arctic, Antarct. Alp. Res. 43, 649–658.

Kohavi, R., 1995. A Study of Cross-Validation and Bootstrap for Accuracy Estimation and Model Selection, in: International Joint Conference on Artificial Intelligence.

Köse, N., Aydın, A., Akkemik, Ü., Yurtseven, H., Güner, T., 2009. Using tree-ring signals and numerical model to identify the snow avalanche tracks in Kastamonu, Turkey. Nat. Hazards 54, 435–449.

L

Larocque, S.J., Hétu, B., Filion, L., 2001. Geomorphic and dendroecological impacts of slushflows in Central Gaspe Peninsula (Quebec, Canada). Geogr. Ann. 83, 191–201.

Larson, P.R., 1994. The vascular cambium. Development and structure. Springer.

Laternser, M., Schneebeli, M., 2002. Temporal trend and spatial distribution of avalanche activity during the last 50 years in Switzerland. Nat. Hazards 27, 201–230.

Laxton, S.C., Smith, D.J., 2008. Dendrochronological reconstruction of snow avalanche activity in the Lahul Himalaya, Northern India. Nat. Hazards 49, 459–467.

Lied, K., Bakkehøi, S., 1980. Empirical calculations of snow-avalanche run-out distance based on topographic parameters. J. Glaciol. 26, 165–177.

Luckman, B.H., 2010. Dendrogeomorphology and snow avalanche research, in: Stoffel, M., Bollschweiler, M., Butler, D.R., Luckman, B.H. (Eds.), Tree Rings and Natural Hazards. Springer Netherlands, Dordrecht, pp. 27–34.

M

Malanson, G.P., Butler, D.R., 1984. Transverse pattern of vegetation on avalanche paths in the northern Rocky Mountains, Montana. Gt. Basin Nat. 44, 453–458.

Martin, E., Giraud, G., Lejeune, Y., Boudart, G., 2001. Impact of a climate change on avalanche hazard. Ann. Glaciol. 32, 163–167.

Mattheck, C., 1993. Design in der Natur. Rombach, Freiburg.

McAuliffe, J.R., Scuderi, L.A., McFadden, L.D., 2006. Tree-ring record of hillslope erosion and valley floor dynamics: Landscape responses to climate variation during the last 400yr in the Colorado Plateau, northeastern Arizona. Glob. Planet. Change 50, 184–201.

McClung, D.M., 1990. A model for scaling avalanche speeds. J. Glaciol. 36, 188–198.

McClung, D.M., 2000. Extreme avalanche runout in space and time. Can. Geotech. J. 37, 161–170.

McClung, D.M., 2003. Magnitude and frequency of avalanches in relation to terrain and forest cover. Arctic, Antarct. Alp. Res. 35, 82–90.

McClung, D.M., 2013. The effects of El Niño and La Niña on snow and avalanche patterns in British Columbia, Canada, and central Chile. J. Glaciol. 59, 783–792.

McClung, D.M., Lied, K., 1987. Statistical and geometrical definition of snow avalanche runout. Cold Reg. Sci. Technol. 13, 107–119.

McClung, D.M., Mears, A.I., 1991. Extreme value prediction of snow avalanche runout. Cold Reg. Sci. Technol. 19, 163–175.

McClung, D.M., Mears, A.I., Schaerer, P.A., 1989. Extreme avalanche run-out: data from four mountain ranges. Ann. Glaciol. 13, 180–184.

McClung, D.M., Schaerer, P.A., 1985. Characteristics of flowing snow and avalanche impact pressures. Ann. Glaciol. 6, 9–14.

McClung, D.M., Schaerer, P.A., 2006. The avalanche handbook, 3rd revised edition, The Mountaineers Books.

McClung, D.M., Tweedy, J., 1993. Characteristics of avalanching: Kootenay Pass. J. Glaciol. 39, 316–322.

Mears, A.I., 1989. Avalanche runout distances and dynamics: current methods and limitations. Avalanche Rev. 7.

Mears, A.I., 1992. Snow-avalanche hazard analysis for land-use planning and engineering. Color. Geol. Surv. 59.

Metropolis, N., Rosenbluth, A.W., Rosenbluth, M.N., Teller, A.H., Teller, E., 1953. Equation of state calculations by fast computing machines. J. Chem. Phys. 21, 1087–1092.

Meunier, M., Ancey, C., 2004. Towards a conceptual approach to predetermining long-return-period avalanche run-out distances. J. Glaciol. 50, 268–278.

Meunier, M., Ancey, C., Naaim, M., 2001. Mise au point d'une méthode de prédétermination statistique des côtes d'arrêt d'avalanches. La Houille Blanche, 92–98.

Mougin, P., 1922. Etudes glaciologiques: Les avalanches en Savoie, Etudes glaciologiques. Imprimerie Nationale, Paris.

Mundo, I., Barrera, M.D., Roig, F., 2007. Testing the utility of *Nothofagus pumilio* for dating a snow avalanche in Tierra del Fuego, Argentina. Dendrochronologia 25, 19–28.

Muntán, E., Andreu, L., Oller, P., Gutiérrez, E., Martínez, P., 2004. Dendrochronological study of the Canal del Roc Roig avalanche path: first results of the Aludex project in the Pyrenees. Ann. Glaciol. 38, 173–179.

Muntán, E., Garcia, C., Oller, P., Marti, G., Garcia, A., Gutiérrez, E., 2009. Reconstructing snow avalanches in the Southeastern Pyrenees. Nat. Hazards Earth Syst. Sci. 9, 1599–1612.

N

Naaim, M., 1998. Contribution to snow drift and avalanches flows modelling. Habilitation thesis. Université Joseph Fourier.

Naaim, M., Durand, Y., Eckert, N., Chambon, G., 2013. Dense avalanche friction coefficients: influence of physical properties of snow. J. Glaciol. 59, 771–782.

Naaim, M., Faug, T., Naaim-Bouvet, F., Eckert, N., 2010. Return period calculation and passive structure design at the Taconnaz avalanche path (France). Ann. Glaciol. 51, 89–97.

Naaim, M., Naaim-Bouvet, F., Faug, T., Bouchet, A., 2004. Dense snow avalanche modeling: Flow, erosion, deposition and obstacle effects. Cold Reg. Sci. Technol. 39, 193–204.

Nagelkerke, N.J.D., 1991. A note on a general definition of the coefficient of determination. Biometrika 78, 691–692.

Nagy, N.E., Franceschi, V.R., Solheim, H., Krekling, T., Christiansen, E., 2000. Wound-induced traumatic resin duct development in stems of Norway spruce (*Pinaceae*): anatomy and cytochemical traits. Am. J. Bot. 87, 302–313.

P

Pallardy, S.G., 2007. Physiology of Woody Plants. Elsevier Inc.

Pederson, G.T., Reardon, B.A., Caruso, C.J., Fagre, D.B., 2006. High resolution tree-ring based spatial reconstructions of snow avalanche activity in glacier national park, Montana, USA, in: Proceedings of the International Snow Science Workshop ISSW. Telluride, CO, pp. 436–443.

Peng, C.-Y.J., Lee, K.L., Ingersoll, G.M., 2002. An introduction to logistic regression analysis and reporting. J. Educ. Res. 96, 3–14.

Perret, S., Stoffel, M., Kienholz, H., 2006. Spatial and temporal rockfall activity in a forest stand in the Swiss Prealps - A dendrogeomorphological case study. Geomorphology 74, 219–231.

Potter, N., 1969. Tree-ring dating of snow avalanche tracks and the geomorphic activity of avalanches, northern Absaroka Mountains, Wyoming, Boulder, CO. Geol. Soc. Am. Special Pa, 141–165.

Pozdnoukhov, A., Matasci, G., Kanevski, M., Purves, R.S., 2011. Spatio-temporal avalanche forecasting with Support Vector Machines. Nat. Hazards Earth Syst. Sci. 11, 367–382.

R

R Development Core Team, 2011. R: A language and environment for statistical computing.

Reardon, B.A., Pederson, G.T., Caruso, C.J., Fagre, D.B., 2008. Spatial reconstructions and comparisons of historic snow avalanche frequency and extent using tree rings in Glacier National Park, Montana, U.S.A. Arctic, Antarct. Alp. Res. 40, 148–160.

Rigling, A., Bräker, O.U., Schneiter, G., Schweingruber, F.H., 2002. Intra-annual tree-ring parameters indicating differences in drought stress of *Pinus sylvestris* forests within the Erico-Pinion in the Valais (Switzerland). Plant Ecol. 163, 105–121.

Rinntech, 2014a. LINTAB - Precision ring by ring. URL: http://www.rinntech.de/content/view/16/47/lang,english/index.html.

Rinntech, 2014b. TSAP Win - Discover the life history of trees. URL: http://www.rinntech.de/content/view/17/48/lang,english/.

Ripley, B.D., 1996. Pattern recognition and neural networks. Cambridge University Press.

Rognon, P.G., Chevoir, F., Bellot, H., Ousset, F., Naaim, M., Coussot, P., 2008. Rheology of dense snow flows: Inferences from steady state chute-flow experiments. J. Rheol. 52.

S

Sachs, T., 1991. Pattern formation in plant tissues. Cambridge University Press.

Salm, B., 1993. Flow, flow transition and runout distances of flowing avalanches. Ann. Glaciol. 18, 221–226.

Salm, B.W., Burkhard, A., Gubler, H.U., 1990. Berechnungen von Fliesslawinen: Eine Anleitung für Praktiker mit Beispielen.

Saporta, G., 2011. Probabilités, analyse des données et statistique, 3rd edition, Paris, France.

Savage, S.B., Hutter, K., 1989. The motion of a finite mass of granular material down a rough incline. J. Fluid Mech. 199, 177–215.

Schaerer, P.A., 1972. Terrain and vegetation of snow avalanche sites at Rogers Pass, British Columbia, in: Slaymaker, O., McPherson, H.J. (Eds.), Mountain Geomorphology: Geomorphological Processes in the Canadian Cordillera. Tantalus Research Ltd, Vancouver BC, pp. 215–222.

Schläppy, R., Eckert, N., Jomelli, V., Stoffel, M., Grancher, D., Brunstein, D., Naaim, M., Deschatres, M., 2014. Validation of extreme snow avalanches and related return periods derived from a statistical-dynamical model using tree-ring techniques. Cold Reg. Sci. Technol. 99, 12–26.

Schläppy, R., Jomelli, V., Grancher, D., Stoffel, M., Corona, C., Brunstein, D., Eckert, N., Deschatres, M., 2013. A new tree-ring-based, semi-quantitative approach for the determination of snow avalanche events: use of classification trees for validation. Arctic, Antarct. Alp. Res. 45, 383–395.

Schneuwly, D.M., Stoffel, M., Bollschweiler, M., 2009a. Formation and spread of callus tissue and tangential rows of resin ducts in *Larix decidua* and *Picea abies* following rockfall impacts. Tree Physiol. 29, 281–289.

Schneuwly, D.M., Stoffel, M., Dorren, L., Berger, F., 2009b. Three-dimensional analysis of the anatomical growth response of European conifers to mechanical disturbance. Tree Physiol. 29, 1247–1257.

Schweingruber, F.H., 1983. Der Jahrring: Standort, Methodik, Zeit und Klima in der Dendrochronologie. Paul Haupt, Bern, Stuttgart, Wien.

Schweingruber, F.H., 1996. Tree Rings and Environment Dendroecology, New Phytologist. Paul Haupt, Bern, Stuttgart, Wien.

Schweingruber, F.H., 2001. Dendroökologische Holzanatomie. Paul Haupt, Bern, Stuttgart, Wien.

Schweingruber, F.H., 2007. Wood structure and environment. Springer.

Schweingruber, F.H., Eckstein, D., Serre-Bachet, F., Bräker, O.U., 1990. Identification, presentation and interpretation of event years and pointer years in dendrochronology. Dendrochronologia 8, 9–39.

Schweizer, J., Jamieson, J.B., Schneebeli, M., 2003. Snow avalanche formation. Rev. Geophys. 41.

Shigo, A.L., 1984. Compartmentalization: A Conceptual Framework for Understanding How Trees Grow and Defend Themselves. Annu. Rev. Phytopathol. 22, 189–214.

Shroder, J.F., 1978. Dendrogeomorphological analysis of mass movement on Table Cliffs Plateau, Utah. Quat. Res. 9, 168–185.

Shroder, J.F., 1980. Dendrogeomorphology: review and new techniques of tree-ring dating. Prog. Phys. Geogr. 4, 161–188.

Smith, M.J., McClung, D.M., 1997a. Characteristics and prediction of high-frequency avalanche runout. Arct. Alp. Res. 29, 352–357.

Smith, M.J., McClung, D.M., 1997b. Avalanche frequency and terrain characteristics at Rogers' Pass, British Columbia, Canada. J. Glaciol. 43, 165–171.

Stoffel, M., 2008. Dating past geomorphic processes with tangential rows of traumatic resin ducts. Dendrochronologia 26, 53–60.

Stoffel, M., Bollschweiler, M., 2008. Tree-ring analysis in natural hazards research – an overview. Nat. Hazards Earth Syst. Sci. 8, 187–202.

Stoffel, M., Bollschweiler, M., 2009a. What Tree Rings Can Tell About Earth-Surface Processes: Teaching the Principles of Dendrogeomorphology. Geogr. Compass 3, 1013–1037.

Stoffel, M., Bollschweiler, M., 2009b. Tree-ring reconstruction of past debris flows based on a small number of samples—possibilities and limitations. Landslides 6, 225–230.

Stoffel, M., Bollschweiler, M., Butler, D.R., Luckman, B.H., 2010. Tree Rings and Natural Hazards. Springer Netherlands, Dordrecht.

Stoffel, M., Bollschweiler, M., Hassler, G., 2006. Differentiating past events on a cone influenced by debris-flow and snow avalanche activity – a dendrogeomorphological approach. Earth Surf. Process. Landforms 31, 1424–1437.

Stoffel, M., Butler, D.R., Corona, C., 2013. Mass movements and tree rings: A guide to dendrogeomorphic field sampling and dating. Geomorphology 200, 106–120.

Stoffel, M., Corona, C., 2014. Dendroecological Dating of Geomorphic Disturbance in Trees. Tree-Ring Res. 70, 3–20.

Stoffel, M., Hitz, O.M., 2008. Rockfall and snow avalanche impacts leave different anatomical signatures in tree rings of juvenile *Larix decidua*. Tree Physiol. 28, 1713–1720.

Stoffel, M., Perret, S., 2006. Reconstructing past rockfall activity with tree rings: Some methodological considerations. Dendrochronologia 24, 1–15.

Stoffel, M., Schneuwly, D.M., Bollschweiler, M., Lièvre, I., Delaloye, R., Myint, M., Monbaron, M., 2005. Analyzing rockfall activity (1600–2002) in a protection forest—a case study using dendrogeomorphology. Geomorphology 68, 224–241.

Straub, D., Grêt-Regamey, A., 2006. A Bayesian probabilistic framework for avalanche modelling based on observations. Cold Reg. Sci. Technol. 46, 192–203.

T

Takeuchi, Y., Torita, H., Nishimura, K., Hirashima, H., 2011. Study of a large-scale dry slab avalanche and the extent of damage to a cedar forest in the Makunosawa valley, Myoko, Japan. Ann. Glaciol. 52, 119–128.

Teich, M., Bartelt, P., Grêt-Regamey, A., Bebi, P., 2012. Snow avalanches in forested terrain: Influence of forest parameters, topography, and avalanche characteristics on runout distance. Arctic, Antarct. Alp. Res. 44, 509–519.

Therneau, T.M., Atkinson, E.J., 1997. An Introduction to Recursive Partitioning Using the RPART Routines. pp. 1–52.

Timell, T., 1986. Compression wood in Gymnosperms. Springer, Berlin.

Trappmann, D., Stoffel, M., 2013. Counting scars on tree stems to assess rockfall hazards: A low effort approach, but how reliable? Geomorphology 180-181, 180–186.

U

Uppala, S.M., Kallberg, P.W., Simmons, A.J., Andrae, U., Da Costa Bechtold, V., Fiorino, M., Gibson, J.K., Haseler, J., Hernandez, A., Kelly, G.A., Li, X., Onogi, K., Saarinen, S., Sokka, N., Allan, R.P., Andersson, E., Arpe, K., Balmaseda, M.A., Beljaars, A.C.M., Van de Berg, L., Bidlot, J., Bormann, N., Caires, S., Chevallier, F., Dethof, A., Dragosavac, M., Fisher, M., Fuentes, M., Hagemann, S., Hólm, E., Hoskins, B.J., Isaksen, L., Janssen, P.A.E.M., Jenne, R., Mcnally, A.P., Mahfouf, J.-F., Morcrette, J.-J., Rayner, N.A., Saunders, R.W., Simon, P., Sterl, A., Trenberth, K.E., Untch, A., Vasiljevic, D., Viterbo, P., Woollen, J., 2005. The ERA-40 re-analysis. Q. J. R. Meteorol. Soc. 131, 2961–3012.

V

Vaganov, E.A., Hughes, M.K., Shashkin, A.V., 2006. Growth dynamics of conifer tree rings. Images of past and future environments. Springer, Berlin, New York.

Van der Burght, L., Stoffel, M., Bigler, C., 2012. Analysis and modelling of tree succession on a recent rockslide deposit. Plant Ecol. 213, 35–46.

Voellmy, A., 1955. Über die Zerstörungskraft den Lawinen. Schweizerische Bauzeitung 73, 159–162, 212–217, 246–249 and 280–285.

Voiculescu, M., 2008. Snow avalanche hazards in the Făgăraş massif (Southern Carpathians): Romanian Carpathians—Management and perspectives. Nat. Hazards 51, 459–475.

Voiculescu, M., Onaca, A., 2013. Snow avalanche assessment in the Sinaia ski area (Bucegi Mountains, Southern Carpathians) using the dendrogeomorphology method. Area 45, 109–122.

Voiculescu, M., Onaca, A., Chiroiu, P., 2012. Spatio-temporal reconstruction of snow avalanche activity using dendrogeomorphological method in Bucegi mountains-Romanian Carpathians, in: International Snow Science Workshop. Anchorage, Alaska.

Vriend, N.M., McElwaine, J.N., Sovilla, B., Keylock, C.J., Ash, M., Brennan, P.V., 2013. High-resolution radar measurements of snow avalanches. Geophys. Res. Lett. 40, 727–731.

W

Weber, U.M., 1997. Dendroecological reconstruction and interpretation of larch budmoth (*Zeiraphera diniana*) outbreaks in two central Alpine valleys of Switzerland from 1470-1990. Trees 11, 277–290.

Weir, P., 2002. Snow avalanche management in forested terrain. Res. Br., B.C. Min.For., Victoria, B.C.

Wigley, T.M.L., Briffa, K.R., Jones, P.D., 1984. On the Average Value of Correlated Time Series, with Applications in Dendroclimatology and Hydrometeorology. J. Clim. Appl. Meteorol. 23, 201–213.

SCHLÄPPY Romain
114 boulevard de Charonne
75020 Paris
romain.schlappy@cnrs-bellevue.fr
Tél. prof.: +33 145 07 55 81
Tél. perso.: +33 625 19 48 88

30 ans
Nationalité suisse

SPÉCIALISTE RISQUES NATURELS ET GÉOSCIENCES

EXPÉRIENCE PROFESSIONNELLE

Chargé de projet scientifique

avril 2010 – à ce jour: **CNRS – Laboratoire de Géographie Physique LGP, Meudon (France)**

- Investigations de terrain et collecte d'échantillons dans plusieurs couloirs d'avalanche dans les Alpes françaises et au Groenland
- Gestion et analyse de données géographiques
- Cartographie de l'aléa avalancheux et évaluation de la période de retour pour les évènements extrêmes dans les Alpes françaises
- Analyses statistiques des relations entre climat et activité avalancheuse
- Publication d'articles scientifiques
- Encadrement d'étudiants

Chargé de mission au sein de la division *Prévention des dangers*

janvier – décembre 2009: **Office fédéral de l'environnement OFEV, Berne**

- Identification des instabilités de terrain fondée sur l'interférométrie radar (InSAR)
- Cartographie des processus naturels et mise en place d'une base de données cantonale
- Rédaction de rapports
- Membre d'équipe de la section *Glissements de terrain, avalanches et forêts protectrices*

Assistant de recherche

octobre – décembre 2008: **Dendrolab.ch, Université de Berne**

- Relevé de terrain, analyse d'échantillons et interprétation de données collectées sur plusieurs cônes de déjection dans le canton du Valais
- Caractérisation de l'aléa «laves torrentielles» à l'aide d'une approche dendrogéomorphologique
- Cartographie des débordements et de l'extension maximale des laves torrentielles, et évaluation de la fréquence évènementielle

FORMATION

avril 2010 – avril 2014: **Doctorat de géographie en cotutelle internationale**

- Université Paris 1 Panthéon-Sorbonne – CNRS – Laboratoire de Géographie Physique LGP
- Université de Berne, Institut de Géologie – Dendrolab.ch

septembre 2006 – septembre 2008: **Master ès Sciences en Géographie**

- Université de Fribourg

septembre 2002 – août 2006: **Bachelor ès Sciences en Géosciences et Environnement**

- Université de Lausanne

août 1998 – juin 2002: **Maturité fédérale Type E**

- Lycée Jean-Piaget à Neuchâtel

INFORMATIQUE

Logiciels : ArcGIS 10.2, Adobe Illustrator, Adobe Photoshop, XLSTAT, R, TSAP Win, MS Office
Environnements : Windows, MAC OS

LANGUES

Français : Langue maternelle

Allemand et Anglais : Très bon niveau

CENTRES D'INTÉRÊT

Badminton : 14 ans de pratique en club
Photographie : passionné depuis 15 ans

Musique : 10 ans de pratique au sein d'un groupe
Voyages : Europe, Canada, Indonésie, Groenland

PUBLICATIONS

Schläppy R., Jomelli V., Eckert N., Stoffel M., Grancher D., Brunstein D., Corona C., Deschatres M. About the assessment of avalanche—climate relations using tree-ring data – case studies in the French Alps. Submitted in *Regional Environmental Change*.

Schläppy R., Eckert N., Jomelli V., Stoffel M., Grancher D., Brunstein D., Naaim, M., Deschatres M. 2013. Validation of extreme snow avalanches and related return periods derived from a statistical-dynamical model using tree-ring techniques. *Cold Regions Science and Technology*, 99, 12—26.

Schläppy R., Jomelli V., Grancher D., Stoffel M., Corona C., Brunstein D., Eckert N., Deschatres M., 2013. A new tree-ring-based, semi-quantitative approach for the determination of snow avalanche events: use of classification trees for validation. *Arctic, Antarctic, and Alpine Research*, 45(3), 383—395.

Bollschweiler M., Stoffel M., **Schläppy R.**, 2011. Debris-flood reconstruction in a pre-alpine catchment in Switzerland based on tree-ring records of coniferous and broadleaved trees. *Geografiska Annaler*, 93(1), 1—15.

BOURSE DE RECHERCHE

Fonds National Suisse de la Recherche Scientifique FNS: projet P1SKP2_148492

RÉFÉRENCES

Dr Vincent Jomelli
Directeur de recherche
LGP — UMR 8591 — CNRS
1 place Aristide Briand
92195 Meudon cedex
FRANCE
Tél. : +33 145 07 55 81

Dr Markus Stoffel
Directeur du Dendrolab.ch
Institut de Géologie, Université de Berne
Baltzerstrasse 1—3
3012 Berne
SUISSE
Tél. : +41 316 31 87 73

Dr Luuk Dorren
Collaborateur scientifique
Office fédéral de l'environnement OFEV
Worblentalstrasse 68
3063 Ittigen
SUISSE
Tél. : +41 313 24 10 24